0-315-01267-6

National Library of Canada | Bibliothèque nationale du Canada

Canadian Theses Division | Division des thèses canadiennes

Ottawa, Canada
K1A 0N4

49125

PERMISSION TO MICROFILM — AUTORISATION DE MICROFILMER

• Please print or type — Écrire en lettres moulées ou dactylographier

Full Name of Author — Nom complet de l'auteur

SUI-MING ANTHONY TSE

Date of Birth — Date de naissance	Country of Birth — Lieu de naissance
March 19, 1954	HONG KONG

Permanent Address — Résidence fixe

Chemistry Department, University of Alberta,
Edmonton, Alberta T6G 2G2

Title of Thesis — Titre de la thèse

Application of Photoelection Spectroscopy in Organic Chemistry

University — Université

Alberta

Degree for which thesis was presented — Grade pour lequel cette thèse fut présentée

Ph.D.

Year this degree conferred — Année d'obtention de ce grade	Name of Supervisor — Nom du directeur de thèse
1980	Prof. R.S. Brown

Permission is hereby granted to the NATIONAL LIBRARY OF CANADA to microfilm this thesis and to lend or sell copies of the film.

The author reserves other publication rights, and neither the thesis nor extensive extracts from it may be printed or otherwise reproduced without the author's written permission.

L'autorisation est, par la présente, accordée à la BIBLIOTHÈQUE NATIONALE DU CANADA de microfilmer cette thèse et de prêter ou de vendre des exemplaires du film.

L'auteur se réserve les autres droits de publication; ni la thèse ni de longs extraits de celle-ci ne doivent être imprimés ou autrement reproduits sans l'autorisation écrite de l'auteur.

Date	Signature
8/5/1980	Anthony Tse

NL-91 (4/77)

National Library of Canada
Collections Development Branch

Canadian Theses on
Microfiche Service

Bibliothèque nationale du Canada
Direction du développement des collections

Service des thèses canadiennes
sur microfiche

NOTICE

The quality of this microfiche is heavily dependent upon the quality of the original thesis submitted for microfilming. Every effort has been made to ensure the highest quality of reproduction possible.

If pages are missing, contact the university which granted the degree.

Some pages may have indistinct print especially if the original pages were typed with a poor typewriter ribbon or if the university sent us a poor photocopy.

Previously copyrighted materials (journal articles, published tests, etc.) are not filmed.

Reproduction in full or in part of this film is governed by the Canadian Copyright Act, R.S.C. 1970, c. C-30. Please read the authorization forms which accompany this thesis.

AVIS

La qualité de cette microfiche dépend grandement de la qualité de la thèse soumise au microfilmage. Nous avons tout fait pour assurer une qualité supérieure de reproduction.

S'il manque des pages, veuillez communiquer avec l'université qui a conféré le grade.

La qualité d'impression de certaines pages peut laisser à désirer, surtout si les pages originales ont été dactylographiées à l'aide d'un ruban usé ou si l'université nous a fait parvenir une photocopie de mauvaise qualité.

Les documents qui font déjà l'objet d'un droit d'auteur (articles de revue, examens publiés, etc.) ne sont pas microfilmés.

La reproduction, même partielle, de ce microfilm est soumise à la Loi canadienne sur le droit d'auteur, SRC 1970, c. C-30. Veuillez prendre connaissance des formules d'autorisation qui accompagnent cette thèse.

THIS DISSERTATION
HAS BEEN MICROFILMED
EXACTLY AS RECEIVED

LA THÈSE A ÉTÉ
MICROFILMÉE TELLE QUE
NOUS L'AVONS REÇUE

Ottawa, Canada
K1A 0N4

NL-339 (Rev. 8/80)

THE UNIVERSITY OF ALBERTA

APPLICATION OF PHOTOELECTRON SPECTROSCOPY IN ORGANIC CHEMISTRY

by

(C)

SUI MING ANTHONY TSE

A THESIS

SUBMITTED TO THE FACULTY OF GRADUATE STUDIES AND RESEARCH

IN PARTIAL FULFILMENT OF THE REQUIREMENTS FOR THE DEGREE

OF DOCTOR OF PHILOSOPHY

IN

DEPARTMENT OF CHEMISTRY

EDMONTON, ALBERTA

FALL, 1980

THE UNIVERSITY OF ALBERTA

FACULTY OF GRADUATE STUDIES AND RESEARCH

The undersigned certify that they have read, and recommend to the Faculty of Graduate Studies and Research, for acceptance, a thesis entitled

APPLICATION OF PHOTOELECTRON SPECTROSCOPY
IN ORGANIC CHEMISTRY

submitted by SUI MING ANTHONY TSE in partial fulfilment of the requirements for the degree of Doctor of Philosophy in Chemistry.

R. S. Brown
Supervisor

Dennis O. Harris

Brian D. Sykes

P. Stefanik

D. Clive

Robert W. Taft
External Examiner

Date April 28, 1980

TO MY MOTHER

ABSTRACT

The technique of photoelectron spectroscopy (pes) was employed in order to investigate some fundamental concepts of physical organic chemistry. A brief qualitative description of the basic theory of pes is given in Chapter I. The essential instrumental aspects of this technique are also introduced in this chapter with the aid of a simple picture of a pe spectrometer.

Chapter II deals with the application of pes to the long standing question of the symmetries of the H-bonded enol forms of some diketones. In this chapter, the advantages of pes over other methods in terms of the time scale for measurement and the simplicity of the spectra is demonstrated. The O_{1S} ionization region of the enolized malonaldehyde, hexafluoroacetylacetone, 9-hydroxy-phenalenone and 6-hydroxy-2-formyl-fulvene as well as that of tropolone show two major peaks from which one concludes that these enols exist in an asymmetric C_S form.

In Chapter III, several series of nitrogen-containing bases are examined, and their N_{1S} binding energies are presented. For pyridines, N_{1S} E_B values are found to correlate well with existing σ-parameters. Comparison of the substituent effect on the N_{1S} E_B with that predicted from two existing theoretical models (GPM and RPM) indicates qualitative, but not quantitative agreement. In addition, the 2-hydroxypyridine $\rightleftharpoons$ 2-pyridone equilibrium is inves-

tigated in the gas phase and the results corroborate existing data with respect to $\Delta G°$ and $\Delta H°$ values. These data are used to predict a gas phase basicity for 2-hydroxypyridine and 2-pyridone, and moreover unambiguously show that the relationship between E_B and gas phase basicity can only be valid when the sites of protonation and photoionization are the same. Further examples concerning this point are also presented. It is also shown that the above relationship will again fail if there is a substantial geometry change accompanying protonation which cannot be probed by photoionization since the latter is a fast process. Utilizing the presented data, one can get some idea of the energetic contribution of such geometry changes to the gas phase basicity. Finally in Chapter III a utilization of the N_{1S} E_B versus basicity data is used to show that the site of protonation in aniline is N-protonated, but *m*-NH_2 aniline and *m*-OCH_3 aniline are ring protonated.

Finally, in Chapter IV, attention is switched from core orbital (E_B) to valence orbital (ip) ionization. By using the technique of UV pes, we have studied the substituent effects of the OH and OCH_3 groups on the π ip in some allylic ethers and alcohols. It was found that the flexible allylic substituted cyclohexenes examined in this study prefer to exist in a conformation in which the π orbital is aligned with the adjacent C-OR bond.

ACKNOWLEDGEMENTS

The author wishes to express his sincere gratitude to his research supervisor, Prof. R.S. Brown, for his constant advice and encouragement throughout this work. His interest and assistance in the preparation of this thesis are also greatly appreciated.

The financial assistance provided by the University of Alberta and the National Science and Engineering Council of Canada is acknowledged.

The author would like to thank the members of the Chemistry Department Machine Shop and Electronic Shop for the maintenance of the photoelectron spectrometer, and Dr. A.M. Hogg, Dr. T.T. Nakashima and Mr. R.N. Swindlehurst and their staffs for providing superior spectral data.

The author would also like to thank Mr. Joan Huguet for his assistance and helpful discussion during his graduate career. He is also indebted to Prof. P. Kebarle and his associates for providing preliminary gas phase basicity data of the *m*-substituted anilines.

Special thanks to Ms. Diane Dowhaniuk for her care and patience in typing this manuscript.

Finally, words cannot express my appreciation to Josephine for her constant support and encouragement.

TABLE OF CONTENTS

	Page
CHAPTER I	
INTRODUCTION	1
Basic Principles of Photoelectron Spectroscopy	1
Ionizing Sources	11
(1) X-ray source	11
(2) Vacuum-UV sources	11
Sample Introduction	12
Heated-inlet Assembly	13
Spectral Measurements	17
CHAPTER II	
DETERMINATION OF THE PREFERRED SYMMETRY OF THE HYDROGEN-BONDED ENOL FORMS OF SOME DIKETONES IN GAS PHASE	18
Introduction	18
Results and Discussion	28
Variable temperature ^{1}H NMR Studies on MA and D-MA	44
Conclusions	54
Experimental	56
CHAPTER III	
N_{1S} BINDING ENERGIES OF NITROGEN-CONTAINING COMPOUNDS: CORRELATION BETWEEN N_{1S} E_B AND GAS PHASE BASICITY, SUBSTITUENT CONSTANTS AND THEORETICAL PREDICTIONS	60

CHAPTER III (continued) Page

Introduction 60

Results and Discussion 72

(I) Substituted pyridines 72

Comparison of N_{1S} binding energy shift (ΔE_B) for substituted pyridines with C_{1S} ΔE_B of substituted benzenes and with ^{14}N NMR chemical shifts of substituted pyridines 72

Comparison of the observed and calculated N_{1S} ΔE_B shifts 81

Correlation between N_{1S} E_B and σ-substituent parameters 85

Correlation between N_{1S} E_B and $\delta\Delta G°$ 91

MINDO/3 studies on the methoxypyridines 94

Tautomeric equilibrium between pyridone and hydroxypyridine ... 102

(II) Circumstances under which N_{1S} E_B-$\Delta G°$ Correlation breaks down 108

Amides 113

Aniline, N-substituted, N,N-disubstituted and *p*-substituted anilines 116

Substituted amino-naphthalenes . 119

MINDO/3 calculations for pyridine, quinuclidine, aniline and *o*-diaminobenzene 120

Site of protonation of *m*-substituted anilines 124

Experimental 134

Page

CHAPTER IV

DEPENDENCE OF THE π-IONIZATION ENERGY ON THE ORIENTATION OF AN ALLYLIC HYDROXYL OR METHOXYL SUBSTITUENT AS DETERMINED BY UV-PHOTOELECTRON SPECTROSCOPY 138

Introduction 138

Results 143

Discussion 153

Conclusion 159

Experimental 160

REFERENCES 165

LIST OF TABLES

Table	Description	Page
1	O_{1S} binding energies for dicarbonyls.	29
2	Gas phase N_{1S} binding energies (E_B), basicities ($\Delta G°$) and proton affinities (PA) for some 2,3, and 4-substituted pyridines.	73
3	Comparison of N_{1S} ΔE_B values for substituted pyridines with calculated C_{1S} ΔE_B values for analogous positions of substituted benzenes.	76
4	^{14}N chemical shift values (ppm) of some 2,3 and 4-substituted pyridines referred to CH_3NO_2 as internal standard.	80
5	Calculated differences in binding energy based upon GPM and RPM approaches.	87
6	MINDO/3 heats of formation for methoxypyridines, methoxy-pyridinium ions and ΔH_r.	98
7	O_{1S} and N_{1S} binding energies (E_B) for hydroxypyridines and pyridones.	103
8	E_B, $\delta\Delta G°$ and $\delta\Delta H°$ values relatives to NH_3.	110
9	MINDO/3 calculated heats of formation for some bases.	122
10	N_{1S} ΔE_B and $\delta\Delta G°$ values of *m*-substituted anilines relative to aniline.	126
11	Vertical ionization energies (ip) and assignments for compounds 53, 54, 55, 64, 65 and 66.	147

LIST OF FIGURES

Figure		Page
1	Potential energy functions of a hypothetical molecule illustrating transitions from the ground state (A) to a final state for which the equilibrium internuclear distance is (a) about the same (B) and (b) quite different from the internuclear separation (r_o) of the ground state (C).	7
2	Schematic diagram of a MacPherson ESCA 36 Photoelectron spectrometer.	9
3	Heated inlet assembly for MacPherson ESCA 36 spectrometer designed for these studies. Upper half of the diagram shows the front view of the heated inlet assembly. Lower half reveals the bottom view at right angle to the upper view of the rest of the assembly inside the sample chamber.	14-15
4	An unrestricted computer fit of the O_{1S} ionization region of dimethylacetylacetone (2).	31
5	An unrestricted computer deconvolution of the O_{1S} ionization region of β-methoxyacrolein (1b).	32
6	An unrestricted computer deconvolution of the O_{1S} ionization region of Malonaldehyde (1a).	33
7	An unrestricted computer deconvolution of the O_{1S} ionization region of acetylacetone (1c).	34
8	An unrestricted computer deconvolution of the O_{1S} ionization region of hexafluoroacetylacetone (1d).	36
9	An unrestricted computer deconvolution of the O_{1S} ionization region of tropolone (3a). There appears to be small but real deviation from baseline to the high binding energy side of the deconvoluted peaks that we tentatively assign to shake-up events (see text).	36

Figure		Page
10	An unrestricted computer deconvolution of the O_{1S} ionization region of 2-methoxytropone (3b) assuming only two main peaks. There appear to be small but real deviation from base-line to the high binding energy side of the main bands that we tentatively assign to shake-up events (see text).	37
11	A computer deconvolution of the O_{1S} ionization region of 9-hydroxyphenalenone (4). Due to the poor statistics we were forced to restrict the deconvolution of the broad experimental peak into two peaks of equal area.	38
12	An unrestricted computer deconvolution of the O_{1S} ionization region of 6-hydroxy-2-formylfulvene (5). The high binding energy peaks are presumably due to shake-up phenomenon accompanying ionization of the oxygen.	39
13	The ^1H NMR spectrum of malonaldehyde (1a) at 153°K in a solvent of 1:1 $CFCl_3$:CD_2Cl_2. The small peak at ~δ6 is attributable to a spinning side band from adventitious $HCDCl_2$.	50
14	The ^1H NMR spectrum of deuterated malonaldehyde at 150°K in a solvent of 1:1 $CFCl_3$:CD_2Cl_2. The large resonance at δ 5.33 is attributable to $HCDCl_2$.	52
15	A plot of N_{1S} ΔE_B against C_{1S} ΔE_B for substituted pyridines and benzenes.	77
16	A plot of N_{1S} ΔE_B (observed) against N_{1S} ΔE_B (calculated) on the basis of GPM.	83
17	A plot of N_{1S} ΔE_B (observed) against N_{1S} ΔE_B (calculated) on the basis of RPM.	86
18	A plot of N_{1S} ΔE_B against σ-substituted parameters from ref. 187.	89
19	A plot of N_{1S} ΔE_B vs $\delta\Delta G°$ (relative to pyridine) for 2,3, and 4-substituted pyridines. Open circles (O) are for 2, (▲) are for 3, and closed circles (●) are for 4 substituents.	92

Figure		Page
20	Unrestricted computer deconvolution of the N_{1S} and O_{1S} ionization region of $\underset{\sim}{7} \rightleftharpoons \underset{\sim}{8}$ at 130°C. The ratio of the two N peaks and O peaks is 0.48 ± 0.05.	104
21	A plot of N_{1S} E_B vs - $\delta\Delta G°$ (relative to NH_3) for the compounds listed in Table 8. Amides are represented by ▲, pyridines as O, anilines as ● and substituted aminonaphthalenes as ■.	109
22	A plot of O_{1S} E_B against - $\delta\Delta G°$ (relative to NH_3) for various amides. The open triangle is the predicted basicity for 2-pyridone.	115
23	A plot of ΔE_B (N_{1S}) against the differences in gas phase basicities ($\delta\Delta G°$) for *m*-substituted anilines.	129
24	N_{1S} ΔE_B vs σ-values for *m*-substituted anilines relative to aniline.	131
25	N_{1S} ΔE_B vs σ-values for *p*-substituted anilines relative to aniline.	133
26	The pe spectra *cis*- and *trans*-*tert*-butyl-2-cyclohexen-1-ol ($\underset{\sim}{53b}$ and $\underset{\sim}{54b}$) using Argon as an internal reference.	148-149
27	The pe spectra of *cis*- and *trans*-3-methoxy-6-*tert*-butylcyclohexene ($\underset{\sim}{53c}$ and $\underset{\sim}{54c}$) using Argon as an internal reference.	150
28	The pe spectra of 5α-substituted-10α-methyl-Δ^3-octalins ($\underset{\sim}{55a,b,c}$) using Argon as an internal calibrant.	151

CHAPTER I

INTRODUCTION

For the present thesis work, photoelectron spectroscopy (pes) was utilized as a tool to gather information about the electronic structure and chemical bonding of several series of organic compounds. The theory and method of pes have been reviewed by several authors, for both X-ray[1-8] and ultraviolet (U.V.) pes[8-18]. In this chapter a qualitative description of pes is given to acquaint the reader with the essentials of the method as it pertains to the work presented, since details of this technique can be found in references 1-18.

Basic Principles of Photoelectron Spectroscopy

Photoelectron spectroscopy is a technique which permits the direct measurement of the energy required to remove an electron from an atom or molecule (equation 1).

$$M + h\nu \longrightarrow M^+ + e^- \qquad (1)$$

$$h\nu = E_B(e^-) + E_K(e^-) \qquad (2)$$

The method provides information about the bonding characteristics of the orbital from which the electron is ejected and hence the electronic properties of the

atom or molecule. The theory behind the experimental technique rests on the photoelectric effect[19] for which according to the law of conservation of energy, an absorbed photon provides energy ($h\nu$) which is equal to the sum of the minimum energy required for the ejection of an electron (held with a binding energy E_B) from a particular orbital and the kinetic energy, E_K of the free electron. The photoelectron spectrometer allows the measurement of the electron kinetic energy (E_K), and together with the known input photon energy ($h\nu$), E_B of the ejected electron can be evaluated from equation 2. In order to interpret the photoelectron spectral data as providing information about orbital energies, one generally invokes Koopmans' theorem[20] which states that the molecular binding energy (E_B) of an electron is equal to the negative of its molecular orbital eigenvalue (ε_i) (equation 3).

$$E_{Bi} = -\varepsilon_i \qquad (3)$$

However, one should be aware of the approximations made in Koopmans' approach so that the photoelectron spectra are not misinterpreted due to the defects in the theorem itself. The approach rests on three major approximations[21].

(a) <u>The reorientation approximation</u>

The general proof of Koopmans' theorem assumes that

all the energy orbitals remain unchanged when going from the molecule's neutral state to its ionic state. This is not necessarily true since electronic relaxation may become important upon ionization. Electronic relaxation occurs during an ionizing process in which the removal of an electron from a molecular orbital causes the remaining electrons in the molecule to polarize towards the resultant positive hole so as to "screen" the hole charge. As a result of this electronic reorganization a more stable ionic state with a different set of orbitals from that of the molecular ground state is formed.

(b) The relativistic energy approximation

In the Hartree-Fock-self-consistent-field calculation[22], only non-relativistic orbital energies are determined. However, in order to equate the experimental E_B values with the theoretical ones, relativistic corrections need to be considered. According to the theory of relativity[23], relativistic effects are only important for particles travelling at high velocity (comparable to the speed of light); the faster the particle travels the greater the relativistic corrections become. Since inner shells require a higher photon energy to ionize their electrons than valence shells (Mg K_α vs HeI radiation respectively), the former generally possess higher E_K's and therefore require larger relativistic corrections than the latter. As Koopman's theorem

assumes that the relativistic energy is the same in both molecule and ion, the ionization energy is then given by the difference between the non-relativistic orbital energy of the molecule and the ion. This assumption may be reasonable if only outer shell electrons are removed because of the smaller relativistic corrections, however, it is not surprising that the assumption breaks down for removal of inner shell electrons.

(c) The correlation energy approximation

Electrons tend to be as far from each other as possible, that is, their motions are correlated. The assumption however is made that the correlation energy is the same in both the molecule and ion. As correlation effects arise largely from interactions between electrons, and the ion has fewer electrons than the parent molecule, the correlation energy would certainly be different and generally less in the ion than its parent molecule.

While Koopmans' theorem is generally invoked to interpret ionization data in terms of molecular orbital (M.O.) energies, several violations of the theorem are documented in the literature[25-27]. For example, *ab initio* calculations[25] on N_2 and N_2^+ failed to predict the correct energy ordering of orbitals in the ionic ground state. The failure is presumably due to the neglect of correlation terms.

In the present thesis work, the E_B data are analyzed with respect to a suitable standard. For example, all the binding energy shifts of substituted pyridines are interpreted relative to the E_B value of pyridine. Since no absolute E_B value is involved in the discussion of spectral results, the errors inherent in the Koopmans' theorem should be minimized when comparison of E_B data is considered.

As the ionization process involves an electronic transition ($\nu = 10^{16}$ sec^{-1})[28], it should be fast compared to molecular motions, the fastest being vibrations occuring with frequency of 10^{14} sec^{-1}[28]. Therefore the transition should follow the Franck-Condon Principle[29-31] which states that the internuclear distances remain constant during an electronic transition. In other words, the transfer of excitation occurs on a time scale which is short compared with that required for the execution of vibrational motion. The principle governs the relative probabilities of ionizing transitions from the molecular vibrational ground state ($\nu' = 0$) to the various ionic vibrational states ($\nu'' = 0, 1 .....$). Under normal circumstances, transitions are all taken as originating from $\nu' = 0$ since it is usually the most populated state at ambient temperatures[32]. According to the Franck-Condon Principle, the transition probability $P_{\nu''\nu'}$ is proportional to the square of the

overlap integral of the ground vibrational ($\psi_{\nu'}$) and ionic vibrational ($\psi_{\nu''}$) wave functions (equation 4).

$$P_{\nu''\nu'} \alpha [\int \psi_{\nu''} \psi_{\nu'} dr]^2 \quad (4)$$

Consider the hypothetical transition shown in Figure 1. The zeroth ground vibrational state ($\nu' = 0$) has its maximum at the equilibrium internuclear position (r_o) so that the maximum probability for transition occurs in the centre of the Franck-Condon region (area between two vertical lines in Figure 1). Significant transition cannot occur outside this region since ψ approaches zero. Transition from A to B represents the situation where equilibrium internuclear distance in ion B is the same or nearly the same as that in A, and hence the most probable transition is to the $\nu'' = 0$ in B. Transition to other vibrational levels in B will have a very low probability which decreases as ν'' increases. The transition from $\nu' = 0$ to $\nu'' = 0$ is called the adiabatic transition which in this case is equal to the "vertical" transition (*vide infra*).

In the case of the transition from A to ion C where equilibrium internuclear distances in both states are different (in this case, the equilibrium internuclear distance is greater in C than in A), the maximum overlap occurs at higher vibrational level than $\nu'' = 0$ in C. This transition of maximum probability is termed

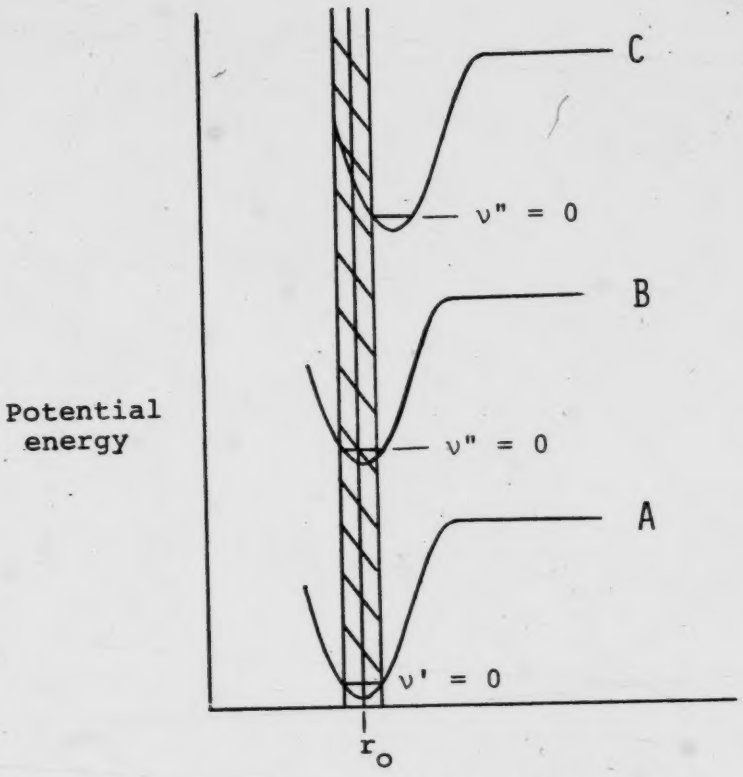

Figure 1. Potential energy functions of a hypothetical molecule illustrating transitions from the ground state (A) to a final state for which the equilibrium internuclear distance is (a) about the same (B) and (b) quite different from the internuclear separation (r_o) of the ground state (C).

"vertical". In principle, one should be able to observe the fine vibrational structure in a photoelectron spectrum provided that the separation of these vibrational levels in the ion state is greater than the resolution of the spectrometer. This is commonly observed in UV

photoelectron spectra[9], but not in the X-ray photoelectron spectra since the usual full width at half maximum (FWHM) of the ionization peak in the X-ray case is in the order of 1-2 eV. For a molecule undergoing core shell or 1s ionization, the equilibrium internuclear distance is almost the same in the ion as for the neutral molecule because the core electrons are essentially non-bonding. Thus for X-ray pes (XPS) the adiabatic and the vertical ionization energies are basically the same. However, this is not always the case for valence shell ionization as they generally arise from orbitals which have some bonding or anti-bonding characteristics. Unless otherwise stated, only vertical ionization energies determined as the maximum intensity of the band, will be considered.

The generalized photoelectron spectrometer basically consists of three compartments, a sample chamber, an energy analyzer and an electron detector, (Figure 2). Each compartment is maintained under high vacuum ($\sim 10^{-6}$ Torr) during spectral runs to allow proper functioning of the X-ray source and electron detector and to provide a collision-free path for the photo-emitted electrons. The sample chamber is comprised of a source of ionizing radiation and either a target chamber for vapor phase studies or a solid target where collisions between sample and photons occur leading to ionization.

Figure 2: Schematic Diagram of a MacPherson ESCA 36 Photoelectron Spectrometer from ref. 35.

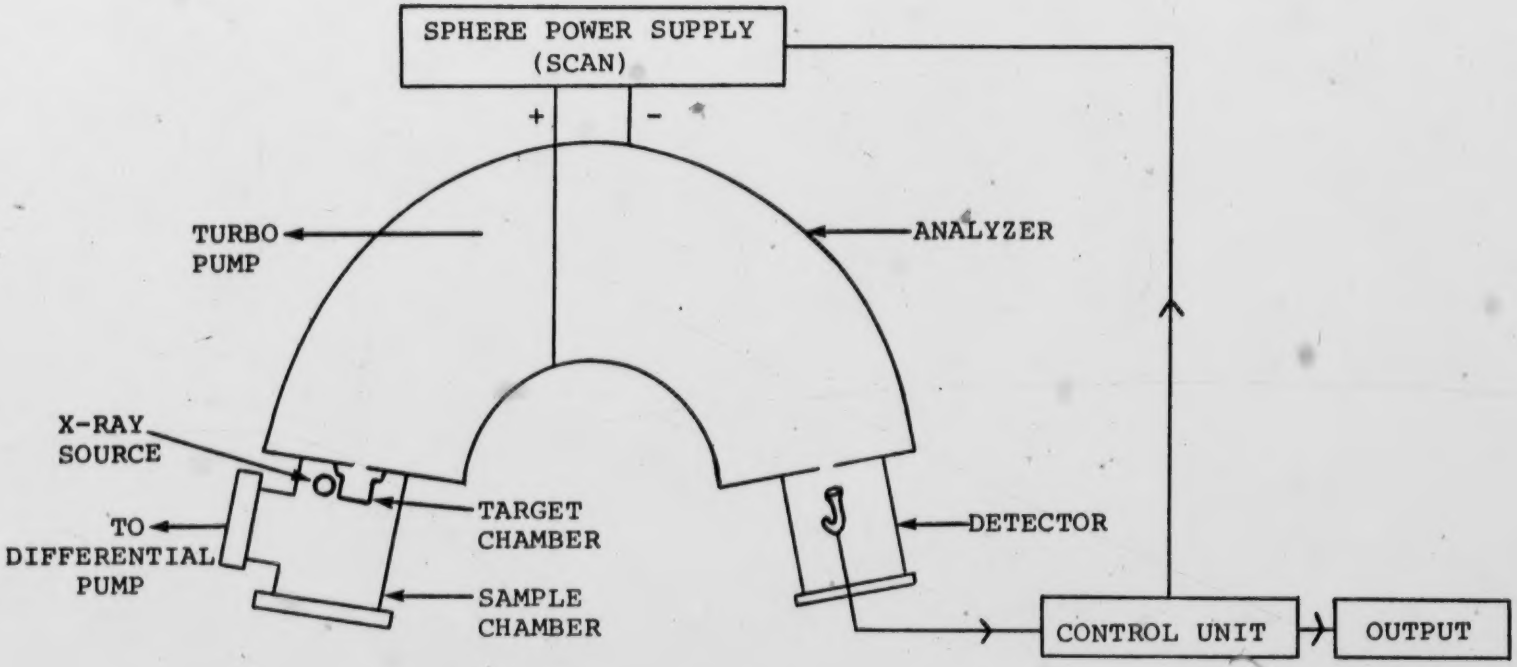

In a typical experiment an electron can be ejected from any energy level in the molecule, provided that the individual E_B is less than that of the incident photon energy and that its ionization cross-section or ionization probability is substantial. These ejected electrons possess E_K given by equation 2 and enter the analyzer if they are within the solid angle of acceptance of the analyzer entrance slit. The trajectories of these electrons in the analyzer are controlled by a potential difference between the analyzer plates. By increasing the potential across the plates, electrons of increasing E_K are brought into focus on the exit slit at the end of the analyzer. Once through the exit slit, the electrons enter the detector (electron multiplier)[33,34] where signals will be amplified. The recorded information consists of electron counts as a function of plate voltage, the latter being directly proportional to E_K.

Two types of pes, ultraviolet (UV) and X-ray, will be considered in terms of their ionizing sources and target chambers. Since the spectrometer used throughout this thesis work is a commercial McPherson ESCA 36[35], discussion will be restricted to the design of this particular instrument.

Ionizing sources

(1) X-ray source

Many X-ray sources[3] have been used in pes, but by far the most important are the characteristic K_α X-rays of Mg and Al. The Mg K_α X-ray (1253.6 eV)[3] was used as the photon source for this work, and it is produced by bombarding a Mg anode with electrons generated from a thoriated tungsten filament of the X-ray cathode. Bombardment of the Mg anode by these electrons creates initial vacancies in the desired inner shell (K-shell) of the magnesium atoms. By filling of the K-shell vacancy with an atomic electron an X-ray is generated by means of a radiative transition. In order to prevent any contamination of the X-ray source by the sample gas molecules which decreases the photon flux, the target chamber (Figure 2) is fitted with an aluminum "window" (100 mm x 50 mm x 0.005 mm) to isolate the sample vapor from the source. The aluminum window also serves the purpose of filtering out the low energy bremsstrahlung[36]. By using Mg K_α X-rays, the typical half-width of an ionization peak is 1.0-1.2 eV for the reference neon Auger line (E_K = 804.56 eV)[37] and about 1.5 eV for the gas molecules studied, although the natural width of Mg K_α radiation is 0.8 eV[3].

(2) Vacuum-UV sources

Two methods have proven successful in producing

HeI resonance lines, gas discharge and microwave discharge. In this work valence shell studies utilized a cathode discharge vacuum-UV lamp producing HeI radiation of 21.2175 eV (584 Å)[15]. Photons from this light source are capable of ionizing the majority of valence electrons and are uncontaminated by any photon of lower energy down to about 4 eV. The spectra generated in the helium discharge lamp exhibit sharp lines, resulting from deexcitation of excited free helium atoms. These lines have a natural linewidth of as low as a few millielectron volts, (meV)[38].

Sample Introduction

In principle, any solid or gas sample can be studied by pes, however, the discussion will be limited to gas phase studies. One of the major problems in measuring pes spectra in the gas phase is that a high sample pressure is desirable in the region of ionization such that a reasonable signal can be obtained. On the other hand, the sample pressure should be low enough so that the photoemitted electron does not suffer collisions during the time it is ejected from the parent molecule until it enters the analyzer. A target chamber (Figure 2) is set up in the sample chamber to permit a high concentration of vapor for ionization while keeping the rest of the spectrometer at low pressure through differential pumping. Typical pressure

in the target chamber is about 10^{-2} Torr whereas in the analyzer is about 10^{-5} or 10^{-6} Torr. For compounds of low volatility, a heated-inlet system was utilized to produce sufficient sample vapor for spectral runs.

Heated-inlet assembly

Shown in Figure 3 is the heated-inlet system with which involatile samples can be introduced into a target chamber. This design allows the minimum modification of the existing sample chamber and hence it can be used as a permanent set up for both volatile and non-volatile samples. However, it suffers from the minor disadvantage of having the heated gaseous molecules travel some distance down a hot stainless steel tube before being bombarded by X-rays. This could produce problems with molecules which thermalize on the steel surface, although we have not observed any problem with the samples studied here.

The heated-inlet assembly consists of three main parts, a piece of machinable glass, an aluminum target chamber, and a piece of stainless steel tube for introducing the sample into the target chamber. The machinable glass simply acts as a support for the target chamber and also provides thermal and electrical insulation from the analyzer. Four 30-Ω pencil heaters[39] (1/8" x 1") connected in parallel are implanted

Figure 3. Heated inlet assembly for McPherson ESCA 36 spectrometer designed for these studies. Upper half of the diagram shows the front view of the heated inlet assembly. Lower half reveals the bottom view at right angles to the upper view of the rest of the assembly inside the sample chamber.

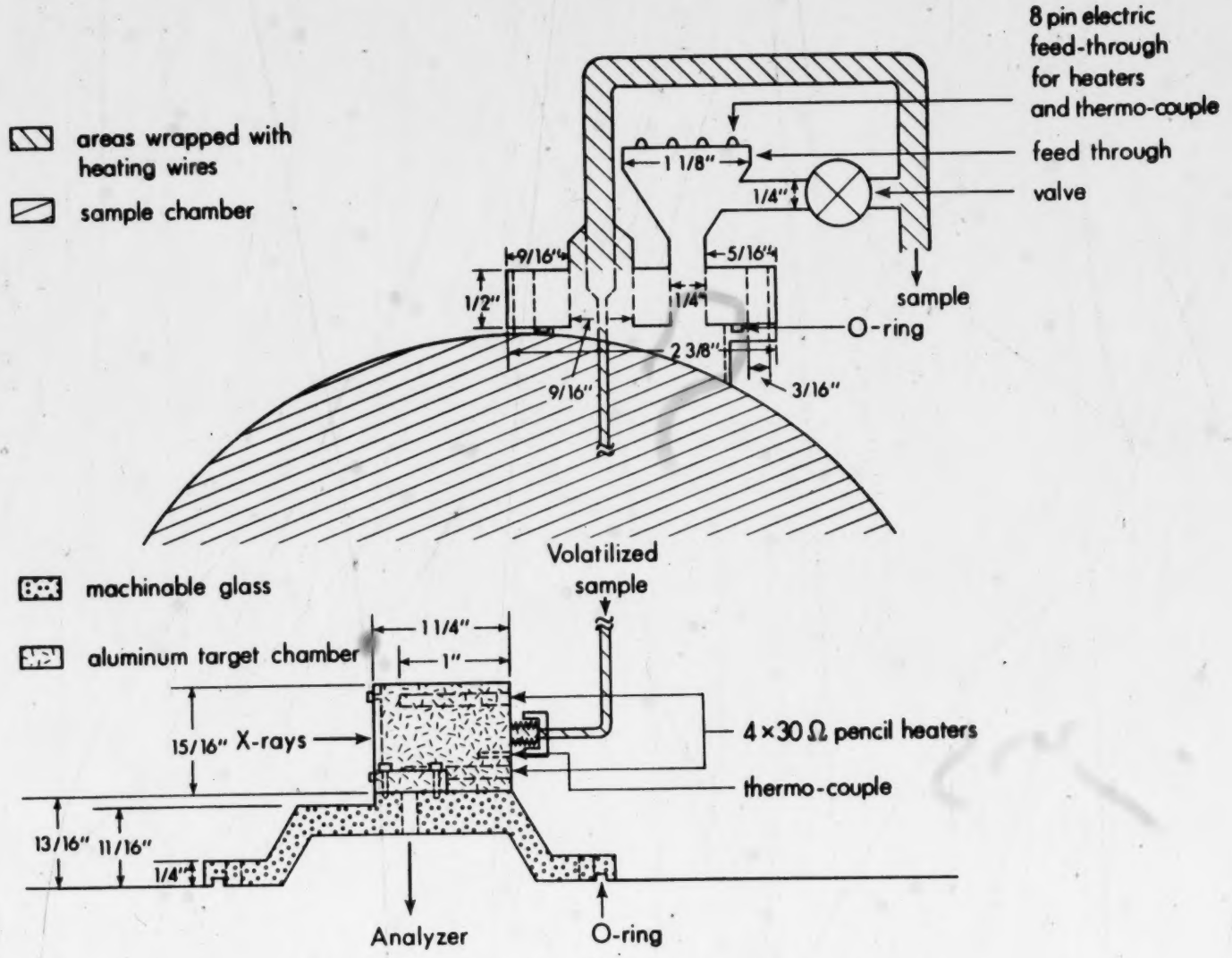
areas wrapped with heating wires
sample chamber
8 pin electric feed-through for heaters and thermo-couple
feed through
valve
1 1/8"
1/4"
9/16"
5/16"
1/2"
1/4"
sample
O-ring
2 3/8"
9/16"
3/16"
Volatilized sample
machinable glass
aluminum target chamber
1 1/4"
1"
15/16" X-rays
4×30 Ω pencil heaters
thermo-couple
13/16"
11/16"
1/4"
Analyzer
O-ring

in the four corners of the target chamber for heating purposes. A thermocouple is also placed in the target chamber body for temperature measurement. Flexible 1/16" stainless steel tubing inside the sample chamber allows easy connection/disconnection of the tube from the target chamber. The other end of this 1/16" stainless steel tube is connected to a 1/4" stainless steel entrance tube by a Kovar seal which minimizes heat transfer from the stainless steel tube to the sample chamber. Tube heating inside and outside the sample chamber is accomplished with 12' of electrically insulated nichrome wire (2.66Ω/foot) bifillar wrapped around the tubes. Electrically insulated feed-throughs allow the entry of the leads for the heating assembly and thermocouple. Binding energies for compounds such as N_2, O_2 and 2-aminopyridine determined with this heated-inlet assembly reproduced values measured at room temperature with the standard gas cell supplied as standard equipment indicating that no anomalous field-effects of the heaters and nichrome wire were influencing the binding energy values. Utilizing this assembly temperature of up to 200°C could routinely be reached although in principle temperatures greater than 250°C should be attainable.

Spectral measurements

XPS spectra were determined on gaseous samples using a neon Auger line[37] as calibrant. The reported E_B values are the average of at least three calibrated runs in which the sample and the calibrant were measured alternately, and each has a precision of ± 0.03 eV unless otherwise noted. For each sample at least two spectra were scanned for a 12 eV range and one spectrum for a 24 eV range; each spectrum was computer stored in 100 or 200 channels. The experimental data were then least-squares analyzed with an ELSPEC program[40] assuming Gaussian peaks and the XPS spectra shown in this thesis were computer plotted using a PLOTTO program[41].

In the UV pes studies, all spectra were measured in the gas phase and were calibrated against the argon $^2P_{1/2}$-$^2P_{3/2}$[18] (E_K are 5.281 and 5.459 eV respectively) lines which had a resolution of 25-35 meV during operation. Spectra were computer stored in 1006 channels for a 10 eV scan and peak positions were determined from an intensity vs channel number listing. Each ionization energy value reported the average of at least three calibrated runs and has a precision of ± 0.02 eV unless otherwise stated.

CHAPTER II

DETERMINATION OF THE PREFERRED SYMMETRY OF THE HYDROGEN-BONDED ENOL FORMS OF SOME DIKETONES IN GAS PHASE

INTRODUCTION

In recent years, the question concerning the symmetry of the hydrogen-bonded enol form of malonaldehyde (MA) proved to be an active area in both experimental and theoretical chemistry (equation 5).

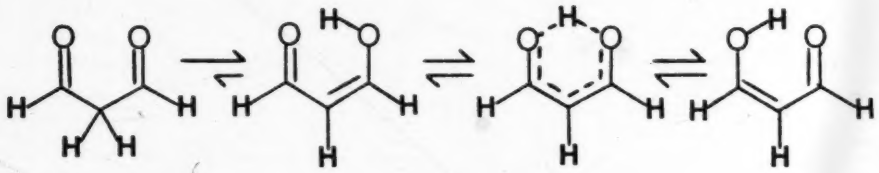

(5)

C_S C_{2V} C_S

The first theoretical calculation on MA was done by Schuster[42] using semi-empirical CNDO/2 methods[43-45] with a fixed geometry of the carbon molecular backbone. This calculation showed an energy difference of 0.5 kcal/mol between the C_S and $C_{2\nu}$ forms with the C_S form being the more stable structure. The two O---H distances were found to be 1.13 Å and 1.33 Å respectively. Recently, Roos et al[46] reinvestigated the MA question by performing *ab initio* calculations on the intramolecularly H-bonded enols with geometry optimization. Based on all the

available X-ray and electron diffraction data on analogous β-dicarbonyl compounds[47-50], MA was considered[46] to be planar. The ratios between angles a:b, c:d, e:f were kept constant and equal to the corresponding values determined by electron diffraction[50] on the enol form of acetylacetone. The result of this calculation agreed

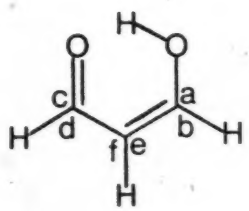

1a

with that of Schuster's[42] with the C_s form being 11.47 kcal/mol more stable than the C_{2v} form. Independently, Morokuma and Isaacson[51] employed both semi-empirical, INDO, CNDO/2 and *ab initio* methods[52] to determine the most stable enol form of MA. They investigated the dependence of the shape of the potential surface on the O---O distance and found that when the O---O separation was less than 2.3 Å, a single minimum corresponding to the C_{2v} form was obtained whereas a double minimum corresponding to an asymmetric enol form was observed when the O---O distance was greater than 2.3 Å. They suggested that Schuster's[42] prediction of an asymmetric MA enol was due to the lack of geometry optimization in his calculation since they demonstrated the dependence of the symmetry on the O---O separation

in both semi-empirical and *ab initio* calculations. However, these authors[51] could not make a conclusive prediction as to whether the enol should have a symmetric H-bond because the CNDO/2 and INDO methods tend to underestimate the H-bonded O---O distance[53,54], and the *ab initio* study they had performed did not involve extensive geometry optimization which included back-bond structural changes.

Del Bene and Kochenour[55,56] carried out other *ab initio* calculations on both the C_s and C_{2v} symmetry forms with geometry optimization. The calculations predicted that the C_s forms is more stable than the C_{2v} form by 6.6 kcal/mol. Although both this study and the one made by Roos[46] support the greater stability of the C_s form, both results had been obtained with limited basis sets, and neither study had taken into account correlation energy corrections, which would be greater for the C_{2v} form. Hence the determination of the favorable symmetry form is sensitive to the parameters used in the calculation. They suggested that the small energy difference between the C_s and C_{2v} forms probably allowed easy interconversion of the two structures.

Other work concerning MA was done by Fukui et al.[57] using CNDO/2 methods to calculate the proton location on the reaction coordinate and the rate of proton exchange between the two C_s forms via a C_{2v} intermediate. They

calculated the rate of proton transfer to be 9.77 x 10^{13} sec^{-1} and the barrier between the C_S and C_{2v} forms of 1.04 kcal/mol with the C_S form being the more stable. They suggested an ellipse-like orbit for the proton motion based on their calculated reaction coordinate. The possibility of proton tunneling[22] between the two C_S forms of MA enol had been examined by Fluder and de la Vega[58] who performed *ab initio* calculations[59,60] to obtain an energy profile for this molecule. The calculated tunneling frequency of the interconversion was found to be 2.25 x 10^{10} sec^{-1} which is an order of magnitude less than that obtained experimentally by microwave spectroscopy[61]. Their results concerning the energies and geometries for the initial and final asymmetric structures (C_S) as well as the symmetric intermediate (C_{2v}) coincide with those obtained by Roos[46]. In view of the previous inconclusive calculations[42,46,51,55-58] on the symmetry of MA enol, Fernandez-Alonso et al.[62] made detailed calculations of the potential energy of MA as a function of the O---O distance using CNDO/2, INDO, and *ab initio* methods. The calculations were carried out by varying the O---O distance from 2.1 to 2.7 Å with full geometry optimization. The results from each method were used to plot a potential energy vs O---O distance curve; in all cases C_{2v} form was favored for short O---O separa-

tion (< 2.3 Å) while the C_S form dominated at long O---O distance (> 2.3 Å). Here they demonstrated that the comparison of the energy between the two symmetry forms is not necessarily the determining factor in deciding which is the more favorable one; it is the variation in the O---O separation that decides the symmetry of the molecule.

Early experimental work[63-67] on MA was mainly done in solution in which the enol conformation varied depending on the solvent used. It had been shown by ^1H NMR[64] that MA exists as a *trans* enol in water and hydroxylic solvents and as an intramolecularly H-bonded *cis* enol in less polar chlorinated hydrocarbons. A gas phase UV-photoelectron study[68] indicated that MA exists predominantly in its enol form. However, no comment was made concerning the preferred symmetry of this molecule. Recently Wilson et al.[61] reported the microwave spectra of a number of isotopic species of MA and suggested that the molecule has a symmetrical double minimum potential surface with a relatively low barrier between the two minima so that rapid proton tunneling can occur between the two asymmetric forms. This explanation is also preferred by Seliskar and Hoffmann[69] who measured the electronic transitions of MA. However, each of these experimental results still was not able to conclusively solve the symmetry question

of the MA enol. Related dicarbonyl compounds, 1c, 1d, 3a, 4 and 5, which can also exist in either C_{2v} or C_s enol forms with five-, six-, and seven-membered H-bonded rings, and are also of interest since the O---O separations and O—H---O angles are altered by the molecular structure. To our knowledge, there have been no theoretical calculations on compounds 3a, 4 and 5, possibly due to their larger sizes when compared to MA.

A number of different techniques have been employed in order to determine the preferred symmetry of tropolone (3a). Early solution IR studies[70,71] suggested an asymmetric structure complimenting results obtained by ^{1}H[72,73] and ^{13}C[74,75] NMR studies in which a rapid proton exchange is believed to occur between two asymmetric C_s structures through a symmetric C_{2v} intermediate. This process appears to be faster than the NMR time scale at room temperature, but in principle, one should be able to observe the C_s structure of 3a by measuring its NMR spectrum at low temperature. We have attempted variable temperature ^{13}C NMR studies[76] on this compound but no change in the spectrum was found at -130°C when compared to that measured at room temperature.

The X-ray crystal structure[77,78] indicated two different C-O bond lengths which is consistent with an asymmetric structure of tropolone. However, the X-ray

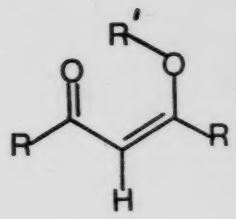

	R	R′
1a	H	H
1b	H	CH_3
1c	CH_3	H
1d	CF_3	H

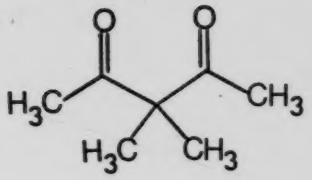

2

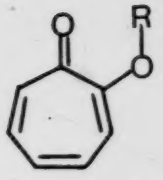

	R
3a	H
3b	CH_3

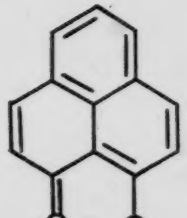

4

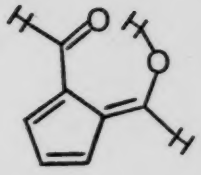

5

analysis also revealed that the crystal is composed of dimers, so this experimental result cannot be used to confirm the preferred symmetry of the individual monomer. On the other hand, gas phase studies should provide information about the intrinsic properties of the individual molecule.

Electron diffraction data[79] gave two slightly different C-O distances (R_{C-O} = 1.34 Å, $R_{C=O}$ = 1.26 Å) supporting a C_S symmetry for 3a. Additionally, the near UV spectroscopic data of Alves and Hollas[80,81] favored rapid equilibrium between the two C_S structure via a C_{2v} intermediate. Thus, the question of the preferred symmetry of 3a is still an ambiguous one based on the experimental evidence[70-81] presented above.

As for compound 4 (9-hydroxy-2-phenalenone) IR studies[82] in solution and solid states showed no absorption due to the O-H stretching vibration. Our variable temperature ^1H and ^{13}C NMR studies[83] appear to support C_{2v} symmetry for 4 at ambient temperature and reveal no significant change down to -130°C. However the possibility of a rapid interconversion between two C_S forms cannot be eliminated. A recent X-ray crystallographic study[84] shows 4 to have a short O---O separation (< 2.5 Å). The only gas phase work on this compound was done by Peel et al.[85] who studied the UV pes of 4 and assigned the spectra with the aid of

SPINDO[86] calculations. No discussion on the preferred symmetry of 4 was made by these authors[85].

A Drieding model of the 6-hydroxy-2-formylfulvene (5) shows that the O—H---O moiety is almost linear (confirmed by X-ray); this suggests that the proton movement between the two oxygens should be relatively facile. Thus it is a very demanding case for the determination of the preferred symmetry. Early ^{1}H NMR data[91] at ambient temperature and our variable temperature ^{1}H and ^{13}C NMR studies[83] down to -130°C are consistent with a C_{2v} symmetry form of 5 or two rapidly interconverting C_s forms. The IR spectrum[91] was interpreted as arising from two equilibrating C_s forms. Gas phase microwave data for 5 and its deuterated analogues are interpreted as arising from either a C_{2v} form or a C_s form with the proton oscillating between the terminal oxygens at a rate faster than 2×10^{12} sec^{-1}[92]. Solid state X-ray and neutron diffraction data[93] give a slightly asymmetric H-bond with O-H distances of 1.343 and 1.214 Å, but it is not certain to what extent crystal packing forces perturb the individual molecular symmetry.

Because of the lack of experimental evidence to unambiguously confirm the preferred symmetry of the above-mentioned compounds (1a, 1c, 1d, 3a, 4 and 5), we decided to attack this particular question using the

technique of X-ray pes. The advantages of this technique over others for this particular problem are the following. First, its time scale for measurement is short enough (10^{-16} sec)[28] to freeze out fast proton transfer between the two oxygen atoms of the enol (suggested to be > 2 x 10^{12} sec^{-1} for 5[92]). Secondly, the simplicity of the pe spectrum allows the unambiguous assignment of the E_B peaks. Consequently, the preferred symmetry of the enols can be identified without any interpretive difficulty. Hence, the pes measurement should provide the most definite evidence for the preferred molecular symmetry of 1-5. We have also conducted variable temperature NMR studies on MA and its deuterated analogue (D-MA), with the aim of retarding the proton exchange process so that the frozen C_S form might be observed. From the measured coalescence temperature, the interconversion barrier between the two C_S forms via the C_{2v} form (which is possibly reduced by proton tunneling[22]) can be determined. In the following discussion, the results concerning these questions will be presented.

RESULTS AND DISCUSSION

Shown in Table I are the O_{1S} E_B for the dominant peaks in the X-PS spectra of 1-5 and their computer deconvoluted spectra are presented in Figures 4-12. The assignment of the observed peaks is based on the argument that the symmetric C_{2v} enol form of these molecules should show a single O_{1S} ionization from the two equivalent oxygens. The asymmetric C_S form should give rise to two different ionizations of 1:1 area ratio, assuming equal ionization cross-sections for the inequivalent oxygens, which may lead to either considerably broadened or even separated peaks. It is therefore expected that the nonenolizable, but symmetric dimethylacetylacetone (2) should give a single O_{1S} ionization peak. Indeed this is observed to be the case as indicated in Figure 4. On the other hand, two O_{1S} ionization peaks of 1:1 area ratio are observed for β-methoxyacrolein (1b) which has two inequivalent oxygens (Figure 5). Based on the argument given above, the results for the enols 1a, c,d, 3a, 4 and 5 are analyzed as follows.

In every observed spectrum, there is at least one low intensity peak on the higher E_B side of the main O_{1S} ionization peaks. One might suspect that these enols could possibly exist in equilibrium between the C_S and the C_{2v} forms to give rise to at least three

Table 1. O_{1s} Binding energies for dicarbonyls.[a,b]

Compound	Peak[e]	Relative Area	E_B (eV)	FWHM[c]
Malonaldehyde[d] (1a) ~~	1	0.16±0.05	542.52	1.60
	2	0.96±0.05	539.71	1.49
	3	1.0 ±0.04	538.14	1.62
3-Methoxyacrolein[d] (1b) ~~	1	0.31±0.03	541.74	2.27
	2	1.0 ±0.04	539.79	1.26
	3	0.91±0.02	537.53	1.52
Acetylacetone[d] (1c) ~~	1	0.1 ±0.01	541.68	1.86
	2	1.43±0.08	538.83	1.95
	3	1.0 ±0.11	537.33	1.65
Hexafluoro-acetylacetone[d] (1d) ~~	1	0.37±0.03	543.06	2.24
	2	1.47±0.17	540.48	1.75
	3	1.66±0.16	539.03	1.91
3,3-Dimethyl-acetylacetone (2) ~	1	1.0	538.08	1.77
Tropolone (3a) ~~	1	1.0	539.27	1.72
	2	0.71± .05	536.95	1.46
2-Methoxytropone (3b) ~~	1	1.0	539.60	1.82
	2	0.71±0.03	537.08	1.63
9-hydroxyphenalenone (4) ~	1	1.0	539.23[f]	2.88
	2	0.99±0.03	536.64	2.88
6-Hydroxy-2-formylfulvene[d] (5) ~	1	0.14±0.02	543.45	2.16
	2	0.15±0.02	541.39	1.61
	3	1.0	539.07	1.69
	4	1.1 ±0.12	537.74	1.68

a. Referenced to a Ne Auger line at 804.56 eV kinetic energy[37].

b. Binding energy values reported are the average of at least three runs and have a precision of ±0.03 eV.

continued.....

Table 1 (continued)

c. Full width at half maximum height.

d. Low intensity peaks (assigned as peaks 1 for $\underset{\sim}{1}a$, $\underset{\sim}{1}b$, $\underset{\sim}{1}c$, and $\underset{\sim}{1}d$, and peaks 1 and 2 for $\underset{\sim}{5}$) are believed to arise from shake up phenomena (see text).

e. Each compound investigated shows the presence of one or more low intensity peak to the high binding energy side of the main ionization lines. The Table includes this peak only if its intensity is greater than 10% of the main lines, but it is clearly present in every case (cf. Figs. 4-12).

f. Average of two calibrated runs; precision ±0.06 eV.

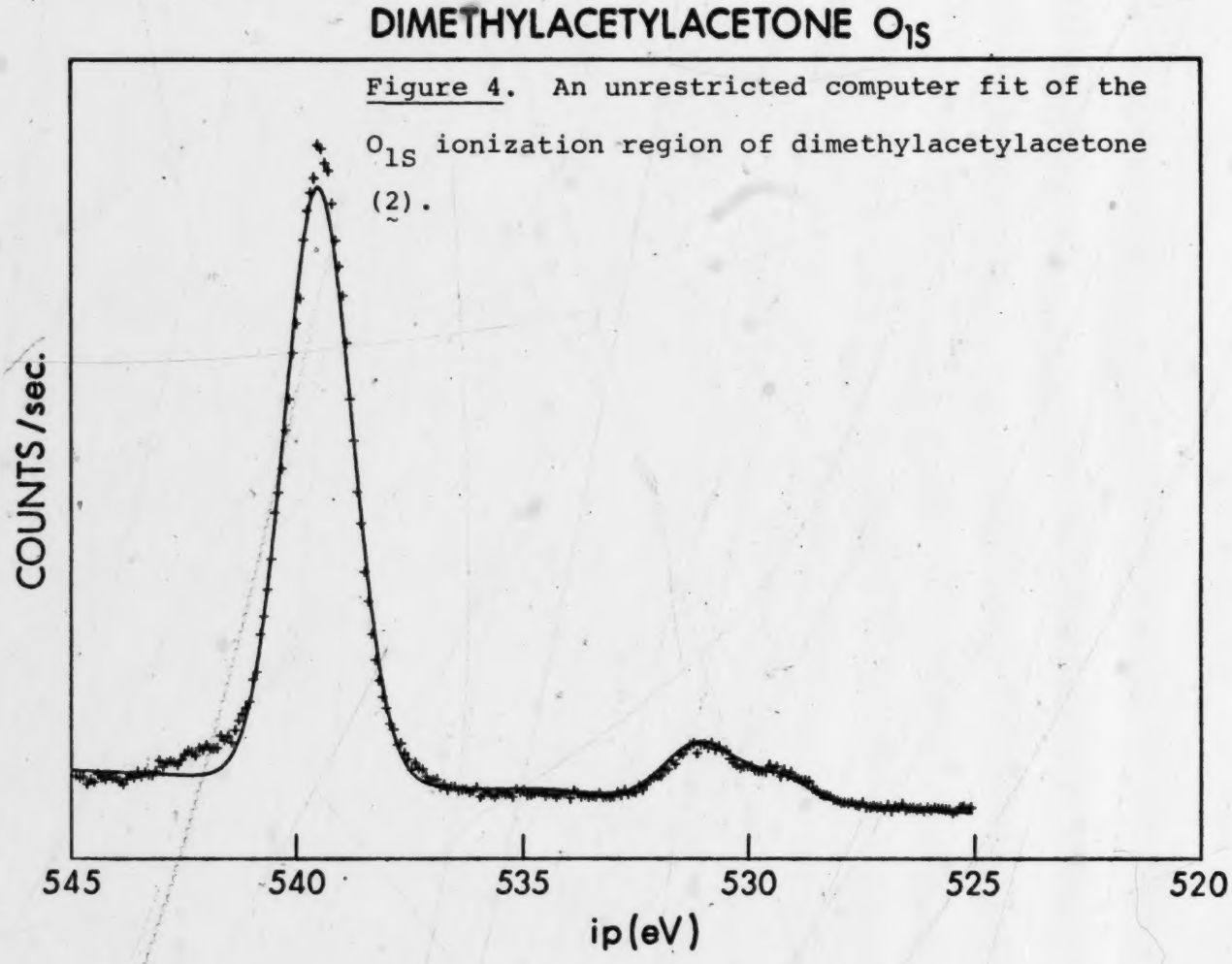

Figure 4. An unrestricted computer fit of the O_{1S} ionization region of dimethylacetylacetone (2).

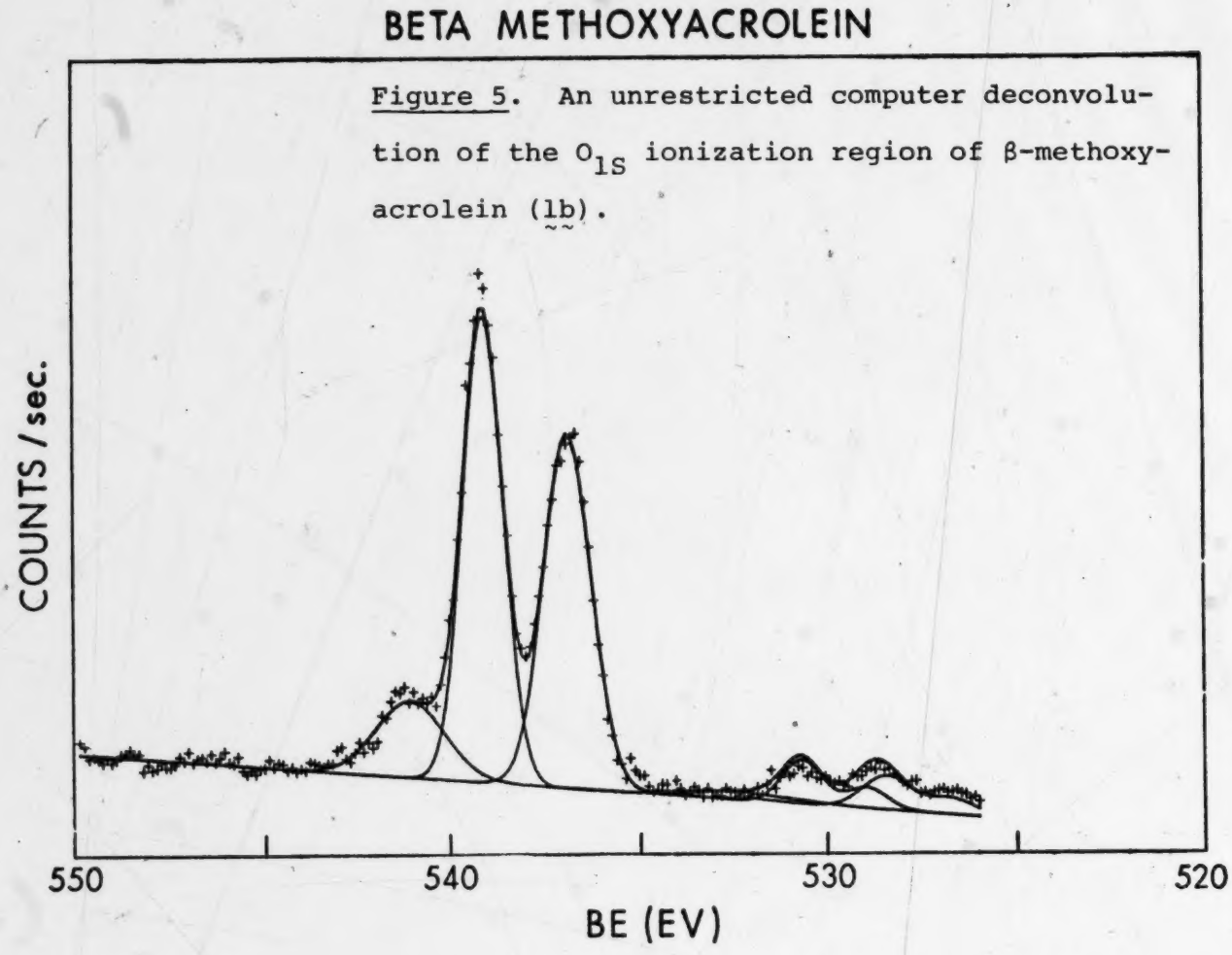

Figure 5. An unrestricted computer deconvolution of the O_{1S} ionization region of β-methoxyacrolein (1b).

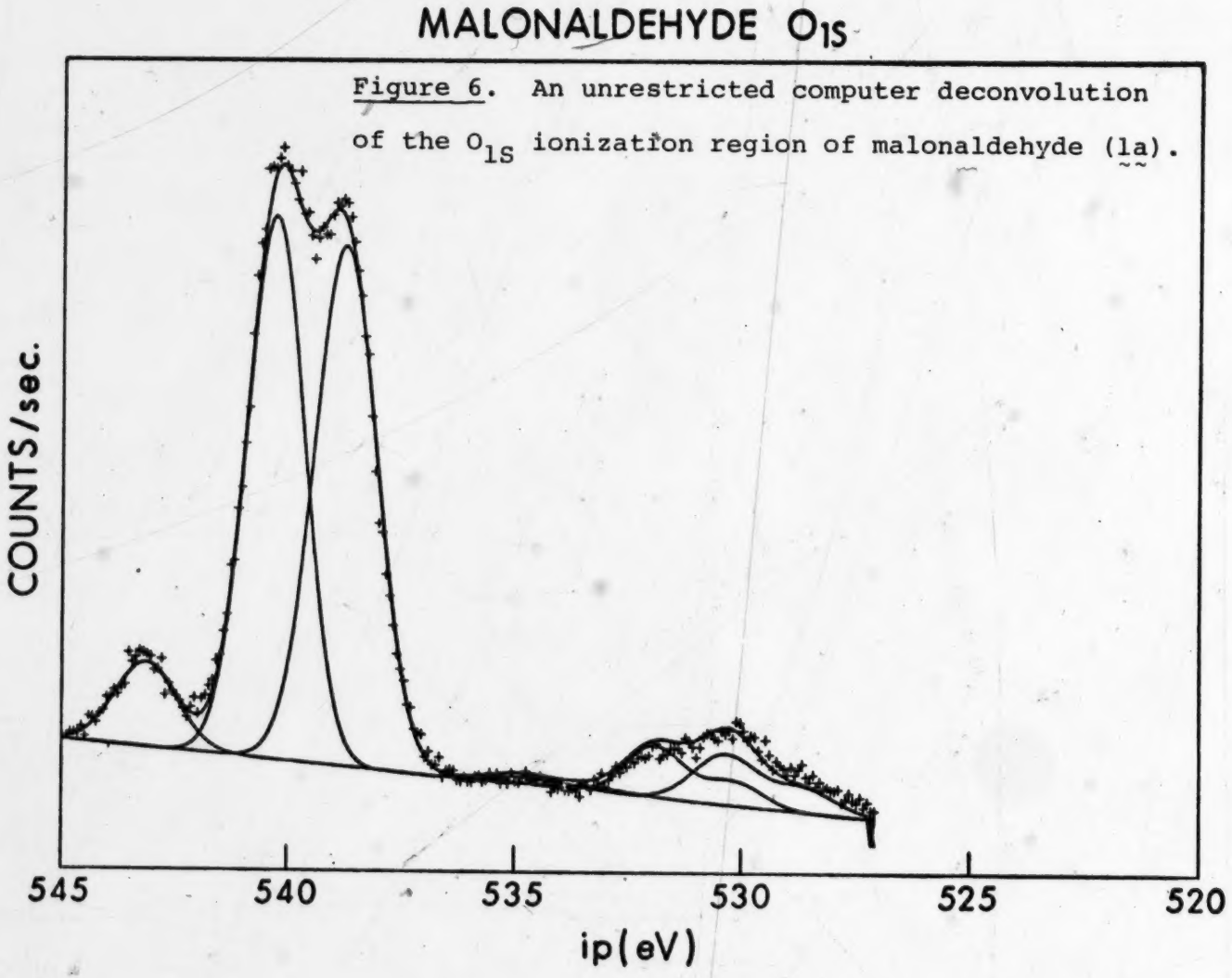

Figure 6. An unrestricted computer deconvolution of the O_{1S} ionization region of malonaldehyde (1a).

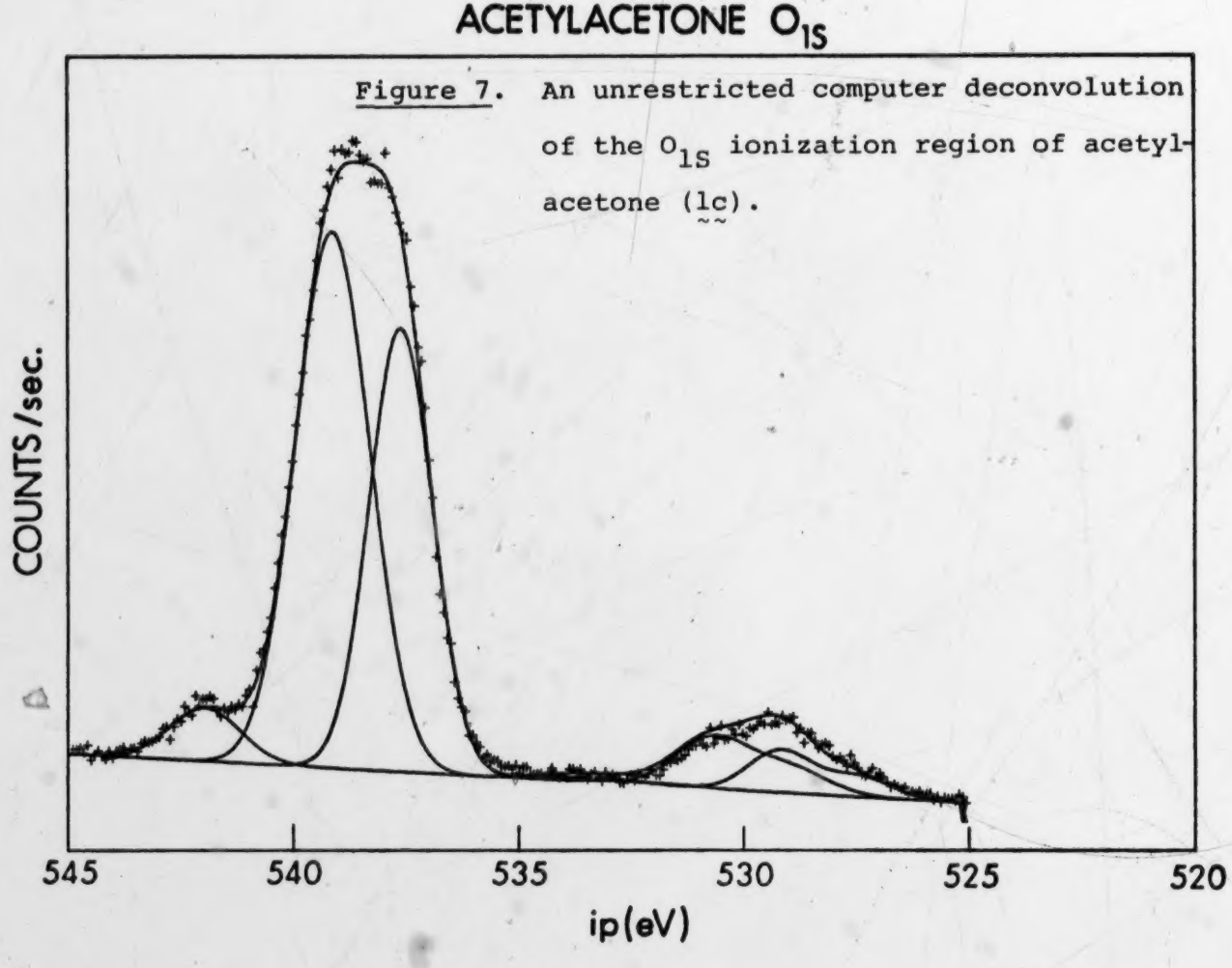

Figure 7. An unrestricted computer deconvolution of the O_{1S} ionization region of acetylacetone (1c).

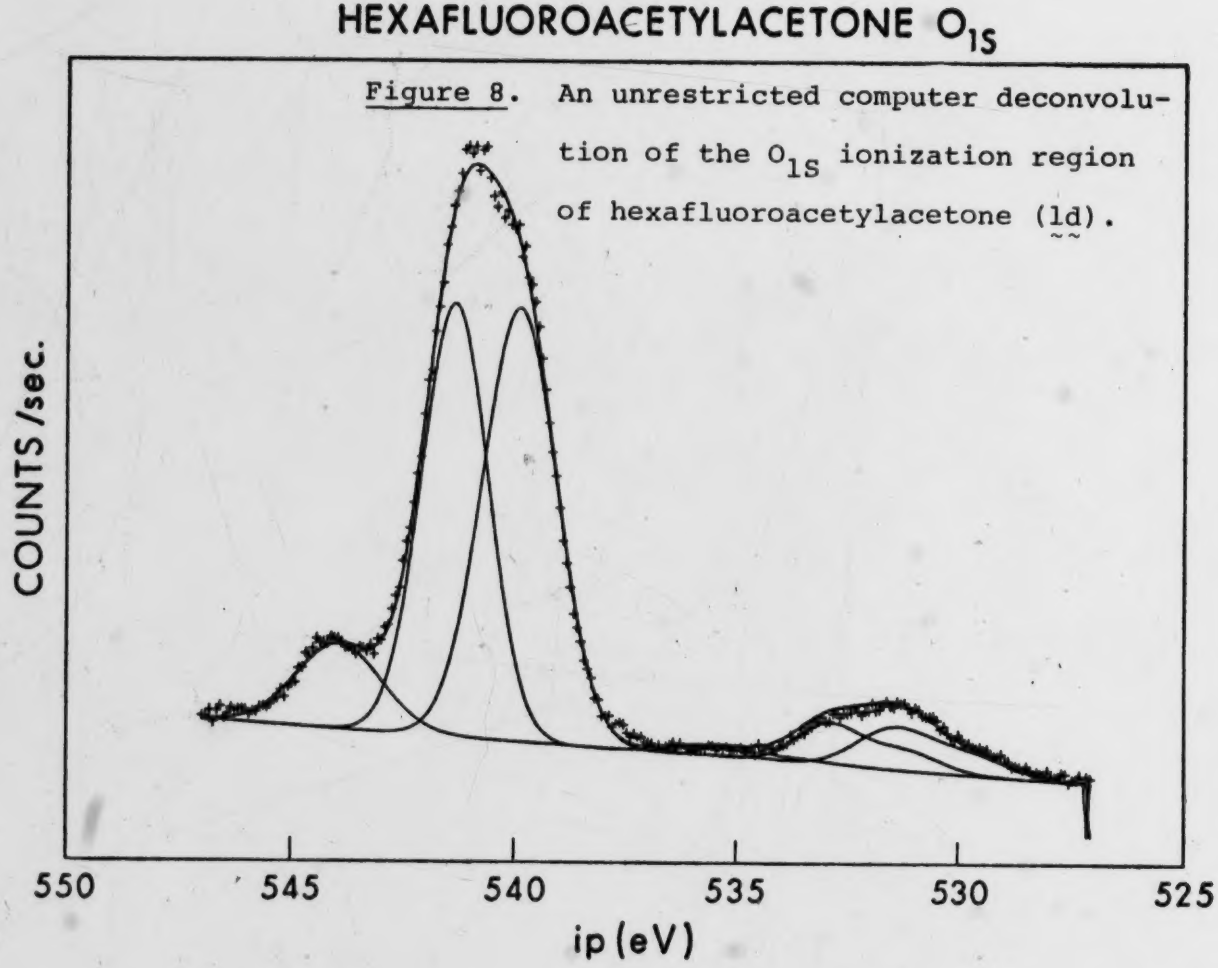

Figure 8. An unrestricted computer deconvolution of the O_{1S} ionization region of hexafluoroacetylacetone (1d).

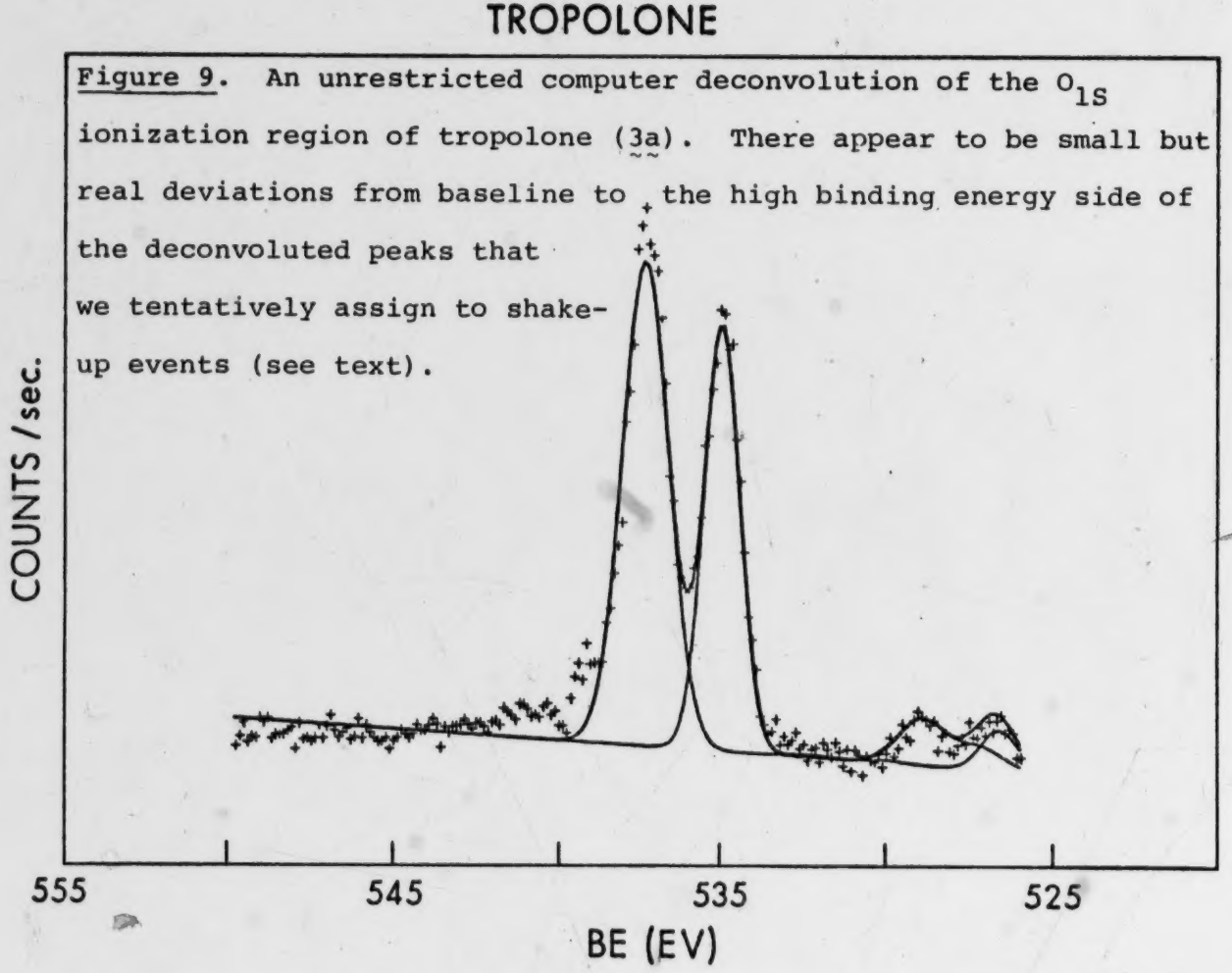

Figure 9. An unrestricted computer deconvolution of the O_{1S} ionization region of tropolone (3a). There appear to be small but real deviations from baseline to the high binding energy side of the deconvoluted peaks that we tentatively assign to shake-up events (see text).

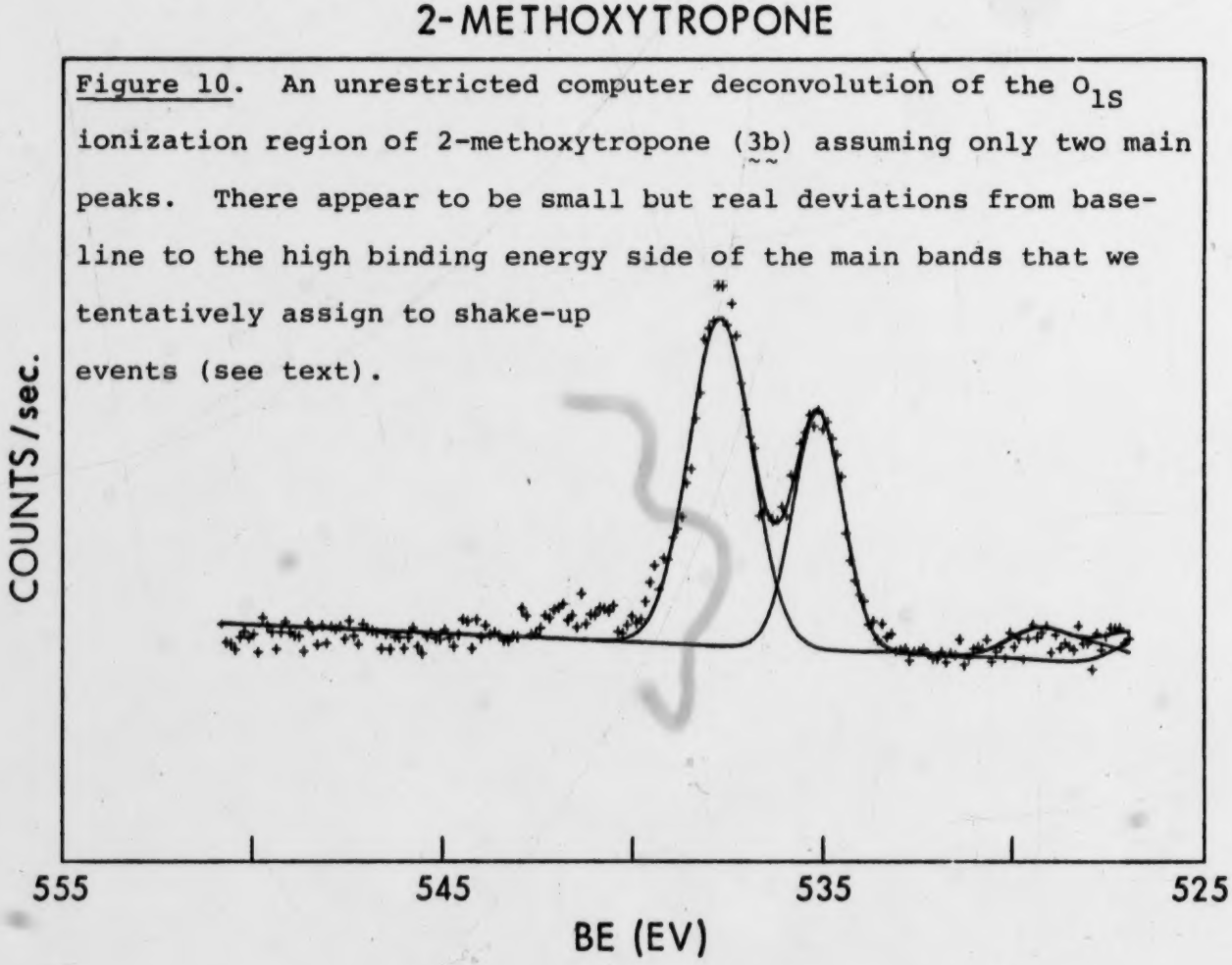

Figure 10. An unrestricted computer deconvolution of the O_{1S} ionization region of 2-methoxytropone (3b) assuming only two main peaks. There appear to be small but real deviations from base-line to the high binding energy side of the main bands that we tentatively assign to shake-up events (see text).

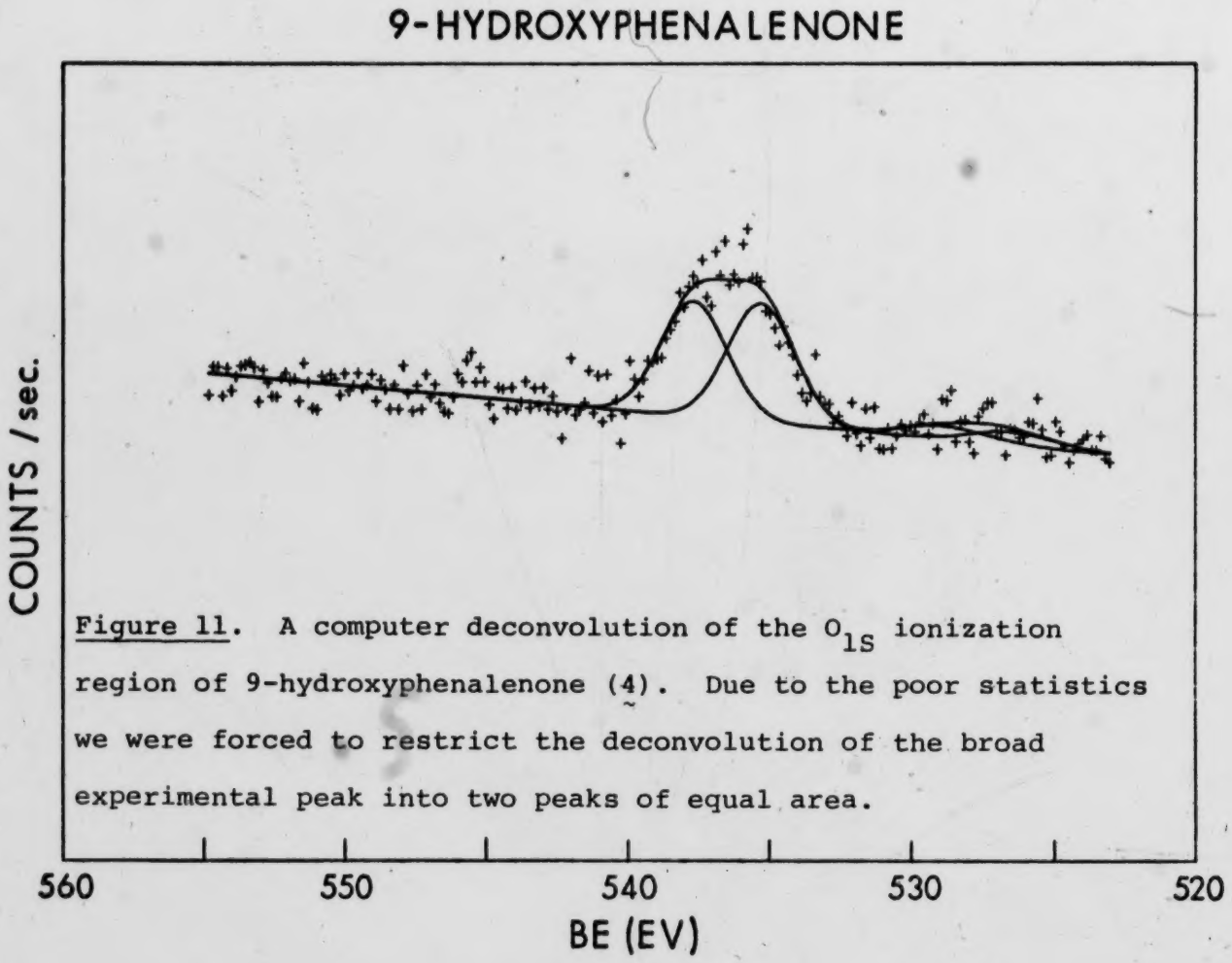

Figure 11. A computer deconvolution of the O_{1S} ionization region of 9-hydroxyphenalenone (4). Due to the poor statistics we were forced to restrict the deconvolution of the broad experimental peak into two peaks of equal area.

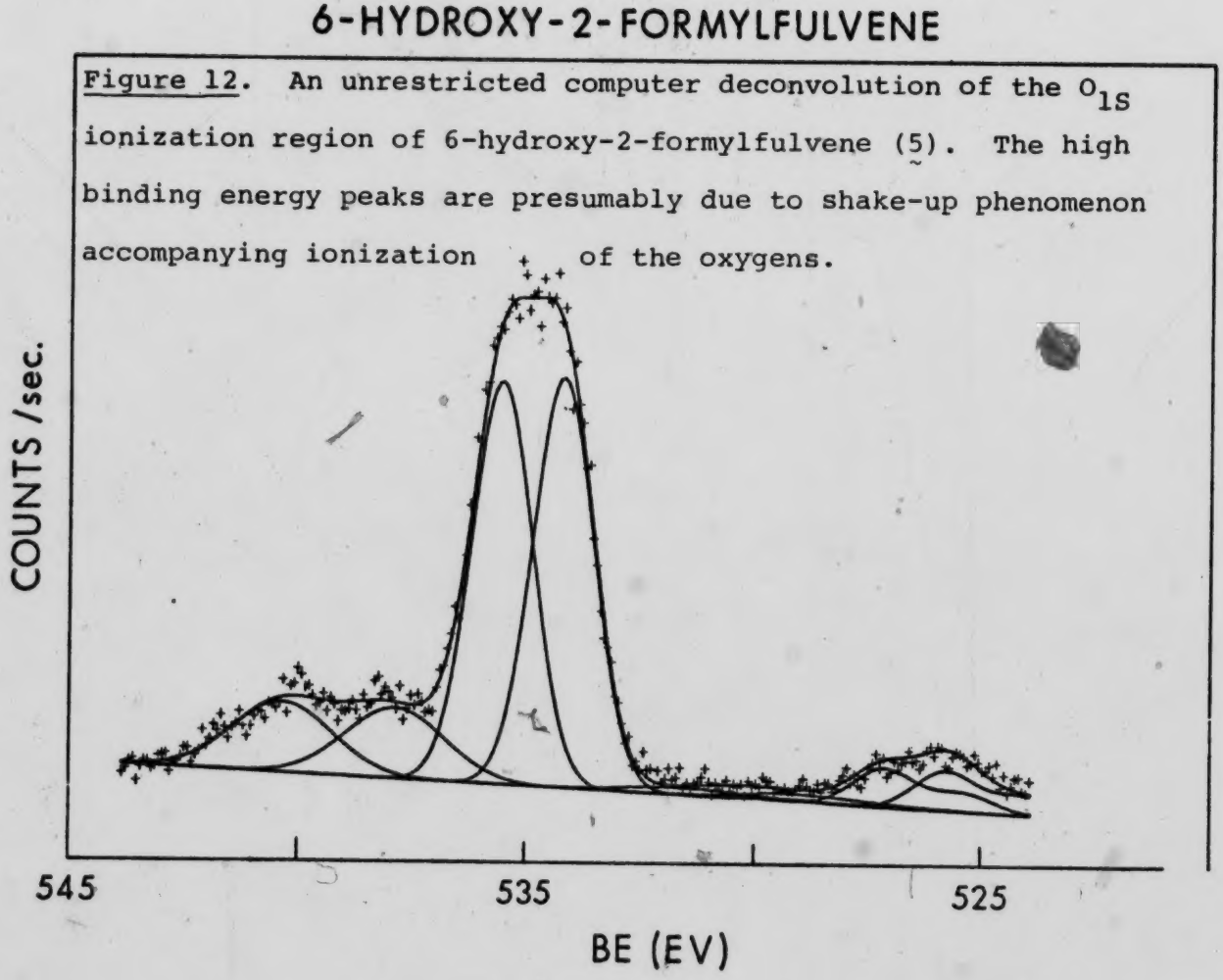

Figure 12. An unrestricted computer deconvolution of the O_{1S} ionization region of 6-hydroxy-2-formylfulvene (5). The high binding energy peaks are presumably due to shake-up phenomenon accompanying ionization of the oxygens.

distinct O_{1S} peaks, two from the C_S form and one from the C_{2v} form. In fact, this was suggested by Fernández-Alonso et al[62] for MA (1a) and hexafluoro-acetylacetone (1d) based on our published data. This possibility can be eliminated based on several lines of evidence. First of all, even the nonenolizable dimethylacetyl-acetone (2) shows such a peak on the higher E_B side of the major peaks, as can be seen in Figure 4, although its intensity is very low. Secondly, the O_{1S} E_B of the C_{2v} form is expected to be somewhere between the two O_{1S} E_B of the C_S structure since the two equivalent oxygens of the C_{2v} form are supposed to be intermediate between a carbonyl oxygen and a hydroxyl oxygen. As the observed low-intensity peaks always lies at the higher E_B side of O_{1S} peaks of the C_S form, it could not possibly arise from the C_{2v} form. Thirdly, the asymmetric β-methoxyacrolein (1b) also shows at least one similar low intensity ionization peak (see Figure 5). Hence it is very unlikely that this low-intensity peak comes from the C_{2v} symmetry form as suggested[92]. Probably the occurrence of this peak is the result of the so-called "shake-up" phenomenon[8] in which an electron in a high-lying occupied M.O. is promoted to a low-lying virtual orbital during core ionization. Because of this simultaneous core electron ejection and valence electron excitation, the observed E_K of the ejected core

electron appears to be lower than that observed in the absence of shake up processes. This phenomenon has been observed for compounds such as carbon suboxide[94] (O=C=C=C=O), furan[95], tetrahydrofuran and diazocyclopentadiene[96].

In the case of acetylacetone (1c) the O_{1S} ionization region was deconvoluted into two major peaks of approximately 6:4 area ratio (Figure 7). However, there is evidence that 1c is not completely enolized in the gas phase. Early gas phase IR studies[97] revealed the presence of both a keto-carbonyl band (1725 cm^{-1}) and an enol-carbonyl band (1625 cm^{-1}). Recent electron diffraction data[49] gave the keto-enol ratio of roughly 1:2 at 105°C. This is supported by the results from the variable temperature UV pes studies[98]. Accordingly the observed XPS spectrum of 1c is most likely a result of the ionization from both keto and enol forms. The observed ionization region may consist of three overlapping peaks, one from the keto-form and the others from the enol-form which is probably asymmetric although this experimental evidence is not as clear cut as in the other cases.

Both MA[68] (1a) (Figure 6) and hexafluoroacetylacetone (1d)[50] (Figure 8) have been shown to exist completely in their enolized form in the gas phase. The present XPS spectra show distinctly two dominant O_{1S}

ionization peaks of 1:1 ratio which can only be consistent with an asymmetric enol having two inequivalent oxygens. The present result for 1d contrasts the assumed symmetric location of the proton derived from the electron diffraction study[50].

Tropolone (3a) represents an interesting case since it demonstrates that an unequal peak area in the two O_{1S} ionization may not necessarily be due to ionization from two or more species. A previous report[99] for this molecule showed that the XPS spectrum consists of a broad O_{1S} peak (FWHM = 2.7 eV) centred at 532 ± 0.2 eV and was interpreted as arising from inequivalent oxygens. However it appears that the measurement was made in the solid state. The present XPS spectra of 3a (Figure 9) and its O-methylated derivative, 3b (Figure 10), show two unequal O_{1S} peaks of area ratio 1:0.7, which seems to suggest a C_S symmetry structure of 3a. The inequivalent area ratio of the O_{1S} peaks can be explained with two alternatives. It may be caused by the preferential shake-up process of the lower E_B oxygen which detracts from its intensity. This process was observed by other workers for carbon suboxide[94], nitrous oxide[100] and N,N-dimethylnitrosamine[101]. Another explanation is the possibility of at least one shake-up peak hidden under the higher E_B ionization which then appears to have higher intensity than the

lower E_B peak.

Due to involatility, the XPS spectrum of 4 was obtained by heating the inlet system to 50°C. Our experiment using fourier-transform (FT) IR on a dilute solution of 4 in tetrachloroethylene has shown no significant spectral change when the sample is heated from room temperature to 100°C and shows no definite C=O or O-H stretches. Assuming that this is applicable to the gas phase, 4 should still be intramolecularly H-bonded at 50°C. Figure 11 shows the XPS spectrum of 4 which exhibits poor statistics. Nevertheless the FWHM as well as the satisfactory deconvolution into two equal area peaks seems to suggest an asymmetric C_S form for 4.

As for 6-hydroxy-2-formylfulvene (5), the XPS spectrum (Figure 12) was deconvoluted into two equal intensity major peaks and two minor peaks, also of equal intensity. The former ones come from the ionization of the inequivalent oxygens and the latter ones which have higher E_B, are believed to arise from some shake up phenomeneon by analogy with our previous results.

On the basis of the above information it seems clear from the XPS spectral data that the enolized diketones investigated are predominantly (if not exclusively) in an asymmetric C_S form. Recently, Maksic et al[102] based on their semi-empirical calculations on 1a,c and d

suggested that the carbonyl oxygen is easier to ionize than the hydroxyl one. This is reasonable since the former has a higher charge density than the latter one. Assuming that this is true, the higher E_B ionization peak in the O_{1S} XPS spectra of 1-5 should arise from the hydroxyl oxygen and the lower one from the carbonyl oxygen.

Variable temperature ^1H NMR studies on MA and D-MA

It has been shown by previous ^1H NMR studies[63,64,66,67] that MA exists in transoid enol form in aqueous or hydroxylic solvents and in cisoid enol form in non-polar, chlorinated hydrocarbons. It has also been demonstrated that the presence of very small amounts of impurities in the chlorinated hydrocarbon could change the conformation of MA from *cis*-enol to *trans*-enol[63]. Nonetheless, the *trans*-enol form in hydroxylic solvents appears to be symmetric based on ^1H NMR data. The mechanism of how the terminal hydrogens (H_A and $H_{A'}$, in structure 6a) become equivalent is of interest.

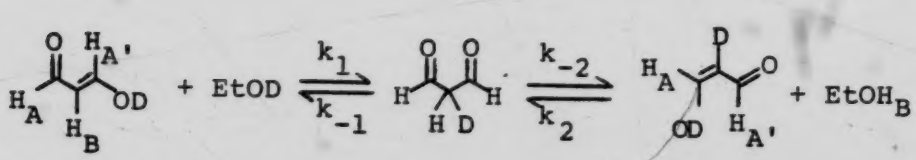

6a 6c 6b (6)

Equation 6 shows one of the possible mechanisms in which the enol form 6a ketonizes and then re-enolizes to 6b. To test this possibility, the rate of exchange of the methine H for D (which can only occur through some keto form) was investigated under pseudo-first order conditions in deuterated ethanol at 303°K by NMR techniques[103]. Assuming a steady-state condition and the reversal of 6b to 6c is negligible[104], the rate expression for this ketonization-enolization process is represented by equation 7.

$$\frac{-d[6a]}{dt} = \frac{d[6b]}{dt} = \frac{k_1 k_{-2}[6a][EtOD]}{k_{-1} + k_{-2}} = k_{obs}[6a] \qquad (7)$$

While the magnitudes of k_{-2} and k_{-1} are not known, they are related by a primary isotope effect[105]. The maximum $k_{-2}:k_{-1}$ ratio is roughly 7:1 and by using this relationship equation 7 can be simplified into the following form.

$$\frac{-d[6a]}{dt} = \frac{d[6b]}{dt} = \frac{k_1[6a][EtOD]}{1.14} = k_{obs}[6a] \qquad (8)$$

On the other hand, if there is no primary isotope effect ($k_{-2} = k_{-1}$) equation 7 becomes

$$\frac{-d[6a]}{dt} = \frac{d[6b]}{dt} = \frac{k_1[6a][EtOD]}{2} = k_{obs}[6a] \qquad (9)$$

Nonetheless, both equations 8 and 9 indicate that k_{obs} is directly proportional to k_1 (rate constant for ketonization) which therefore serves as a good measure of the rate of ketonization. In order to determine k_{obs}, a plot of the concentration of 6a as a function of time t was made[106]. The [6a] was evaluated by calculating the ratio of the integrated area of 6a to the total integrated areas of both 6a and 6b, determined on the basis of H_A and $H_{A'}$. By determining the rate of disappearance of 6a, k_{obs} was found to be 1.7×10^{-3} sec^{-1} at 303°K.

After the completion of deuterium exchange (as indicated by the absence the methine hydrogen in the NMR spectrum of 6b), this same sample was subjected to variable temperature studies in order to determine the coalescence temperature of H_A and $H_{A'}$. At ambient temperature H_A and $H_{A'}$ are equivalent and appear as a ^2H-coupled singlet centred at δ8.52. Gradual cooling of the sample down to lower than 145°K causes this singlet to separate into two broadened singlets centred at δ9.38 and 7.67 which correspond to the formyl ($H_{A'}$) and hydroxyvinyl (H_A) proton, respectively[107]. The rate of equilibration of H_A and $H_{A'}$, (k_{eq}) is given by equation 10, where Δν is the difference in chemical shift between H_A and $H_{A'}$.

$$\frac{\Delta\nu}{k_{eq}} = \frac{1}{\pi\sqrt{2}} \text{ (at coalescence)}^{108} \qquad (10)$$

Comparison of k_{eq}, which is found to be 2.26×10^2 sec^{-1}, with k_{obs} shows the latter process is far too slow to account for the apparent equivalence of H_A and $H_{A'}$, as measured by NMR. Therefore, the present result seems to suggest some intermolecular proton transfer mechanism for the apparent equivalence of H_A and $H_{A'}$. It is found that the exchange process is not strictly first order in MA, since as the concentration of MA is reduced, the coalescence temperature is increased, so that very dilute solution show considerable broadening of the terminal C-H signals even at 25°C. It is also found that small quantities of acids, Hünigs base, and even solid Na_2CO_3 added to the NMR solution reduce the coalescence temperature and thus the exchange process must be very sensitive to trace catalysis by both acid and base. On the basis of the above observations, a mechanism for the proton transfer process of MA is proposed as shown in equation 11. A higher coalescence temperature at low concentration of MA is probably due to the slower exchange between MA and EtOD than between two or more MA molecules, the latter being more important at higher MA concentration.

For the intramolecularly H-bonded cis enol case which can be generated in a 1:1 mixture of $CFCl_3$-CD_2Cl_2, the ^1H NMR spectrum at ambient temperature shows a triplet centered at $\delta 5.68$ (J = 3.5 H, 1 H), a doublet

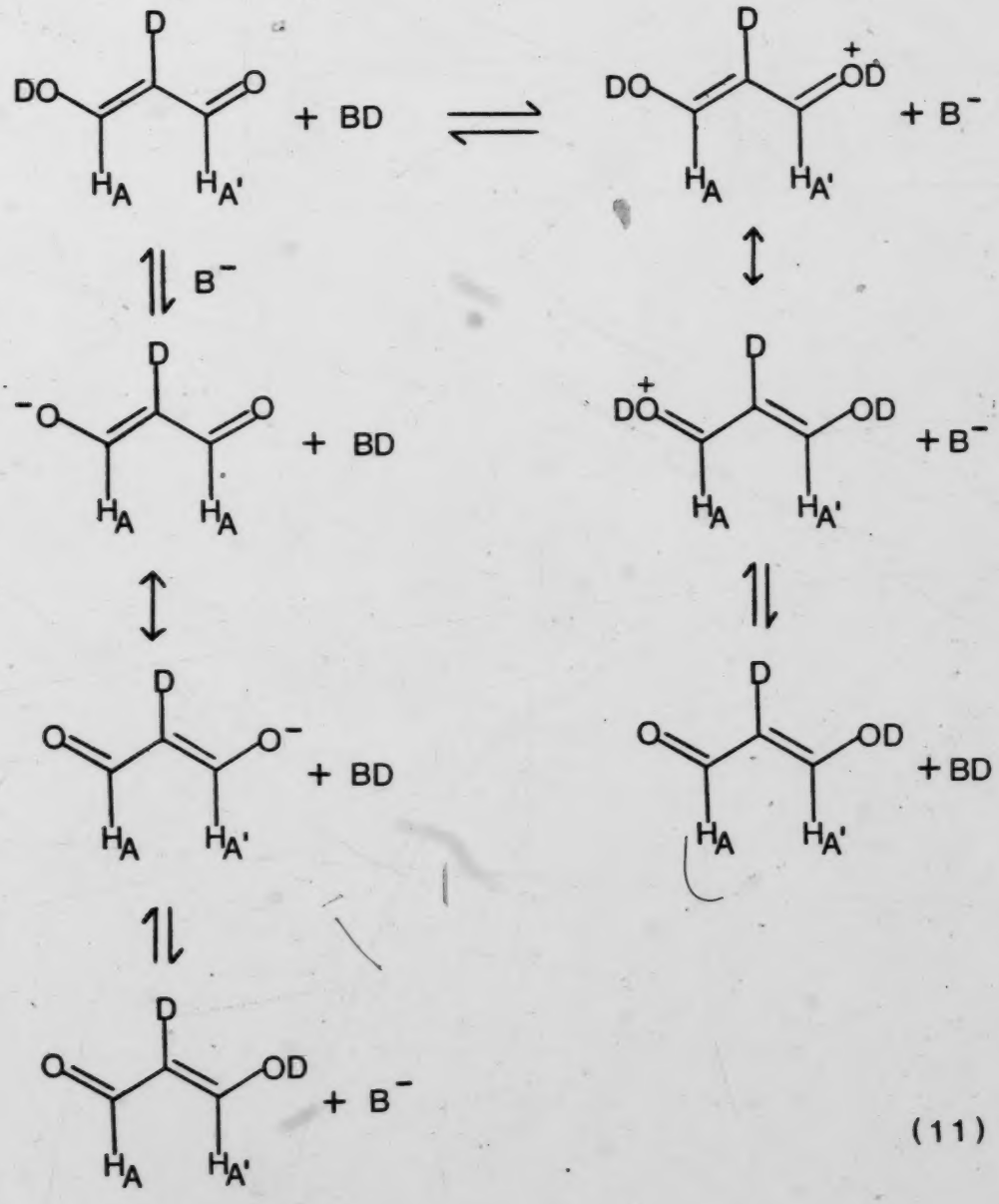

(11)

BD = ETOD , MA , acid

centred at δ8.37 (J = 3.5 Hz, 2 H) and no indication of a low-field intramolecularly H-bonded OH. At temperatures lower than 200°K, the spectrum reveals unambiguously an intramolecularly H-bonded OH triplet at δ16.60 (J = 6.1 Hz), coupled equivalently to the terminal hydrogens, which themselves appear as a doublet of doublets centred at δ8.37 (J = 3.5 Hz, J' = 6.1 Hz) (Figure 13). This small value of J demonstrates that MA, under these conditions, exists in a cisoid conformation. Nonetheless it appears as a C_{2v} symmetric structure on the NMR time scale and remains as such down to 133°K, where the solution freezes. No broadening of the terminal hydrogens' signal other than that attributable to viscosity effects was observed at low temperature. Assuming that the chemical shift difference between the formyl and hydroxyvinyl hydrogens in the cisoid form is the same as that in the transoid form, the upper limit for the barrier to interconversion of the two C_s form via a C_{2v} form is found to be 6.1 kcal/mol using equation 12[108] where $\Delta G^{\ddagger}$ is the activation

$$\Delta G^{\ddagger} = 2.303RT\ (10.319 + \log T - \log k_{eq}) \qquad (12)$$

energy in kcal/mol and T is the temperature in degrees Kelvin (°K).

A possibility exists that replacing OH by OD might slow down the D transfer between the oxygens because

Figure 13. The ^{1}H-NMR spectrum of malonaldehyde (1a) at 153°K in a solvent of 1:1 $CFCl_3$:CD_2Cl_2. The small peak at ~δ 6 is attributable to a spinning sideband from adventitious $HCDCl_2$.

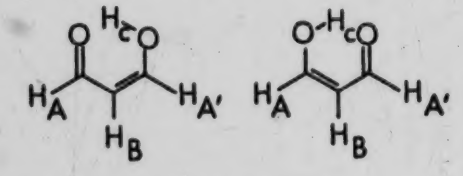

$H_{A,A'}$ = 8 8.37 ($J_{A\,A',B}$ = 3.5Hz, $J_{A\,A',C}$ = 6.1Hz)

H_B = 8 5.68 ($J_{B,A\,A'}$ = 3.5 Hz)

H_C = 8 16.40 ($J_{C,A\,A'}$ = 6.1 Hz)

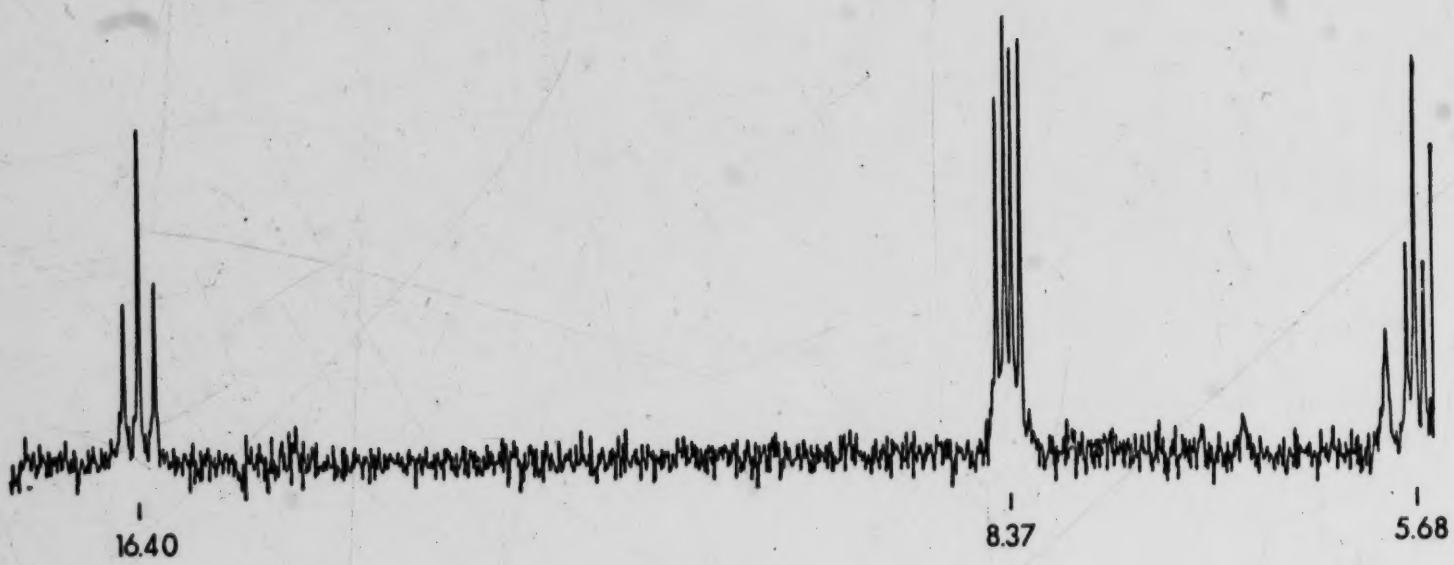

of a primary isotope effect and reduced efficiency of deuterium tunneling, and hence the coalescence temperature of the deuterated cisoid form was attempted. Figure 14 illustrates the ^1H NMR spectrum at 150°K where only a singlet centred at δ 8.37 (terminal hydrogens) was observed. No observable change was found at temperatures down to 130°K, at which point the solution freezes. Thus the intramolecular exchange of the OD is still rapid enough to prevent the measurement of coalescence temperature. Again utilizing the same assumptions as for the MA case, the same interconversion barrier for D-MA as that for MA is obtained. The upper limit of the effective barrier to interconversion of the C_s form via the C_{2v} form therefore cannot be greater than 6 kcal/mol. This is considerably smaller than the interconversion barrier predicted by the calculations (10.5-11.5 kcal/mol)[46,58,62].

One can estimate the lower limit of the interconversion barrier by assuming that the observed XPS spectrum of MA contains no more than 10% of the C_{2v} form which is hidden in the O_{1s} ionization peaks of the C_s form (equation 13).

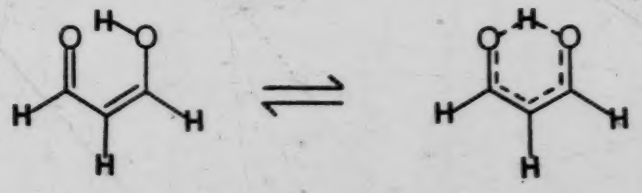

90% 10% (13)

Figure 14. The ^{1}H-NMR spectrum of deuterated malonaldehyde at 150°K in a solvent of 1:1 $CFCl_3$: CD_2Cl_2. The large resonance at δ 5.33 is attributable to $HCDCl_2$.

$H_{A,A'}$ = δ 8.37

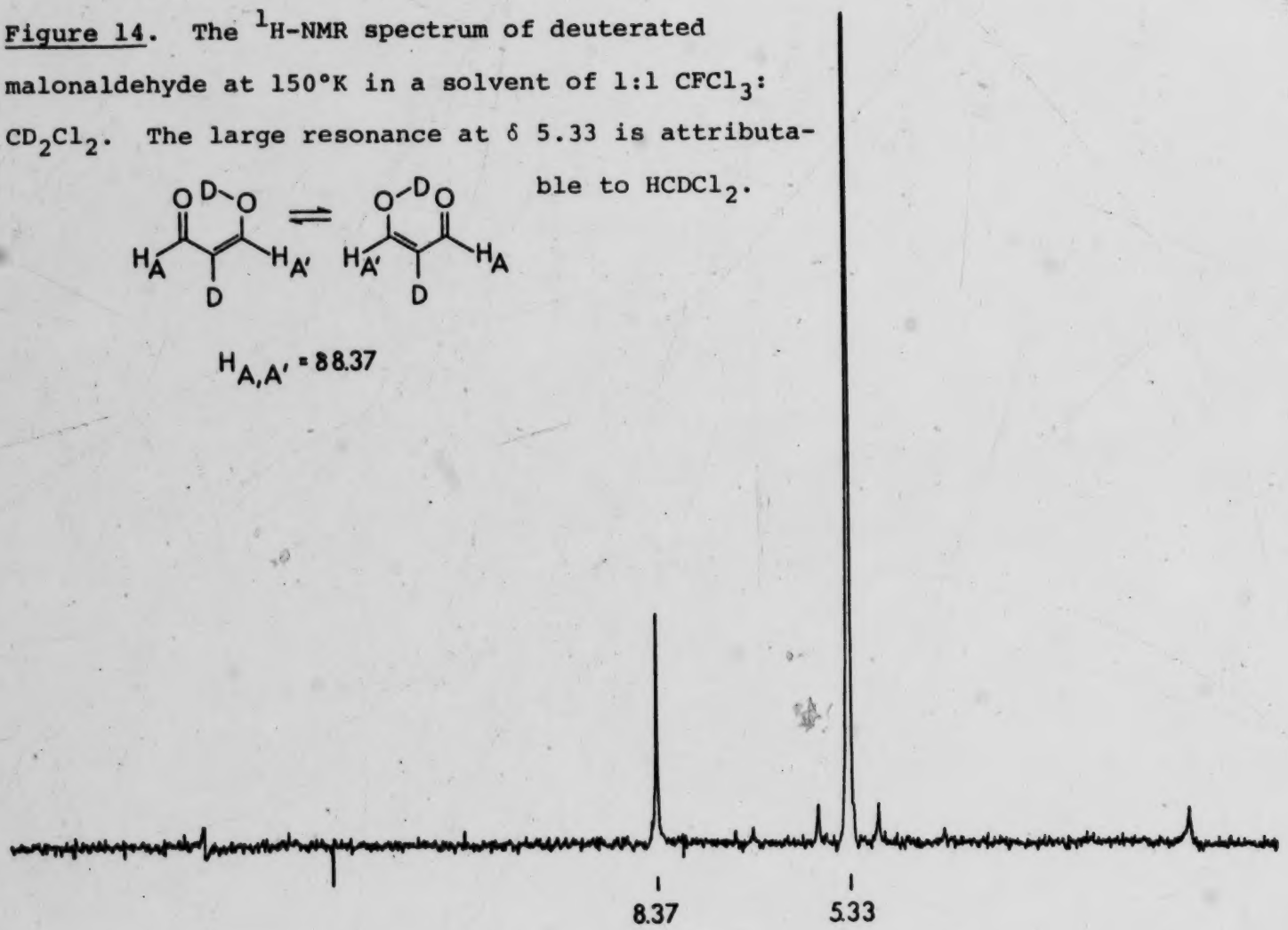

This assumption is based on the total uncertainty in the determination of the relative areas of the two inequivalent oxygens in MA. Using this assumption, k_{eq} is evaluated using equation 14 and is equal to 0.11.

$$k_{eq} = \frac{[C_{2v}]}{[C_S]} \tag{14}$$

Substituting k_{eq} into equation 15, $\Delta G°$ (T = 300°K) is found to be 1.3 kcal/mol, which is the lower limit of the C_S-C_{2v} interconversion barrier.

$$\Delta G° = -RT \ln k_{eq}^{28} \tag{15}$$

CONCLUSIONS

(1) The technique of XPS has demonstrated its ability to identify unambiguously the preferred symmetry form of the enols 1-5. The observation of a C_S form for 5 is particularly significant considering the apparently near-linear H-bond and the close proximity of the oxygens which favor an extremely rapid O:---H—O $\rightleftharpoons$ O—H---:O transfer (said to be > 10^{12} sec^{-1}[92]). Nevertheless, the time scale of the XPS measurement (10^{-16} sec) is sufficient to differentiate between the terminal oxygens.

(2) Variable temperature ^1H NMR and deuterium exchange studies on MA (1a) in deuterated ethanol indicate that the ketonization-enolization process is not fast enough to account for the apparent equivalence of the terminal hydrogens (H_A and $H_{a'}$) in 6a. Other intermolecular proton transfer reactions must account for this apparent symmetry.

(3) Recent calculations[46,58,62] on the cis-enol forms of H-MA place the C_{2v} form about 10.5-11.5 kcal/mol higher in energy than the C_S form. The barrier to interconversion between the two C_S form via the C_{2v} form is postulated to be reduced by proton tunneling[58,61]. The effective barrier to interconversion evaluated from the present ^1H NMR studies on H-MA and D-MA give an upper limit of no higher than 6 kcal/mol and a lower

limit of 1.3 kcal/mol.

(4) A low intensity peak of higher E_B than the major O_{1S} ionization peaks is observed in all the XPS spectra of the compounds under study. It was suggested that this low intensity peak arises from the C_{2v} form[62]. This is proved not to be the case since even dimethylacetylacetone (2) also show such a peak. It is believed that this peak arises from shake-up phenomenon.

EXPERIMENTAL

Routine IR, ^1H NMR and exact mass spectra were recorded on a Nicolet FT IR spectrophotometer, a Varian Associates HA-100 spectrometer and an AEI MS-50 spectrometer, respectively. ^{13}C NMR spectra were measured using a Bruker HFX-90 spectrometer.

Variable-temperature NMR studies of MA (1a) and D-MA were determined on a Bruker WP-60 FT NMR spectrometer using 5×10^{-3} to 4×10^{-2} M solutions of MA or D-MA in a solvent of 1:1 $CFCl_3$-CD_2Cl_2. All the solvents used for the NMR studies were dried over $CaSO_4$ (which had been flamed dry under vacuum) and then distilled into holding receivers using vacuum-line techniques.

Malonaldehyde (1a)

Malonaldehyde was prepared by the method of Hüttel[109] and sublimed five times into a holding receiver where it could be stored at -78°C for several weeks without visible signs of decomposition. NMR samples were then made up as required using vacuum-line techniques to ensure the absence of moisture. ^1H NMR (acetone-d_6): δ 5.61 (1 H, t, J = 9 Hz), 8.52 (2 H, d, J = 9 Hz), 9.34 (1 H, br.S).

Deuterated Malonaldehyde (6b)

Deuterated MA was prepared with great precaution

since the high acidity of system (pKa of MA = 4.46[65]) leads to extremely rapid OD-OH exchange even if the slightest source of exchangeable proton is present. Sodium malonate[110] was dried under vacuum over refluxing xylene for 2 days. All glassware which would be in contact with 6b, including the vacuum rack, was conditioned with D_2O and either oven dried or flamed out under vacuum. Two grams (0.021 mol) of sodium malonate was dissolved with stirring at 0°C in a solution of 20 ml of D_2O (99.7%) containing 4 grams of P_2O_5 in a serum-stoppered 100 ml Erlenmeyer flask. The 6b produced was then extracted via syringe techniques with 10 ml aliquots of sodium-dried ether (for removal of traces of protium) and the combined extracts were transferred via syringe to a second serum-stoppered Erlenmeyer flask which contained 15 grams of a 1:1 mixture of $CaSO_4$-Na_2CO_3 which had been flamed dry under vacuum. After standing at -5°C overnight the mixture was filtered in a glove bag and the ether was removed under house vacuum. The pale yellow solid residue was immediately flushed with N_2 and connected to the vacuum rack where it was manipulated as described for 1a. The NMR tube used was freshly conditioned with D_2O, then flamed out under vacuum; otherwise, the sample invariably showed residual traces of protium. Employing the above procedure, samples of 6b could be routinely

prepared which contained no detectable 1a by NMR.

β-Methoxyacrolein (1b)

β-Methoxyacrolein was prepared following the procedure of Kalinina et al[111]: ^{1}H NMR ($CDCl_3$) δ 3.77 (s, 3 H), 5.58 (d of d, J = 13.0, 8.0 Hz, 1 H), 7.45 (d, J = 13.0 Hz, 1 H), 9.43 (d, J = 8.0 Hz, 1 H). The large vinyl coupling constants suggest that 1b exists completely in a solution as a *trans* enol ether.

Acetylacetone (1c)

Reagent grade acetylacetone was obtained from the Fischer Scientific Co. (glpc purity, 99.46%) and was used as supplied.

Hexafluoroacetylacetone (1d)

Reagent grade (glpc purity 99.38%) was used as supplied by the Pierce Chemical Co.

Tropolone (3a)

Commercially available tropolone was sublimed twice under high vacuum at 40°C bath temperature before used.

2-Methoxy-tropone (3b)

The hemihydrate of 3b was prepared according to the method of Cook et al[112] and the water of crystallization removed using the following procedure. To 1 ml

of benzene was added 0.48 gm of hydrated 3b and the benzene-water azetrope was distilled under nitrogen. A small amount of oven-dried silica gel was added to the residue from which distillation (95°C bath temperature/0.3 mm) gave the anhydrous ether 3b as a yellow oil: 100 MHz ^{1}H NMR ($CDCl_3$) δ 3.94 (s, 3 H), δ 7.04 (m, 5 H).

Dimethylacetylacetone (2)[113], 9-hydroxyphenalenone[114], and 6-hydroxy-2-formylfulvene[115] were prepared by literature methods without modification.

CHAPTER III

N_{1S} BINDING ENERGIES OF NITROGEN-CONTAINING COMPOUNDS: CORRELATION BETWEEN N_{1S} E_B AND GAS PHASE BASICITY, SUBSTITUENT CONSTANTS AND THEORETICAL TREATMENTS.

INTRODUCTION

Basicity, one of the fundamental concepts in chemistry, has been of interest to chemists since it was first proposed by Brönsted[116] and Lewis[117] in 1923. Brönsted defined basicity as the tendency of a molecule B: to accept a proton (equation 16).

$$B: + \overset{+}{H}B_1 \underset{}{\overset{K_{eq}}{\rightleftharpoons}} \overset{+}{B}H + :B_1 \qquad (16)$$

$$\Delta G^\circ = -RT\ell_n K_{eq}$$

$$-\Delta H^\circ = \Delta PA$$

In the gas phase, the negative of the enthalpy change ($-\Delta H^\circ$) in equation 16 is defined as the proton affinity of B: (PA), while the gas phase basicity (ΔG°) is related to the equilibrium constant (K_{eq}) of the proton transfer reaction in equation 16. A more general definition was given by Lewis who described a base as a molecule which tends to donate a valence electron "lone pair" to an electron acceptor (Lewis acid). Recently, Martin and Shirley[118-119], noting the formal

similarity between the removal of a core electron from an atom in a molecule (equation 17) and the addition of a proton to that same atom (equation 16), extended the idea of Lewis basicity to include the ease with which core electrons are removed (E_B or binding energy).

$$B \xrightarrow{h\nu} B^+ \text{ (core hole)} + e^- \qquad (17)$$

They, and independently Davis and Rabalais[120], had shown a correlation between E_B and gas phase PA in a series of simple alkyl-substituted compounds containing oxygen, nitrogen, sulfur and phosphorus. They suggested that both E_B and PA were dependent on two terms, the initial state (inductive and mesomeric)[121] effects and the final state (polarization, or relaxation)[122] effects. The former rely on the electrostatic potential at the site in the neutral molecule on which the positive charge is located while the latter reflect the ease with which the positive charge can be delocalized over the entire molecule by rearrangement of the remaining electrons. It was proposed[119] but not demonstrated that the E_B-PA correlation would fail if there is a change in hybridization or geometry at the site of protonation since this cannot be probed by the photo-emission process which is vertical in the Franck-Condon sense. Thomas et al[123-125] extended these studies by investigating a number of doubly-bonded oxygen compounds,

such as carboxylic acids, esters, CO_2, CO, NO, N_2O and O_2, and found good correlations between E_B and PA except for the simple molecules CO, NO and O_2. No explanation was given by these authors for the above "exceptions". Further work was done by Benoit and Harrison[126] on a wide variety of oxygenated compounds and they explained that the failure of O_{1S} E_B of CO to correlate with its PA was due to the difference in site of protonation and ionization. This explanation was also suggested by Cavell and Allison[127] on the basis of the deviation of some amides and pyrrole from the N_{1S} E_B vs PA graph. In addition, they[127] also suggested the observed deviation of N,N-dimethyl aniline from the correlation is either due to the different site of protonation and ionization, a destabilization of the N_{1S} hole state in this compound relative to the hole state in aniline or a stabilization of the ground state relative to the ground state of aniline. More recent work by Ashe et al[128] on the E_B of As_{3S} and P_{2P} electrons in arsabenzene and phosphabenzene, respectively, showed that the rigid heterocyclic structure did not allow geometry rearrangement upon protonation and therefore the E_B-PA correlation failed. They explained that the ionization process only depends on inductive and relaxation effects whereas the protonation process relies, in addition to the above effects, on the ability

of the molecule to undergo geometry rearrangement. Thus the observed PA's for arsa- and phosphabenzene were lower than that predicted from their E_B's.

Based on the explanations offered for the above "exceptions" in the E_B-PA correlation, two conditions under which the correlation will fail are as follows; the site of protonation and ionization are different, and within a series of closely related compounds there are large energetically different geometry changes accompanying protonation. Certainly in every protonation process, geometry reorganization takes place but only those that show unusually large geometry changes would deviate from the E_B-PA correlation line. This is also supported by some semi-empirical calculations which will be discussed later on in this chapter. To our knowledge there are no detailed studies on circumstances where the E_B-PA correlation will break down and thus it is interesting to experimentally investigate molecules which are expected to deviate from the correlation for one or both of the above reasons. We have therefore investigated several series of compounds, pyridines, anilines, amides and amino-naphthalenes, for which deviations from some N_{1S} E_B-$\Delta G°$ correlation will be explained in terms of these reasons. Previous workers have used PA($-\Delta H°$) for the correlation since the original derivation[118] for the correlation directly

connects E_B with $\Delta H°$. In our case we have used $\Delta G°$ values since they are obtained from the direct measurement of the equilibrium position in the proton transfer reactions and they should be consistent for $\Delta G°$ values abstracted from various published works[129-131] which employ different techniques of measurement. In principle, $\Delta G°$ values can be converted to $PA(-\Delta H°)$ by the expression $\Delta G° = \Delta H° - T\Delta S°$ provided that the entropy term ($\Delta S°$) is known. In most cases, the magnitude of $T\Delta S°$ is rather small, 1-2 kcal/mol[131-132], when compared to that of $\Delta G°$ and is usually roughly constant[132] within a series of related compounds. Although only $\Delta G°$'s and E_B's are being discussed in this chapter, $\Delta H°$'s are also given along with the above data when they are available in the literature.

Because of pyridine's molecular rigidity, minimal geometry rearrangement is allowed to occur on protonation, the site of which is most certainly nitrogen. Hence both the ionization and protonation process are affected by the same factors, inductive, mesomeric and and relaxation. It is then expected a good correlation exists between N_{1S} E_B and $\Delta G°$ and this correlation line should provide the "standard" with which to compare situations where correlation fails. A recent *ab initio* study[133] showed the calculated N_{1S} E_B of 3 and 4-substituted pyridines correlate with the corresponding

experimental PA using only the ground state geometry.

While our primary target was the investigation of circumstances under which the E_B vs $\Delta G°$ correlation failed, the large number of examples of N_{1S} E_B for a virtually complete series of pyridines allowed assessment of other correlations which had been given in the literature on the basis of fewer and more ambiguous examples. Although there have been studies[134-140] of substituent effects on the C_{1S} E_B of substituted benzenes, virtually no experimental work had been done on the E_B of substituted pyridines which in fact, possess several advantages over the benzene series. Firstly the assignment of the benzene C_{1S} E_B peak is rather difficult since in most cases, the C_{1S} peaks are badly overlapped. They were assigned either with the aid of CNDO/2 calculations[138] or empirically in terms of two groups, one from the carbon that is directly attached to the substituent and the other being due to all the remaining benzene carbons. The latter approach invariably leads to assignment ambiguity. For the former model, CNDO/2 calculations provide charge densities of the molecule which are related to the relative binding energy shift (ΔE_{Bi}) by the following equation given by the electrostatic potential model[138], where

$$\Delta E_{Bi} = k_c q_i + \sum_{j \neq i} \frac{q_j}{R_{ij}} \qquad (18)$$

q_i and q_j are the charge densities of the ith and jth atoms, respectively, R_{ij} is the interatomic distance in atomic units, and k_c is a constant which commonly has a value of ~22 eV/unit charge for the benzene carbons. This approach suffers from whatever short comings might be inherent in the CNDO/2 calculation. On the other hand, the pyridine N_{1S} ionization peak can be identified unambiguously because it is far removed from other core ionization bands. Comparison of the observed N_{1S} E_B shift for pyridines with that predicted from the CNDO/2 calculations for benzenes would then offer experimental evidence to test the strength of this CNDO/2 model provided that substituent effects for nitrogen are roughly equivalent to those for carbon.

Secondly, the measured N_{1S} E_B shifts could be used to test the scope of two other models, the ground state potential model (GPM) and relaxation potential model (RPM)[141-144] which have been shown to predict quite well the E_B shifts of a large number of molecules containing carbon, nitrogen and oxygen.

Thirdly, it is also of interest to examine the correlation between N_{1S} E_B and the substituent parameters (σ values) which have been derived from solution chemical processes, specifically, from the dissociation of substituted benzoic acids at 25°C in H_2O[122] (equation 19).

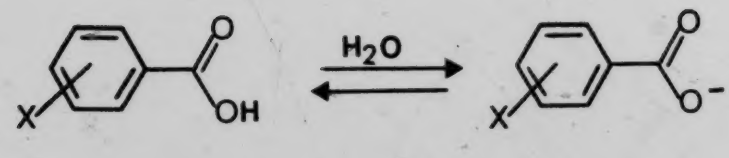

(19)

$$\log \frac{K_{eq}(X)}{K_{eq}(H)} = \rho\,\sigma \qquad \left[\rho = 1 \text{ for benzoic acid ionization}\right]$$

The $K_{eq}(X)$, $K_{eq}(H)$ terms are the equilibrium constants of the dissociation reaction in equation 19 with substituents X and H respectively. The σ value for a particular substituent represents its ability to influence the benzoic acid equilibrium in comparison to its parent molecule and therefore it is only remotely related to the ionization process. However it would be of general interest to see if the solution-derived parameters are useful for the gas phase photoemission process.

In the course of investigating the pyridine series, the tautomeric equilibrium of 2-pyridone $\rightleftharpoons$ 2-hydroxypyridine as a function of temperature was studied (equation 20).

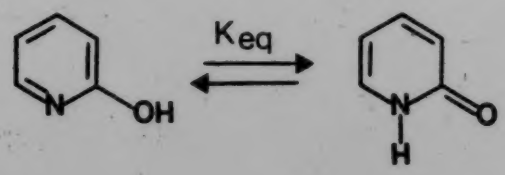

(20)

7 8

This equilibrium has been examined by a number of workers[145-154] using various techniques, from which 7 was found to be the preferred species in the gas phase. Our XPS studies on the N_{1S} and O_{1S} E_B's for 7 and 8 confirm the above results (*vide infra*). Tautomer 8 is an amide, examples of which have been shown to protonate at the oxygen in both solution and solid phases[155-160] with some theoretical confirmation[161-162]. It is therefore expected that the N_{1S} E_B of 8 should not correlate with its $\Delta G°$ but the correlation should be good between O_{1S} E_B and $\Delta G°$. For this reason, a number of amides, whose $\Delta G°$ values are known, were also investigated in order to substantiate this point.

As far as the question of geometry reorganization is concerned, recent gas phase basicity studies[131] of a number of substituted anilines and amino-naphthalenes suggested that the "anomalous" $\Delta G°$ values of some anilines and amino-naphthalenes were due to either different site of protonation or geometry changes on protonation. One of these molecules, 1,8-*bis*-(dimethylamino)-naphthalene (proton sponge, drawn in three dimensions as structure 9), has received

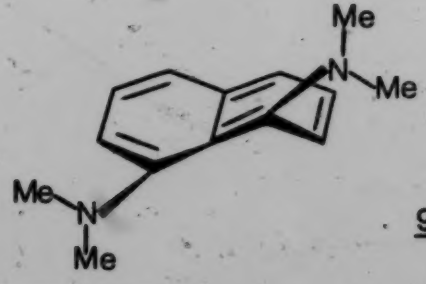

9

much attention for its unusually high basicity in both gas[131] and solution phases[163-165]. X-ray crystallographic studies[166-167] of the non-protonated species revealed that the *bis*-dimethylamino groups experience severe *peri* interaction causing a large distortion from planarity for the naphthalene ring. However, the protonated species of 9 allows the *bis*-dimethylamino groups to reorient themselves in order to share the proton and thus permit the flattening of the naphthalene ring although not to complete planarity[167]. As a result, part of the basicity of 9 must be ascribed to a relief of ground state strain on protonation, a process which cannot be probed by the photoemission process. Therefore compound 9 and other substituted naphthalenes, and anilines which possess unusually high basicities should provide good examples for which the correlation between E_B and $\Delta G°$ fails. Furthermore, the deviation of $\Delta G°$ for these compounds from the correlation line allows an indirect experimental measurement of the energy associated with such geometry changes or different site of protonation.

In order to demonstrate how geometry rearrangement affects $\Delta G°$, semiempirical MINDO/3 calculations[168] on pyridine, quinuclidine, aniline and *O*-diaminobenzene were performed. Pyridine and quinuclidine represent the situation where geometric rearrangement

accompanying protonation is minimized due to their molecular rigidity. On the other hand, aniline and *o*-diaminobenzene may involve geometry changes upon addition of a proton.

Recently, much attention was addressed to aniline as to whether it should protonate on the ring or at the nitrogen atom. Taft et al[169-170] have shown that aniline, all *para*-substituted anilines and *m*-fluoroaniline prefer to protonate at the nitrogen while *m*-toluidine and *m*-anisidine are ring-protonated species. These findings seem to suggest that within the *m*-substituted anilines, the electron-withdrawers tend to favor N-protonation and the electron-donors prefer ring-protonation. In other words, if one plots an N_{1S} E_B vs $\Delta G°$ graph for *m*-substituted anilines, two correlation lines of different slope are expected, one for the electron-withdrawers and the other for the donors. The two lines should intersect at some point indicative of a change in the site of protonation from nitrogen to the ring carbon. It is therefore interesting to investigate the N_{1S} E_B's of the *m*-substituted anilines and compare with the corresponding $\Delta G°$ values.

Due to the large number of compounds investigated, the following discussion is divided into two sections. Section I deals with the pyridine series, in which comparisons between N_{1S} E_B values and ^{13}C and ^{14}N NMR

chemical shifts, predicted N_{1S} E_B shifts from GPM and RPM, σ-parameters and the $\Delta G°$ values are made. In section II, examples whose N_{1S} E_B's did not correlate with the corresponding $\Delta G°$ values are presented and the deviations are discussed in terms of different site of protonation and geometry rearrangement accompanying protonation.

RESULTS AND DISCUSSION

(I) Substituted pyridines

The observed N_{1S} E_B's for the pyridine series and the available $\delta\Delta G°$'s and $\delta\Delta H°$'s[129,130,132,171] are summarized in Table 2. Part of the N_{1S} E_B's are reproduced again in Table 3, where they are compared with the calculated C_{1S} E_B's of the analogously substituted benzenes.

Comparison of N_{1S} binding energy shift (ΔE_B) for substituted pyridines with C_{1S} ΔE_B of substituted benzenes and with ^{14}N NMR chemical shifts of substituted pyridines

Pyridine and benzene are both aromatic compounds and substituent effects on the ring should in principle be similar in both systems. There have been studies on the correlation of ^{13}C NMR shifts between substituted pyridines and substituted benzenes[172-174]. However no comparison of the substituent effects on the nitrogen atom in the pyridines and the corresponding carbon in the benzene series has been made. It is therefore interesting to see if the N_{1S} ΔE_B of the pyridine derivatives correlates with the corresponding C_{1S} ΔE_B in the benzene series. Shown in Figure 15 is a plot of N_{1S} ΔE_B of pyridine derivatives (relative to pyridine) vs C_{1S} ΔE_B of the substitued benzenes (relative to benzene). Because of the overlap of all C_{1S} E_B peaks

Table 2. Gas phase N_{1S} binding energies (E_B), basicities ($\Delta G°$) and proton affinities (PA) for some 2,3 and 4-substituted pyridines.[a,b]

Compound	E_B (eV)	ΔE_B (kcal/mol)[c]	$\delta\Delta G°$[d,e] = $\delta\Delta H°$[i] (kcal/mol)
pyridine	404.94	0.0	0.0
2-CH_3	404.63	7.15	-3.7
2-OH[f]	404.96	-0.46	-
2-NH_2	404.48	10.61	(-3.4)
2-OCH_3	404.68	5.60	-1.2
2-$N(CH_3)_2$	404.05	20.52	(-8.8)
2-Br	405.22	-6.46	6.8[g]
2-Cl	405.23	-6.68	6.7
2-F	405.34	-9.22	10.4
2-CF_3	405.54	-13.84	9.7
2-CN	405.54	-13.84	13.3
2-NO_2	405.89	-21.91	-
2-$COCH_3$	405.12	-4.15	-
3-CH_3	404.75	4.38	-2.9
3-OH	404.97	-0.69	-
3-OCH_3	404.87	1.6	-3.2
3-NH_2	404.67	6.22	(-0.6)
3-$N(CH_3)_2$[h]	404.57	8.53	(-9.5)
3-Br			
3-Cl	405.20	-6.0	6.2

continued.....

Table 2 (continued)

Compound	E_B(eV)	ΔE_B (kcal/mol)[c]	$\delta\Delta G^{\circ}$[d,e] = $\delta\Delta H^{\circ}$[i] (kcal/mol)
3-F	405.34	-9.22	7.0
3-CF_3	405.41	-10.84	8.6
3-CN	405.55	-14.07	12.1
3-NO_2	405.67	-16.83	-
3-$COCH_3$	405.11	-3.92	4.0
4-CH_3	404.68	6.00	-4.3
4-OCH_3	404.49	10.38	-7.2
4-NH_2	404.26	15.68	(-9.4)
4-OH	404.95	-0.23	-
4-$N(CH_3)_2$	404.03	20.90	-15.6
4-Cl	405.08	-3.23	3.3
4-Br	405.18	-5.53	(2.5)
4-F	405.12	-4.15	4.2
4-CN	405.58	-14.76	11.2
4-NO_2	405.66	-16.60	12.7
4-$COCH_3$	404.98	-0.92	3.7
4-CF_3	405.44	-11.53	8.3

a. N_{1S} E_B values are reported as the average of at least 3 runs and have a precision of >±0.03 eV.

b. Calibrated against an internal standard neon Auger line (E_K = 804.56 eV)[37].

continued.....

Table 2 (continued)

c. N_{1S} ΔE_B = N_{1S} E_B (pyridine) - N_{1S} E_B (substituted pyridine); a positive value indicates the base is easier to ionize than pyridine.

d. $\delta\Delta G°$ = $\Delta G°$ (pyridine) - $\Delta G°$ (substituted pyridine); a negative value for $\delta\Delta G°$ indicates the base is stronger than pyridine.

e. Values are from ref. 129, 132; values in brackets are those from ref. 130.

f. 2-Hydroxypyridine exists in the gas phase in equilibrium with 2-pyridone, and different N_{1S} E_B's are seen for each (*vide infra*).

g. Value is taken from ref. 171.

h. The N_{1S} ionization region for 3-$N(CH_3)_2$-pyridine shows a single broad peak (FWHM = 1.9 eV) which was deconvoluted assuming two equal half-width ionizations. We assign the low E_B peak to the pyridine N_{1S} in analogy to the 3 and 4-substituted systems: precision ± 0.1 eV.

i. $\Delta G°$ is less than $\Delta H°$ by 0.8 kcal/mol.

Table 3. Comparison of N_{1S} ΔE_B values for substituted pyridines with calculated C_{1S} ΔE_B values for analogous positions of substituted benzenes.[a,b]

Substituent	ΔE_B (eV)					
	2-position		3-position		4-position	
	C_{1S} ΔE_B	N_{1S} ΔE_B	C_{1S} ΔE_B	N_{1S} ΔE_B	C_{1S} ΔE_B	N_{1S} ΔE_B
H	0.0	0.0	0.0	0.0	0.0	0.0
CH_3	0.1	0.3	0.1	0.19	0.2	0.26
NH_2	0.4	0.46	-0.1	0.27	0.6	0.68
OH	0.1	-0.02	-0.3	-0.03	0.1	-0.01
F	-0.4	-0.4	-0.6	-0.4	-0.2	-0.18
Cl	-0.7	-0.29	-0.2	-0.26	-0.5	-0.14
Br	0.0	-0.28	-0.4	-	0.2	-0.24
CN	-1.7	-0.6	-1.0	-0.61	-1.0	-0.64
NO_2	-1.0	-0.95	-0.7	-0.73	-0.8	-0.72

a. Benzene values from ref. 138.

b. Best fit straight line is C_{1S} ΔE_B = 1.14 N_{1S} ΔE_B - 0.09 (r = 0.82).

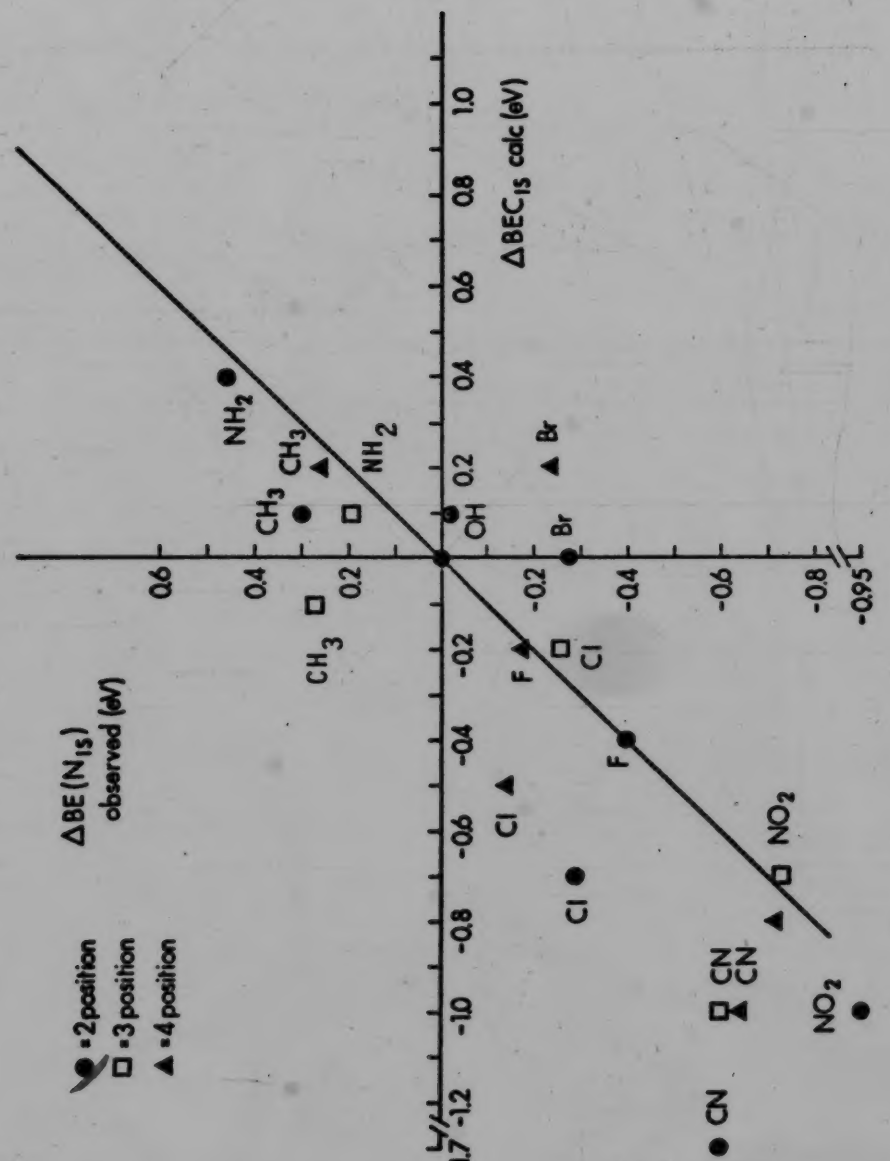

Figure 15. A plot of N_{1S} ΔE_B against C_{1S} ΔE_B for substituted pyridines and benzenes.

in each substitued benzene, they were assigned with the aid of a spectrum simulation program[138], which made use of the electrostatic potential model (equation 18) to evaluate C_{1S} ΔE_B's and fit them into the X-ray pes spectra measured at the C_{1S} region. However, this electrostatic potential model assumes that the molecular reorganization energy accompanying photoionization cancels within a series of closely related molecules such that only ground state effects (inductive or mesomeric) influence the C_{1S} E_B's. Comparison of the C_{1S} ΔE_B for benzene series with the N_{1S} ΔE_B for pyridines should then provide some measure of the validity of this model for this particular system.

A least squares analysis of the C_{1S} ΔE_B vs N_{1S} ΔE_B plot shows a slope of near-unity (1.14) but with considerable scatter in the points (correlation coefficient, $r = 0.82$) indicating a serious shortcoming in the correlation. In general, the plot indicates the expected trends of the substituent effects on these compounds, except for the 3-methyl, 4-bromo and 2-cyano substituents. The lack of correlation between C_{1S} and N_{1S} ΔE_B may be due to some deficiencies in the CNDO/2 parameterization[175], the inapplicability of applying a point charge electrostatic model to π-systems, and/or the inability of the electrostatic potential model to account for the molecular reorganization energy accompanying photo-

ionization.

The correlation between NMR-E_B shifts was first attempted in a theoretical paper by Basch[176], where he pointed out that there should exist a close relationship betwen the chemical shift in NMR and the electrostatic potential, which describes the E_B shift based on the ground state effects (inductive or mesomeric) of the substituents. Recent work by Gelius et al[177] has questioned the overall validity of ΔE_B vs NMR chemical shift correlations although the correlations between C_{1S} ΔE_B and ^{13}C chemical shifts for a series of closely related halomethanes have been presented by some workers[178-180]. Lindberg[181], based on the correlations for an expanded set of substituted methanes and *p*-substituted fluorobenzene ^{19}F chemical shifts, concluded that useful correlations between NMR and E_B shifts should be expected "provided that the objects for correlation are wisely chosen". In this study, a comparison of N_{1S} ΔE_B from Table 2 with the existing ^{14}N NMR chemical shift values[182] for a limited number of pyridines (Table 4) reveals a rather poor correlation ($r < 0.65$) especially for electron-withdrawers for which large observed changes in ΔE_B did not lead to large ^{14}N shifts. This result seems to support the conclusion made by Gelius et al[177] that the NMR-E_B correlations may not be valid even for a

Table 4. ^{14}N chemical shift values (ppm) of some 2, 3 and 4-substituted pyridines referred to CH_3NO_2 as internal standard.[a]

Substituent	Position		
	2	3	4
H	63±2	63±2	63±2
NH_2[b]	128±4	88±4	105±4
OH[b]	209±2	85±4	201±2
OCH_3	110±3	59±4	90±6
CH_3	72±3	68±3	74±3
Cl	67±3	59±3	69±4
Br	61±3	55±3	56±5
CN	62±4	64±4	54±4
$COCH_3$	72±5	48±12	38±12
NO_2[b]	80±5	56±5	35±6

a. Data abstracted from ref. 182.

b. These ^{14}N shift values determined in acetone while the remaining values were determined as neat liquids.

series of closely related compounds.

Comparison of the observed and calculated N_{1S} ΔE_B shifts

Computations of the N_{1S} ΔE_B using GPM and RPM[141-144] based on CNDO/2 methods were done on the present series of substituted pyridines. The GPM deals with the electrostatic potential (V) experienced by the core electron in the ground state while RPM, in addition to the V term, also takes into consideration a relaxation energy (V_R) that arises from redistribution of electronic charge during ionization.

According to the GPM, the electrostatic potential experienced by an electron at a nucleus is given by

$$V = e^2 \sum_i \frac{I}{r_i} - e^2 \sum_j \frac{Z_j}{R_{ij}} \qquad (21)$$

where r_i and R_{ij} refer to the distance between the parent nucleus and the ith electron and jth other nucleus respectively, and Z_j is the nuclear charge on the jth nucleus. It was shown by Basch[176] and Schwartz[183] that the shift in the orbital energy ($\Delta\varepsilon$) relative to a reference is approximately equal to the shift in the potential energy of the electron (ΔV) (equation 22).

$$\Delta\varepsilon \simeq \Delta V \qquad (22)$$

By using Koopmans' theorem, equation 22 then becomes

$$\Delta E_B \simeq -\Delta V \qquad (23)$$

Based on the CNDO/2 wave functions, ΔV at a given nucleus can be evaluated from which ΔE_B can be determined. Figure 16 shows the plot of $N_{1S}\ \Delta E_B$ (GPM predicted) vs $N_{1S}\ \Delta E_B$ (observed) for the substituted pyridines. Standard bond lengths and angles were assumed for the substituents[175] and the geometry of the pyridine ring was taken from the experimental data as determined for pyridine by electron diffraction[184]. In this case, an imperfect correlation is observed due to the large scattering of data points although least-squares analysis gives a near-unity slope as predicted from the theory (equation 24).

$$\Delta E_B(\text{predicted}) = 1.07\ \Delta E_B(\text{observed}) + 0.13 (r = 0.88) \quad (24)$$

Qualitatively, the theory reproduces the observed E_B trend for each 2, 3 and 4-substituent, but quantitatively the agreement is poor. As has been shown by previous workers, this approach gave more or less satisfactory agreement between observed and predicted shifts for some series of closely related compounds[141-144]. The lack of quantitative agreement in this pyridine series could be related to some shortcoming in the CNDO/2 method (parametrization) or the incorrect geometries used or more fundamental difficulties in treating delocalized π-systems with point charge models.

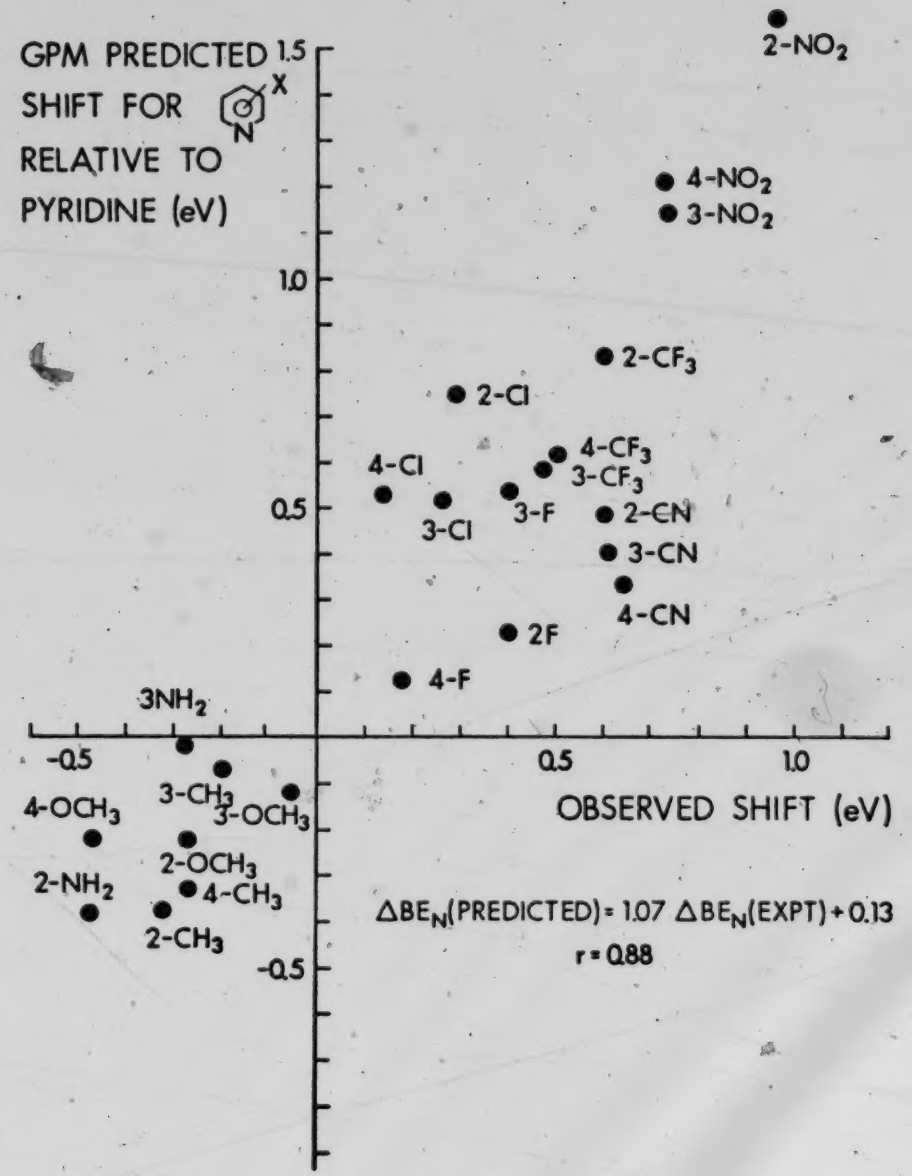

Figure 16. A plot of N_{1S} ΔE_B (observed) against N_{1S} ΔE_B (calculated) on the basis of GPM.

Since the GPM approach was not very successful on the pyridine series, the RPM approach was then examined in order to see if the introduction of relaxation terms would improve the correlation. The RPM approach makes use of an "equivalent-core" approximation to calculate the nitrogen "hole state" whereby the ionized atom (N) is replaced by the next higher element (O). By using this "equivalent-core" approximation, E_B was found to be best represented[185-186] by the following expression,

$$E_B = -1/2\ [\varepsilon(Z) + \varepsilon(Z+1)] \qquad (25)$$

where $\varepsilon(Z)$ and $\varepsilon(Z+1)$ represent the orbital energies in the ground and the hole states respectively, and Z is the nuclear charge of the neutral atom. Accordingly, the E_B shift relative to the parent nucleus is given as follows,

$$\Delta E_B = -1/2\ [\Delta V(Z) + \Delta V(Z+1)] \qquad (26)$$

In order to compare with the GPM expression (equation 23) it is instructive to write equation 26 as

$$\Delta E_B = -\Delta V(Z) - \Delta V_R \qquad (27)$$

where V_R is the relaxation energy which is equal to 1/2 [V(Z+1) - V(Z)]. It has been shown that the introduction of this relaxation term in the RPM approach

provides better agreement between the observed and predicted ΔE_B's for unlike molecules[141,144].

Shown in Figure 17 is a plot of N_{1S} ΔE_B (RPM predicted) vs N_{1S} ΔE_B (observed) for the substituted pyridines and the best fit straight line from the least-squares analysis is

$$\Delta E_B(\text{predicted}) = 1.04\ \Delta E_B(\text{observed}) - 0.06\ (r = 0.88) \quad (28)$$

Upon examining both correlation equations 27 and 28, one sees that the RPM does not show a better correlation than the GPM, but RPM calculations tend to lower the ΔE_B values by an average of 0.2 eV when compared to those from the GPM calculations. Nevertheless, a closer examination of the N_{1S} ΔE_B values reveals that for a given substituent the order of importance of relaxation is 2 > 4 > 3. This is illustrated in Table 5 which lists the calculated differences in E_B between GPM and RPM calculations. It appears from Table 5 that relaxation is between two and three times as important for 2 and 4 substituents as for 3 substituents for a given substituent. This implies that 2 and 4 substituents can better respond to N_{1S} photoionization through electronic relaxation than can 3 substituents.

Correlation between N_{1S} E_B and σ-substituent parameters

The process of XPS involves the removal of a core

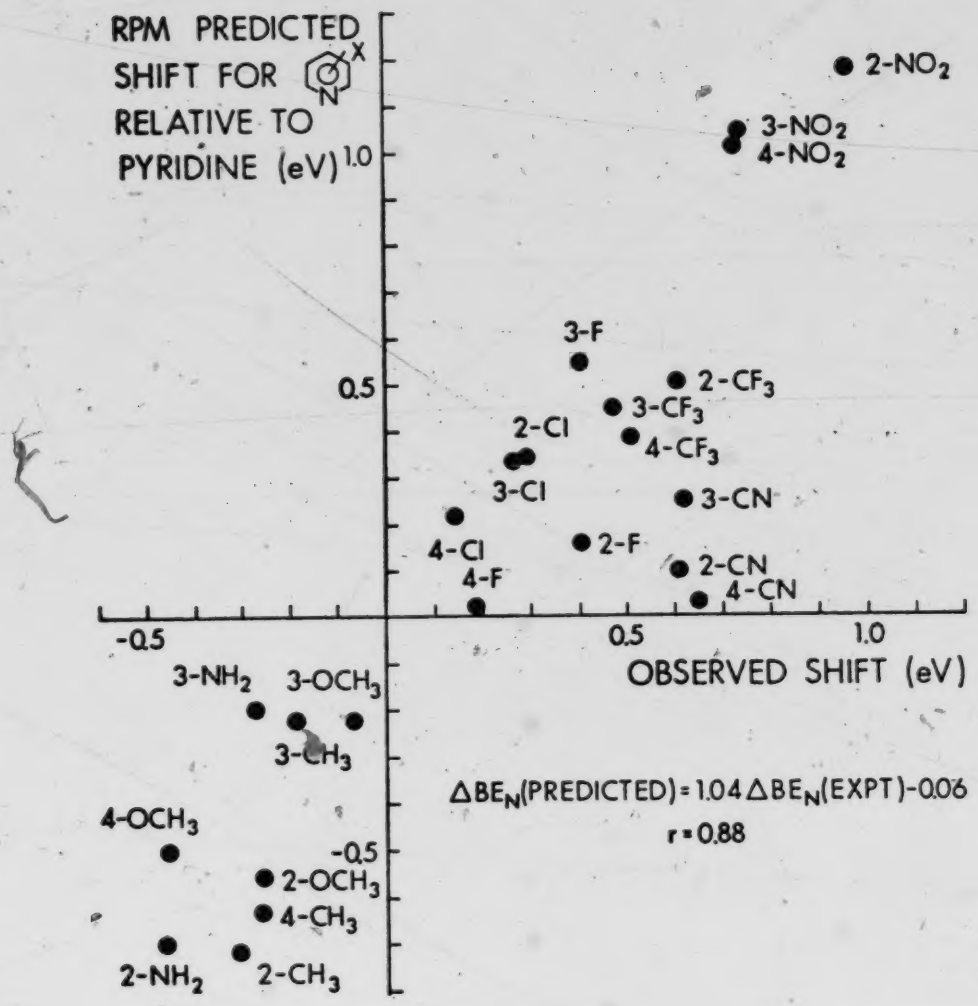

Figure 17. A plot of N_{1S} ΔE_B(observed) against N_{1S} ΔE_B(calculated) on the basis of RPM.

Table 5. Calculated Differences in Binding Energy Based Upon GPM and RPM Approaches.[a,b]

	$\delta\Delta BE_{N_{1S}}$ (GPM - RPM) (eV)		
Substituent	2	3	4
-F	0.07	-0.02	0.09
-Cl	0.39	0.18	0.20
$-CF_3$	0.32	0.13	0.22
$-CH_3$	0.33	0.14	0.29
$-OCH_3$	0.31	0.14	0.27
-CN	0.38	0.15	0.30
$-NO_2$	0.38	0.10	0.29
$-NH_2$	0.30	0.16	-

a. Calculations based upon CNDO/2 methods in ref. 144.

b. These values represent differences in the vertical axes for Figures 16 and 17.

electron in which direct resonance interaction is not expected to play a significant role in stabilizing the positively charged core hole since resonance only deals with valence electrons (equation 29).

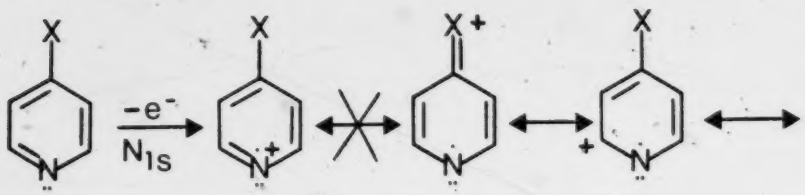

(29)

However resonance effects should affect the ionization process through relaxation which influences the electron density surrounding the ionized center. On the other hand, the σ-parameter measures the total substituent effect which includes inductive, mesomeric and solvent factors, the former two being the intrinsic properties of the substituent. Figure 18 illustrates a plot of N_{1S} ΔE_B for 3 and 4-substituted pyridines vs the corresponding σ-values[187] and the correlation equation determined from the least-squares analysis is N_{1S} ΔE_B = -1.07 + 0.06 eV (r = 0.985), excluding the points for the 4-hydroxy and 4-acetyl-pyridines. Considering that the substituent σ-values were determined in aqueous media for a chemical process which is only remotely related to N_{1S} photoionization, the correlation is remarkably good. The fact that both 3- and 4-substituents lie on the same line would tend to indicate that the mechanism by which they affect the

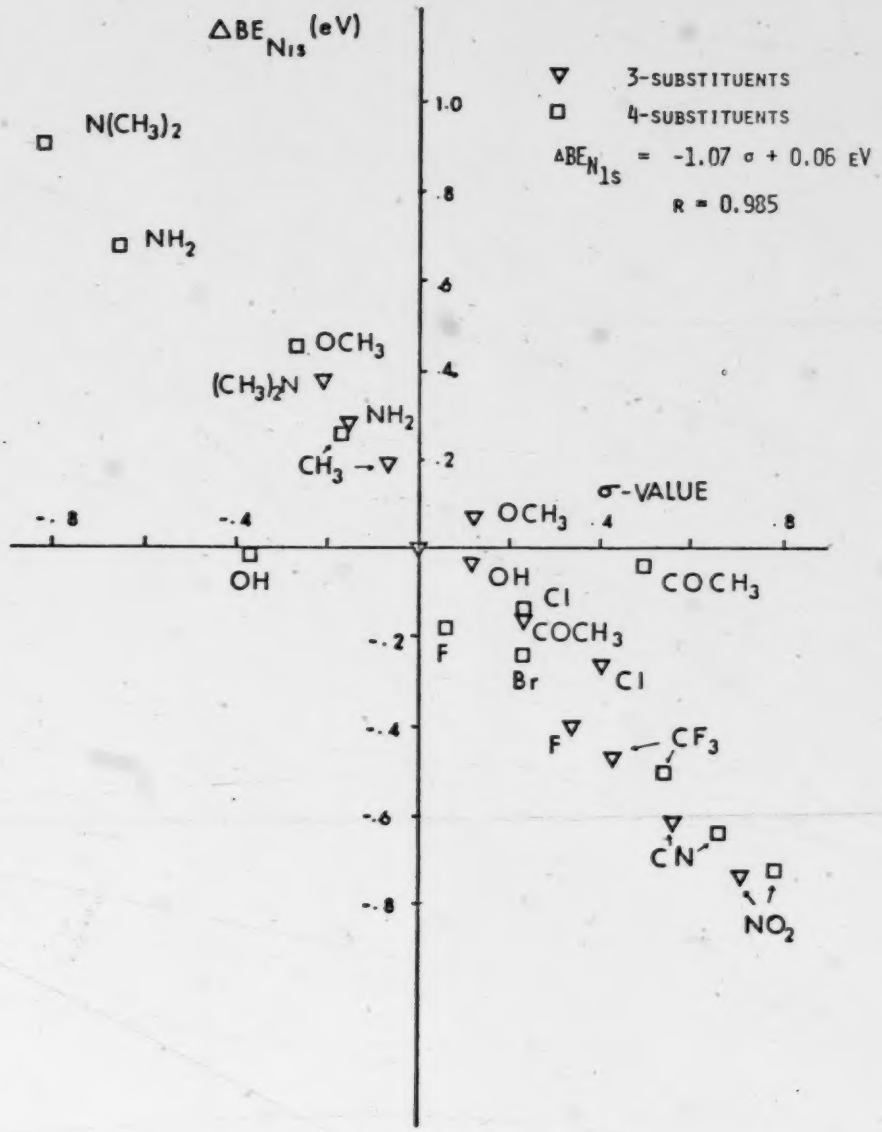

Figure 18. A plot of N_{1S} ΔE_B against σ-substituted parameters from ref. 187.

core ionization is not markedly different and that the substituents respond similarly to both benzoic acid ionization and pyridine N_{1S} photoionization provided that no substituent-solvent interaction such as H-bonding is present.

It is interesting to note that 4-hydroxy and 4-acetylpyridines fall badly off the correlation line, but not 3-hydroxy and 3-acetylpyridines. The hydroxyl substituent has been shown[188-191] to exhibit H-bonding effects in solution. It could be that the H-bonding effects influence the resonance interaction of the OH substituent with the benzene ring leading to the observed large negative σ-values (equation 30).

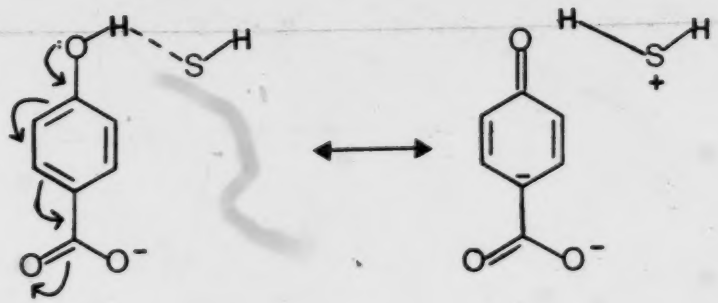

(30)

This does not occur in 3-OH since there is no direct resonance between the 3-substituent and the carbon to which the COO^- is attached. Similarly, the substituent-solvent interaction may allow the electron-withdrawing 4-acetyl group to exert stronger inductive effects

giving a substantially larger positive σ-value (equation 31).

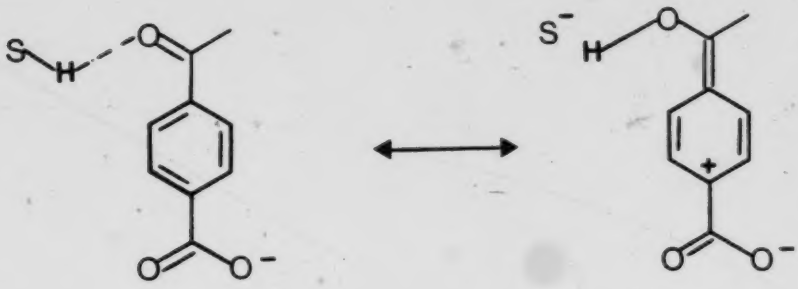

(31)

Correlation between N_{1S} E_B and $\delta\Delta G°$

The correlation between E_B and $\Delta G°$ has been studied for a large number of compounds and it is generally good within a series of closely related compounds[118-120,123-127].

In the present pyridine series, the correlation between N_{1S} ΔE_B vs gas phase basicity shift ($\delta\Delta G°$), both relative to pyridine, is illustrated in Figure 19. The best fit straight line from the least-squares analysis for 24 pyridines substituted at the 2,3 and 4-position is

$$N_{1S}\ \Delta E_B = -1.40\ (\delta\Delta G°) + 2.0 \text{ kcal/mol } (r = 0.980) \qquad (32)$$

The best fit straight line for each series is given as follows.

2-substituted pyridines ; $N_{1S}\ \Delta E_B = -1.5\ (\delta\Delta G°) + 3.65$ kcal/mol ($r = 0.980$)

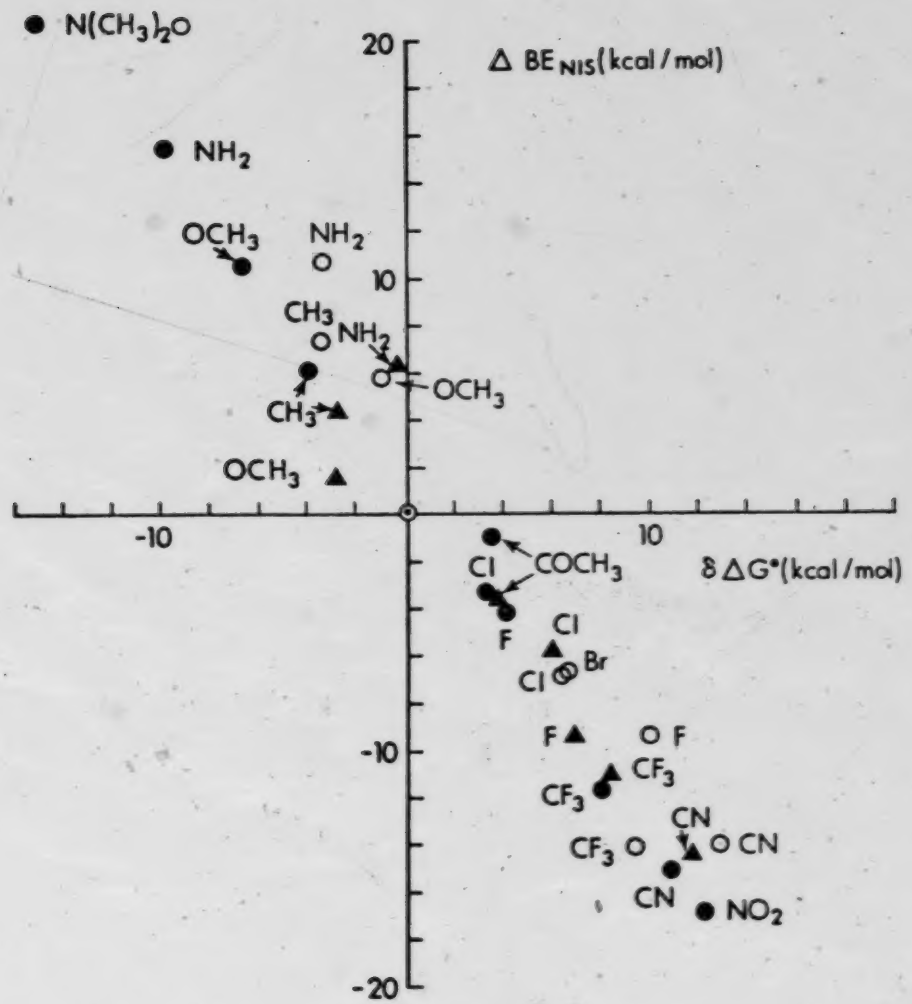

Figure 19. A plot of N_{1S} ΔE_B vs $\delta\Delta G°$ (relative to pyridine) for 2, 3, and 4-substituted pyridines. Open circles (O) are for 2, (▲) are for 3, and closed circles (●) are for 4 substituents.

3-substituted pyridines; N_{1S} ΔE_B = -1.36 ($\delta\Delta G°$) + 1.55 kcal/mol (r = 0.988)

4-substituted pyridines; N_{1S} ΔE_B = -1.34 ($\delta\Delta G°$) + 0.16 kcal/mol (r = 0.996)

The fact that all the correlation equations presented above have slopes less than (-) one suggests that the change in molecular environment affects E_B's more than their corresponding $\Delta G°$'s. Although the original proposal[118] indicated that the variation in PA should be nearly equal to the variation in E_B, there is no reason to expect this to be valid in every case. The reason is that the original derivation of the ΔE_B- PA correlation on alkyl substituted alcohols[118] indicated that both ΔE_B and ΔPA are approximately equal to the change in relaxation energy (ΔE_R), and therefore there should exist a one to one ratio between ΔE_B and ΔPA. This non-unity correlation was also reported by several workers on some phosphorus-[119], nitrogen-[119] and oxygen-[125-126] containing compounds.

In general, the fit for substituted pyridines is quite good and one can utilize this correlation equation to predict those gas phase basicity values, which are not yet available in the literature provided that the N_{1S} E_B's are known. One should note that there is a lack of correlation between N_{1S} E_B and $\Delta G°$ in the methoxypyridines whose order of basicity is

2 < 3 < 4 while the N_{1S} E_B order is 3 < 2 < 4. No clear-cut reason is apparent for this observation and therefore MINDO/3 calculations were performed in order to attempt to obtain some insight into this problem.

MINDO/3 studies on the methoxypyridines

The photoionization process is a vertical one in the Franck-Condon sense which requires the ground and ion state geometry remain the same. Hence factors influencing the photoionization process are those related to electronic (inductive and mesomeric) effects on the ground and ion states.

On the other hand, basicity values are adiabatic ones since the protonated bases at equilibrium are fully relaxed electronically as well as geometrically. Therefore, lack of correlation between ΔE_B and $\delta\Delta G°$ values could arise from either differences in the site of protonation and ionization or geometric relaxation of the protonated species which cannot be probed in the photoionization process.

Our goal in attempting these calculations on the methoxypyridines was to see if geometric relaxation or different site of protonation does indeed account for the different trend in the measured $\Delta G°$ values and in the observed N_{1S} E_B values. According to the resonance theory, one would predict the trend in $\Delta G°$

to be the same as that in N_{1S} E_B. As typified by equation 33, the nitrogen atom becomes more negative due to resonance interaction with the methoxy-substituent in the 2-position (similarly in the 4-position). No such interaction is possible in the 3-position and thus on this basis its tendency to accept a proton at the nitrogen should be less than that in the case of 2- or 4-methoxypyridines.

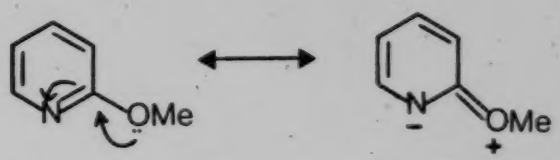

(33)

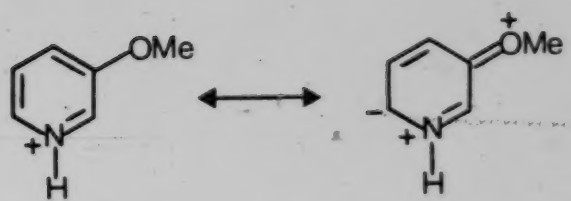

(34)

However, there is a possibility that geometric relaxation is more important in the protonated 3-methoxypyridine (equation 34) because there is no direct resonance interaction to stabilize the positively charged nitrogen and such relaxation seems to be the only way to accommodate the incoming proton.

It has been shown that MINDO/3 calculations give

reasonable heats of formation (ΔH_f) for a wide variety of compounds[168,192] and have been used to provide some insight into the protonation of some dihydropyridines[193]. It therefore appeared that this method might allow one to study the possible cause of the observed basicity order for methoxypyridines.

Consider the hypothetical protonation process listed below.

$$\underset{\text{optimized base}}{B:} \overset{H^+}{\rightleftharpoons} \underset{\text{vertical ion}}{[B:H]^+} \rightleftharpoons \underset{\text{adiabatic ion}}{\overset{+}{B}-H} \qquad (35)$$

The first step of the protonation process in equation 35 is the simple attachment of a proton to the molecule while the second step involves relaxation of this protonated vertical ion to its most stable conformation (adiabatic ion). The calculation of the vertical ion involves simply the attachment of a proton to the geometry optimized neutral methoxypyridine in the ground state. The second process represents a full geometry optimization of the vertical ion leading to the adiabatic ion. The overall calculated protonation processes are shown in equation 36 for 3-methoxypyridine, and the 2- and 4-methoxypyridines can be considered in a similar manner. According to the calculations, the addition of a bare proton in equation 36

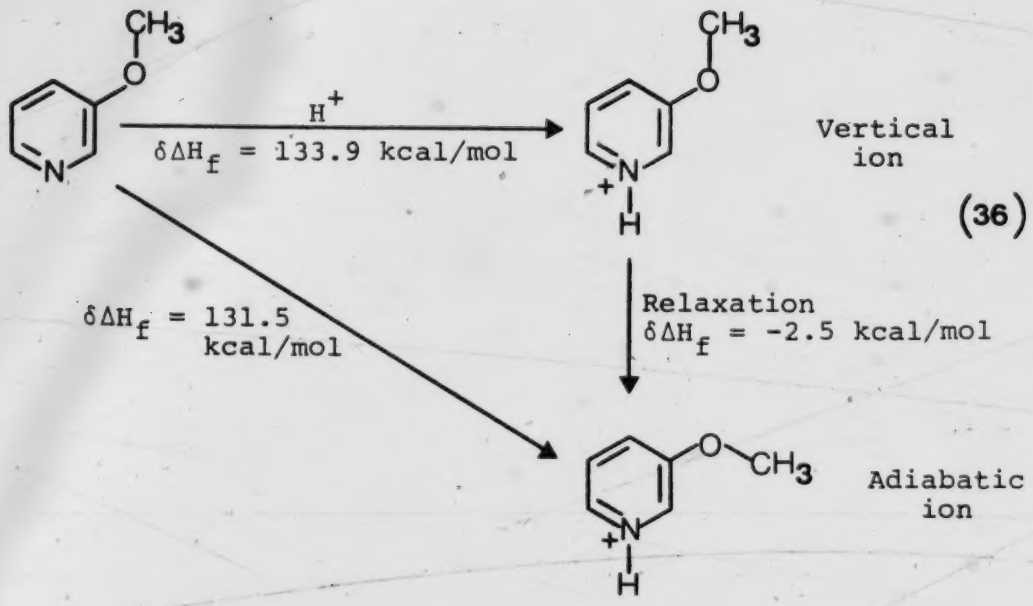

to form a vertical ion raises ΔH_f by 133.9 kcal/mol. Geometric relaxation which appears to involve the reorientation of the OCH_3 group releases 2.5 kcal/mol and thus the overall process of adding a proton to the neutral species is endothermic by 131.5 kcal/mol. Similarly, the changes in heat of formation for the overall protonation process of 2- and 4-methoxypyridines are 130.9 and 127.3 kcal/mol, respectively. In principle, one can determine the $\Delta H°$(-PA) values for the protonation process in each methoxypyridine (equation 37) provided that the calculated values of NH_4^+ and NH_3[192] are known.

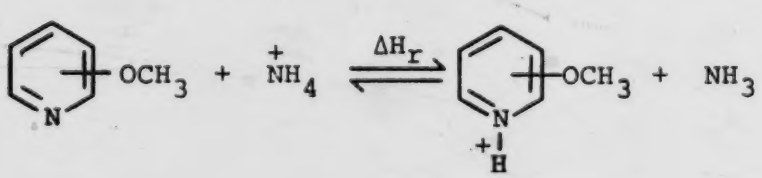

(37)

Table 6. MINDO/3 heats of formation for methoxy pyridines, methoxy pyridinium ions and ΔH_r.[a,b]

Species	ΔH_f (kcal/mol) B:	Vertical BH^+	Adiabatic BH^+	ΔH_r (kcal/mol)
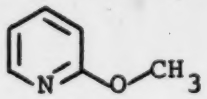	-20.96	113.69	109.32	-32.35
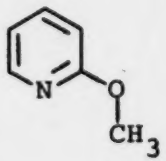	-22.24	113.36	108.71	-
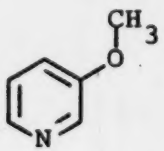	-13.36	120.60	118.16	-31.94
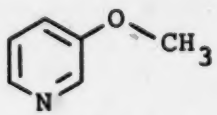	-12.82	120.82	118.10	-
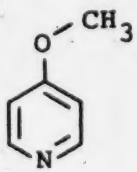	-15.83	115.63	111.43	-36.03

continued.....

Table 6 (continued):

Species	B:	ΔH_f (kcal/mol) Vertical BH^+	Adiabatic BH^+	ΔH_r (kcal/mol)
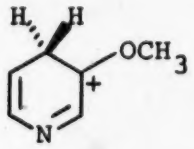	-	-	148.08	-
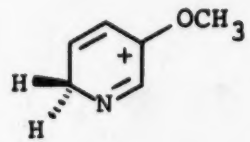	-	-	145.81	-
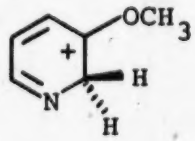	-	-	147.78	-
NH_3 [c]	- 9.4	-	153.9	-

a. $\Delta H_r = \Sigma\Delta H_f(\text{products}) - \Sigma\Delta H_f(\text{reactants})$.

b. For equation 37.

c. Values are taken from ref. 192.

Shown in Table 6 are the calculated ΔH_f's for methoxypyridines and their protonated ions, and the ΔH_r's for the reaction listed in equation 37. Comparison of the ΔH_r values for the methoxypyridines indicates the same trend as that in the N_{1S} E_B. The 3-OCH_3 is less basic than the 2-OCH_3 by ~0.5 kcal/mol, and less basic than the 4-OCH_3 by ~4.1 kcal/mol. Accordingly, these calculations suggest that geometry relaxation is not responsible for the observed behavior in methoxypyridines although one does not know how much value to place in the validity of the method for such small energy differences.

One may argue that the 3-methoxy pyridine protonates on the ring since there have been reports that ring protonation occurs in some substituted benzenes[170,194-196]. However calculations in which a proton is placed on the positions *ortho* and *para* to the methoxy substituent indicate that ring protonation is not a favorable process since the aromaticity of the ring is lost (Table 6). Hence the possibility of protonation on the ring (i.e. different site of protonation) can be eliminated. Thus charge-separated ionic forms as in equation 34 might be quite important in determining the basicity of 3-methoxypyridine.

The calculations for the methoxypyridines also indicate that geometry relaxation in passing from the

"vertical" ion to the "adiabatic" ion releases more energy for 2 and 4-substituents (~4.5 and 4.2 kcal/mol) than for 3-substituent (~2.5 kcal/mol). This is probably due to the better interaction of the substituent with the positive charge in the former cases (equations 33 and 34). Analysis of the calculated geometry changes for all species showed that the plane of the methoxy group was tilted slightly (~1°) downward from the ring plane so as to allow large interaction between the ring and oxygen "P" type lone pair. In all cases, the geometry relaxation of the protonated species (10) causes the shortening of N_1-C_4 distance by ~0.05 Å, lengthening of the C_2-C_6 distance by ~0.10 Å and a decrease in the ring carbon-oxygen bond length by ~0.04 Å relative to the neutral species.

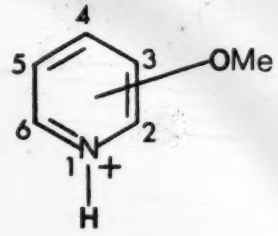

10

The introduced positive charge is basically accommodated by the N_1, N-H, the ring carbon to which the methoxy group is attached and the methyl hydrogens.

Tautomeric equilibrium between pyridone and hydroxypyridine

The prototropic equilibrium of 2-hydroxypyridine (7) with 2-pyridone (8) has been much studied. Recently, solution UV studies[150,152] showed that 8 is the major species down to a concentration of 10^{-7} M in cyclohexane where 7 becomes detectable. However, in the gas phase, 7 is the favored species. This further supported by gas phase IR[148] and UV pes studies[153-154] of this equilibrium. In the present study, the N_{1S} and O_{1S} E_B's for 7, 8 and related derivatives as well as the analogous 2-hydroxypyridine-N-oxide (11a) and N-ethoxy-2-pyridone (12b) were measured and are listed in Table 7. The deconvoluted spectra of the N_{1S} and O_{1S} regions for $7 \rightleftharpoons 8$ obtained at 130°C are presented in Figure 20, and the assignment of the ionization peaks is made by comparison with 2-methoxypyridine (13) and N-methyl-2-pyridone (14). Relative to pyridine (N_{1S} E_B = 404.94 eV) the N_{1S} orbitals of pyridones 8 and 14 are more difficult to ionize by 1.67 eV and 1.39 eV respectively. On the other hand 7 is harder to ionize than pyridine by 0.02 eV while 13 is easier by 0.26 eV. Assuming equal ionization cross-sections for $7 \rightleftharpoons 8$, K_{eq} can be determined by considering the ratio of the deconvoluted intensities of both species in the N_{1S} and O_{1S} regions and is found to be 0.48 ± 0.05 at 130°C

Table 7. O_{1S} and N_{1S} Binding Energies (E_B) for Hydroxypyridines and Pyridones.[a]

Compound	Binding Energy (eV)[b] N_{1S}	O_{1S}
Pyridine	404.94 (404.82)[c]	
2-Hydroxypyridine (7)	404.96	539.45
2-Methoxypyridine (13)	404.68	538.91
2-Pyridone (8)	406.61	536.66
N-Methyl-2-pyridone (14)	406.33	536.36
N-Hydroxy-2-pyridone (12a)	408.07[d]	540.08 (O-H) 537.01 (C=O)
N-Ethoxy-2-pyridone (12b)	407.41	539.58 (OEt) 536.49 (C=O)
Pyridine-N-oxide	408.65[d]	536.00[d]

a. Each E_B is the average of at least three determinations and has a precision of ±0.03 eV unless otherwise noted.

b. Calibrated against a neon Auger line with 804.56 eV kinetic energy[37].

c. Ref. 127.

d. Precision ±0.10 eV.

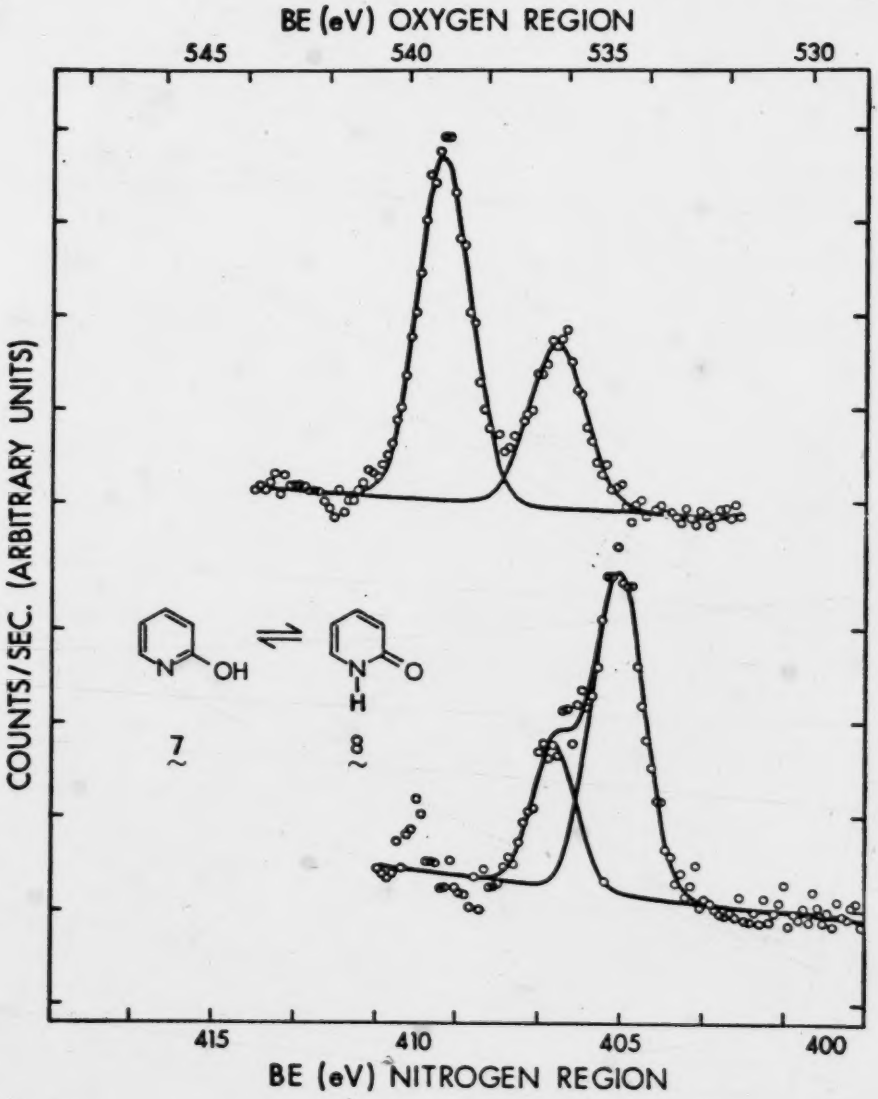

Figure 20. Unrestricted computer deconvolution of the N_{1S} and O_{1S} ionization region of 7 ⇌ 8 at 130°C. The ratio of the two N peaks and O peaks is 0.48±0.05.

with 7 clearly dominating. Thus $\Delta G°$ for 7 ⇌ 8 is evaluated to be 0.58 ± 0.08 kcal/mol in excellent agreement with the $\Delta G°$ of 0.8 kcal/mol at 132°C found by Beak et al[152].

Our temperature studies on this equilibrium 7 ⇌ 8 indicate no significant change between the spectra at 130°C (K_{eq} = 0.48 ± 0.05) and 240°C (K_{eq} = 0.51 ± 0.02). However, one can estimate the enthalpy change ($\Delta H°$) by considering the uncertainty limit in the K_{eq} values determined at the above-mentioned temperatures and using van't Hoff's expression[197], where K_{T_2} and K_{T_1} are the equilibrium

$$\ln \frac{K_{T_2}}{K_{T_1}} = \frac{-\Delta H°}{R}\left(\frac{1}{T_2} - \frac{1}{T_1}\right) \qquad (38)$$

constants at temperatures T_2 and T_1 respectively, and R is the gas constant. Hence $\Delta H°$ is estimated to be 0.23 ± 0.55 kcal/mol which is in agreement with the value determined by Beak et al[152], $\Delta H°$ = -0.3 ± 0.3 kcal/mol using gas phase UV-spectroscopic techniques.

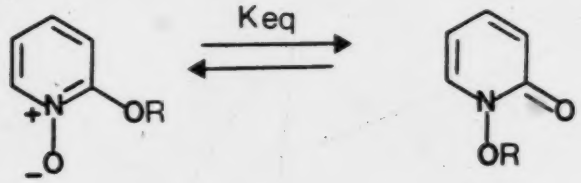

	R		R
11a	H	12a	H
11b	ET	12b	ET

The assignment for the equilibrium 11a ⇌ 12a is not so straightforward. N_{1S} and O_{1S} ionization regions show only one and two peaks respectively indicating that there is one dominating species in the gas phase. Comparison of the separation between the O_{1S} ionizations for the blocked derivative 12b (3.09 eV) and that found for 11a ⇌ 12a (3.07 eV) suggests that the oxygens in both cases are of similar charge type and thus the equilibrium must be lying on the side of 12a. Further support comes from a comparison of the difference in N_{1S} E_B for pyridine and its N-oxide (ΔE_B = 3.71 eV). Assuming that this ΔE_B can be applied to the difference in N_{1S} E_B between 7 and 11a, the estimated N_{1S} E_B of 11a then becomes 408.67 eV. The observed E_B for 11a ⇌ 12a is less than this value by some 0.6 eV suggesting that the dominant species does not have such a positive nitrogen and is therefore more compatible with 12a. It would be desirable to investigate 11b for further evidence to support the proposal that 12a is the dominant species. Unfortunately, under the conditions of the experiment, heating of 11b causes it to rearrange to 12b and the XPS spectrum obtained showed only 12b and no other species.

From consideration of the thermodynamic cycle in equation 38, the gas phase basicity of the pyridine and pyridone forms cannot differ by more than

0.58 kcal/mol, even though the former is N-protonated while the latter is O-protonated.

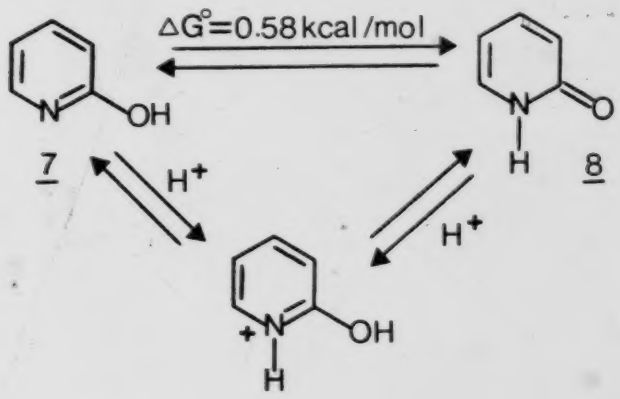

(38)

That the N_{1S} E_B for 8 is 1.65 eV greater than that for 7 even though the basicities cannot be appreciably different provides unquestionable evidence for the lack of correlation between E_B and ΔG° when the sites of protonation and photoionization are different. One should therefore expect a correlation between O_{1S} E_B and ΔG° for compound 8 (*vide infra*). Since both pyridine and 7 have similar N_{1S} E_B, their ΔG° values are expected to be roughly the same according to the correlation equation 32. Consequently, compound 8 is also expected to have similar ΔG° value as that of the parent pyridine.

(II) Circumstances under which N_{1S} E_B-$\Delta G°$ correlation breaks down

The main assumptions under which correlations between E_B and $\Delta G°$ will hold are that (a) the site of protonation and ionization are the same, and (b) within a series of closely related compounds there are not large energetically different geometry changes accompanying protonation. In this section, examples whose deviation from the defined E_B-$\Delta G°$ correlation line are explained by either or both of the above reasons.

Figure 21 shows the plot of N_{1S} E_B vs $(-)\delta\Delta G°$ whose values are taken from Table 8. Selected pyridine data were abstracted from Table 2. All $\Delta G°$ values were obtained from the published work of Kebarle[131], Taft[129,132], and Aue[198], the latter two sets of data being determined by ICR experiments at 300°K and the former one by high pressure mass spectrometry at 600°K, but are corrected to 300°K[199]. The three straight lines on the graph represent the upper and lower limits (± 1 kcal/mol) for the correlation for which (a) the site of protonation is undoubtedly nitrogen, i.e., pyridines, quinuclidine (32) and diazabicyclooctane (34) and some anilines and (b) the geometry changes accompanying protonation are small because of molecular rigidity. The best straight line

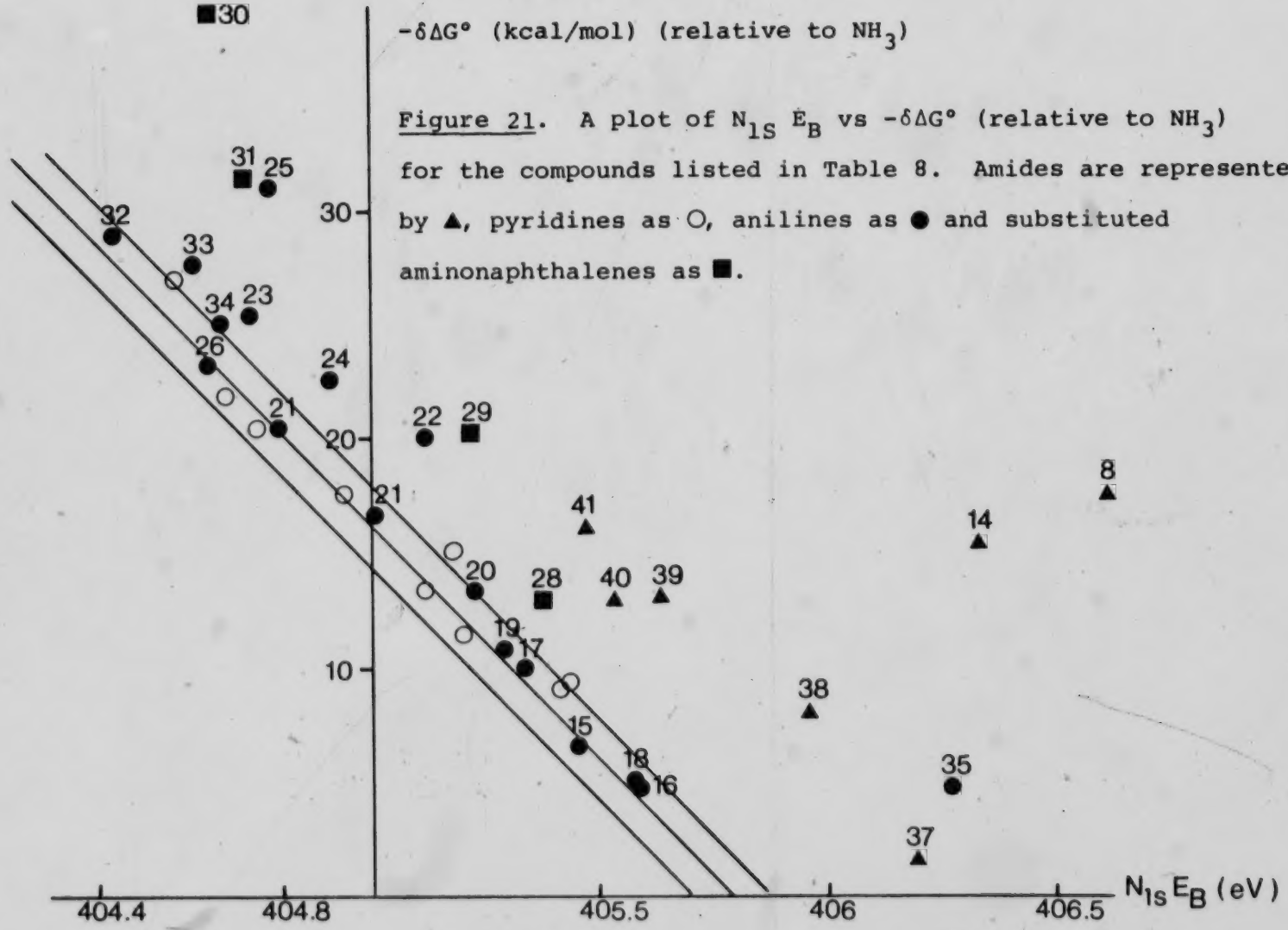

Figure 21. A plot of N_{1S} E_B vs $-\delta\Delta G°$ (relative to NH_3) for the compounds listed in Table 8. Amides are represented by ▲, pyridines as ○, anilines as ● and substituted aminonaphthalenes as ■.

Table 8. E_B, $\delta\Delta G°$ and $\delta\Delta H°$ Values Relative to NH_3.[a]

	Compound	N_{1S} E_B (eV)	$\delta\Delta G°$ (kcal/mol)	$\delta\Delta H°$ (kcal/mol)[c]
15	aniline	405.45	- 6.7[b]	-
16	p-fluoroaniline	405.59	- 4.6[c]	- 4.4
17	p-methylaniline	405.33	-10.1[c]	- 9.9
18	p-chloroaniline	405.58	- 5.1[c]	- 4.9
19	p-methoxyaniline	405.29	-10.9[d]	-10.7
20	N-methylaniline	405.22	-13.5[b]	-
21	N-ethylaniline	405.01	-16.9[b]	-
22	N,N-dimethylaniline	405.11	-20.1[b], -19.8[c]	-
23	N,N-diethylaniline	404.73	-25.4[b]	-
24	N-methyl-N-ethyl-aniline	404.91	-22.7[b]	-
25	O-bis-dimethylaminobenzene	404.78	-31.0[b]	-
26	N-phenylpiperidine	404.64	-23.3[c]	-23.0
27	N-phenylpyrrolidine	404.79	-20.6[c]	-20.4
28	1-aminonaphthalene	405.37	-13.1[b]	-
29	1,8-diaminonaphthalene	405.22	-20.3[b]	-
30	1,8-bis-(dimethylamino)naphthalene	404.65	-38.4[b]	-
31	1-(N,N-dimethylamino-8-(N-methylamino)naphthalene	404.72±0.04	-31.4[b]	-
32	quinuclidine	404.43	-28.9[c]	-28.1

continued.....

Table 8 (continued):

	Compound	N_{1S} E_B (eV)	δΔG° (kcal/mol)	δΔH° (kcal/mol)[c]
33	benzoquinuclidine	404.61	-27.7[c]	-27.8
34	1,4-diazabicyclooctane	404.67	-25.1[c]	-
35	pyrrole	406.27	- 4.8[b]	-

Amides

		N_{1S} E_B (eV)	O_{1S} E_B (eV)	δΔG° (kcal/mol)	δΔH° (kcal/mol)
36	formamide	406.45	537.96	-	-
37	N-methylformamide	406.19	537.48	- 1.8[c]	- 0.5[c]
38	N,N-dimethylformamide	405.96	537.09	- 8.1[c]	- 7.1[c]
39	N,N-dimethylacetamide	405.63	536.78	-13.2[c]	-12.4[c]
40	N-methylpyrrolidone	405.53	536.79	-13.0[e]	-11.5[e]
41	N-methylpiperidone	405.47	536.60	-16.2[e]	-14.0[e]
14	N-methyl-2-pyridone	406.33	536.36	-15.5[e]	-14.7[e]
8	2-pyridone	406.61	536.66	f	-
42	N,N-diethylacetamide	405.33	536.59	-	-

continued.....

Table 8 (continued):

a. E_B precision ±0.03 eV unless otherwise noted. $\Delta G°$ values corrected to 300°K and are relative to NH_3.

b. Ref. 131.

c. Ref. 129,132.

d. Ref. 169, 170.

e. Ref. 198.

f. No $\Delta G°$ value reported, but estimated to be close to that of pyridine (*vide supra*).

encompassing 21 bases within the upper and lower lines is

$$\delta\Delta G^\circ = 20.6486\ (E_B\ N_{1S}) - 8379.37\ \text{kcal/mol}\ (r = 0.994) \quad (39)$$

Other points which lie considerably off the correlation line are the subject of discussion here.

One should note that the deviating points are all above the correlation line indicating that these compounds appear to be more basic than that predicted from the N_{1S} E_B's. This is due to the energy gained from either changes in molecular geometry accompanying protonation or change in site of protonation in order to better stabilize the positive charge.

Amides (36-42, 8, 14)

Because of the observed difference in N_{1S} E_B but similarity in ΔG° values of 7 $\rightleftharpoons$ 8, we decided to investigate a series of amides. The triangular points in Figure 20 represent amides which generally are located above the N_{1S} correlation line. The amides 37-41 form a reasonably straight line ($r = 0.98$) with a slope (17.43 kcal/mol/eV) roughly parallel to the main line. However, the pyridones (8, 14) do not fit even this correlation line and appear to be far more basic than expected on the basis of their N_{1S} E_B's although ΔG° value of 8 is a predicted one from the correlation studies of N_{1S} E_B and

$\delta\Delta G°$ in pyridines (*vide supra*). This deviation can be understood if one considers that on protonation the pyridones relax to an aromatic species which provides an extra stability to the molecule (equation 40) and this cannot be monitored by the N_{1S} photoemission process.

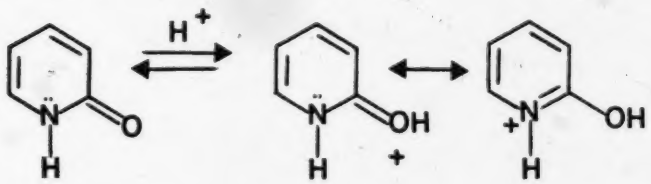

(40)

Shown in Figure 22 is a graph of O_{1S} E_B vs $\delta\Delta G°$ for the amides (37-41, 8, 14) in which excellent correlation is found for amides 37-41 and rather good correlation for 8, 14. The best fit straight line for the amides 37-41 is

$$\delta\Delta G° = 15.844\,(O_{1S}\ E_B) - 8517.96 \text{ kcal/mol} \quad (r = 0.999) \qquad (41)$$

which should allow one to predict the basicity of other amide compounds. For example, the $\delta\Delta G°$ predicted for formamide is 1.8 kcal/mol (less basic than ammonia) from equation 39 and is 5.7 kcal/mol from the O_{1S} E_B-$\Delta G°$ correlation equation. However, the better fit in the O_{1S} E_B vs $\Delta G°$ plot allows a higher degree of confidence in the number predicted from equation 41 than in the basicity predicted on the basis of the N_{1S} E_B (equation 39).

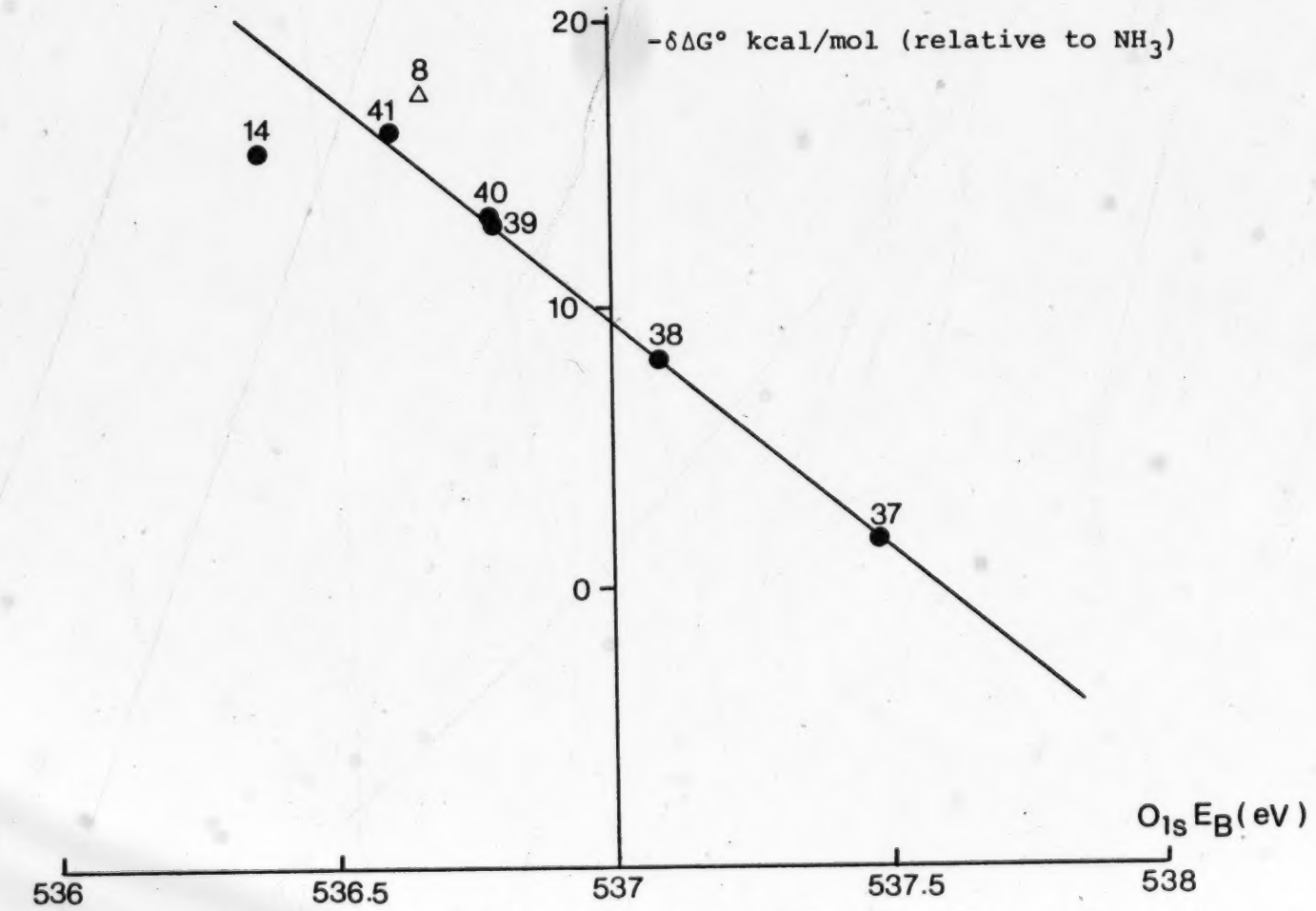

Figure 22. A plot of O_{1S} E_B against -δΔG° (relative to NH_3) for various amides. The open triangle is the predicted basicity for 2-pyridone.

Aniline, N-substituted, N,N-disubstituted and *p*-substituted anilines

Recently, much attention was devoted to the gas phase basicities of aniline derivatives with an eye to determining the site of protonation[127,131,169-170]. It was suggested[169-170] that aniline, N,N-dimethylaniline and some p-substituted anilines favor N-protonation. Figure 21 reveals that the anilines 15-19, 20, 21, 26, 27 fall within the correlation limit in agreement with the belief[169-170] that these molecules are nitrogen protonated. Although N,N-dimethylaniline (23) is predicted to favor N-protonation[169], it deviates from the correlation line. The speculated reason for the deviation is discussed in the following.

N-methylated anilines represent an interesting case since the angle (θ) between the RNR plane and the aromatic ring (equation 42) depends on the number and type of substituents attached to the nitrogen atom.

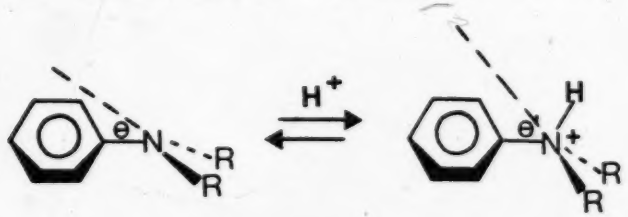

(42)

Upon protonation, the nitrogen atom in the N-methylated anilines adopts an approximately tetrahedral geometry which allows θ' to be as high as 55° if the CNR

angle (θ) is assumed to be 109.5°, and hence if the starting aniline is close to planarity (i.e., $\theta \simeq 0$) a significant geometry change will occur. The magnitude of this change becomes smaller as θ increases towards θ'.

Aniline has been demonstrated to be non-planar in the gas phase by microwave[200], UV[201], and far IR studies[202-204] with support from theoretical calculations[205]. The angle θ is found to be between 42° and 46° from these studies. MINDO/3 calculations on the anilium ion (*vide infra*) gives θ' a value of 56° from which one finds an increase of 10° in angle θ upon protonation of the aniline molecule based on the experimental value of θ = 46°. Apparently, this geometry change (10-15°) is not large enough to cause aniline to deviate from the N_{1S} E_B-ΔG° correlation line so its energetic advantage must be quite small. For N-methylaniline 20 (and analogously N-ethylaniline) θ is estimated to be 38.5° from solution dipole moment measurements[206] and thus this compound also falls on the correlation line with aniline. A similar explanation can also be applied to *p*-fluoroaniline whose θ is reported to be between 43°[204] and 46.4°[207]. Solution phase data for substituted anilines indicate θ is large (close to θ value in aniline) for electron donors and smaller for electron withdrawers being near 0° for

p-nitroaniline[208-209], which is therefore not expected to fall on the correlation line because of large geometry changes accompanying protonation.

As for N,N-dimethylaniline (22), a previous suggestion[127] for its failure to correlate on the N_{1S} E_B vs PA graph for various amines was considered to arise either from "stabilization of its ground state or destabilization of the N_{1S} hole state" relative to those for aniline. Our present results tend to favor the explanation based on geometry changes accompanying protonation. The reason is that the ground state geometry is close to planarity for the nitrogen atom as is determined by gas phase electron diffraction measurements[210], and protonation would then cause a large geometry change at the nitrogen. Since this protonation-rehybridization step cannot be probed by photoionization, the relative basicity value therefore appears to be higher (20 kcal/mol) than that can be predicted by N_{1S} E_B (15 kcal/mol). This 5 kcal/mol increase in energy can be regarded as a result of change in geometry to stabilize the positive charge. A similar explanation is also applied to compounds 23 and 24.

While little structural information is available for N-phenylpiperidine (26) and N-phenylpyrrolidine (27), Drieding models indicate the saturated ring should

hold the ring approximately tetrahedral so that minimal geometry changes are expected to occur on protonation. That 26 and 27 lie on the correlation line supports this idea.

Substituted amino-naphthalenes (28-31)

All amino-naphthalene compounds (28-31) investigated here deviate considerably from the correlation line with the most severe case being 30 (9). Compound 28 has been suggested by Kebarle et al[131] to be ring-protonated consistent with the present finding. By analogy with the structure of aniline and some substituted anilines it is unlikely that the amino group in 28 will undergo energetically significant geometry changes on protonation and thus a different site of protonation and ionization seems to be a reasonable explanation for the deviation. It is also suggested that 29-31 (as well as 25) are nitrogen protonated and that the unusually high basicities are due to H-bond formation resulting after protonation (equation 43).

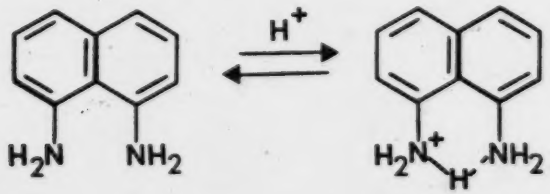

(43)

As stated before, X-ray crystallographic data on 30 (9) and its protonated derivative[166-167] indicate that the distortion from planarity of the naphthalene ring of 30 is relieved upon protonation, the two nitrogens contracting from 2.79 Å in 30 to 2.65 Å in the protonated species. This relief of ground state strain with the H-bond formation between the two nitrogen lone pairs permits a substantial increase in basicity (15 kcal/mol) of 30 as measured by its deviation from the correlation line. The smaller deviation of 29 and 31 from the correlation line is probably due to less ground state steric strain as predicted by Drieding models. Similarly, the 11 kcal/mol deviation of 25 can be explained based on the N-lone pair reorientation to chelate the proton.

MINDO/3 calculations for pyridine, quinuclidine, aniline and *o*-diaminobenzene

The purpose of these calculations is the same as those for the methoxypyridines discussed in Section I, i.e., to determine how important geometry reorganization is upon addition of a proton to the nitrogen. Again, the same hypothetical protonation process as that shown in equation 35 is considered. If the molecular structure opposes such geometry changes the difference between the calculated adiabatic and vertical ions should be

small. However, if the hybridization of the atom (nitrogen) changes from Sp^2 in the neutral state to Sp^3 in the ionic state, then the calculated differences in ΔH_f for the adiabatic and vertical ions should reflect this by giving a large stabilization for the former ion. Table 9 lists the heats of formation (ΔH_f) of the various hypothetical steps for the compounds considered. Pyridine and quinuclidine are examples in which geometry reorganization should not be important because of their molecular rigidity, and this can be seen from the calculated differences between adiabatic and vertical ions which are both -2.3 kcal/mol.

While the calculated ΔH_f for 15 reproduced the previously published value[192,211], the calculation fails to produce the experimental geometry and prefers instead to favor a planar conformation for the amino group such that the lone pair electrons can conjugate with the ring. Nevertheless this calculation should give indication on the magnitude of the rehybridizational energy associated in passing from Sp^2 neutral to Sp^3 ion since the anilium ion should possess a tetrahedral nitrogen. As the vertical ion is a hypothetical entity no significance should be attached to its calculated ΔH_f, other than as a reference number with which to compare the adiabatic ion. The calculated difference

Table 9. MINDO/3 Calculated Heats of Formation for Some Bases.

	ΔH_f in kcal/mol				
	B: $\xrightarrow{H^{\oplus}}$		$B\text{-}H^{\oplus}$	$\longrightarrow$	$BH^{\oplus}$
Base	Base	$\Delta\Delta H_f$	Vertical ion	$\Delta\Delta H_f$	Adiabatic ion
pyridine (42)	34.1	135.3	169.4	- 2.3	167.1
quinuclidine (32)	22.9	142.9	165.8	- 2.3	163.5
4-methoxypyridine[a]	-15.8	131.4	115.6	- 4.2	111.4
o-diamino benzene (43)	12.6	148.7	161.3	- 2.2 - 8.4	159.1[b] 152.9[c]
aniline[d] (15)	17.9	182.8	200.7	-35.1	165.6

a. Table 4

b. H-bonded and N lone pairs $\perp$ to benzene π-system (see text).

c. Non-H-bonded (see text) with remaining N lone pair conjugated with benzene π-system.

d. Calculated geometry of aniline nearly planar contrasting experimental data of ref. 200-205.

between the vertical and adiabatic ion is found to be larger (-35 kcal/mol) than that for 32 and 42, supporting the idea that correlation between E_B and $\Delta G°$ will break down if significant geometry changes occur during protonation.

O-diaminobenzene 43 should resemble its N-methylated derivative, 25, which has been suggested to exist as a H-bonded structure in the protonated state[131]. The calculations for 43 indicate that the most stable form of the ion (after full geometry optimized calculation) does not involve H-bonding, but has one amino group in a planar conformation (with respect to the benzene ring) and the other one as tetrahedral (equation 44). The ΔH_f value for this adiabatic ion is found to be 152.9 kcal/mol.

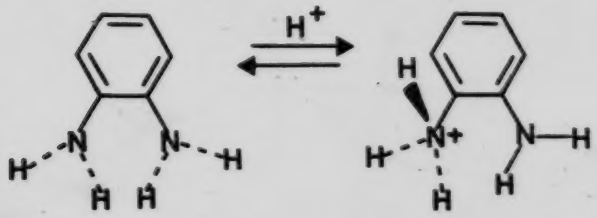

(44)

A calculation on the H-bonded ion structure with full geometry optimization indicates that it is a local minimum with a ΔH_f of 159.1 kcal/mol, 6.2 kcal/mol higher than the ion structure shown in equation 44.

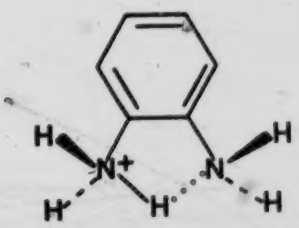

44

However, the higher energy of the optimized structure (44) is suspect since it has been shown[212-213] by other workers that the MINDO/3 method fails to reproduce the energetics of intermolecularly H-bonded systems and probably the intramolecularly H-bonded systems as well. Therefore the validity of the calculation for systems where the conjugate acids are H-bonded may be doubtful.

Site of protonation of *m*-substituted anilines

The question of the preferred site of protonation of substituted aromatics in the gas phase has been the subject of some recent publications[169,170,194-196]. Aniline was determined[169] to favor N-protonation over ring protonation by 1-3 kcal/mol and because of this small energy difference, selective substitution might be expected to influence the site of protonation. Our findings concerning the preferred site of protonation of *m*-substituted anilines are presented as follows.

It was suggested[169,170] that the *meta* electron-

donating substituents CH_3, OCH_3 and NH_2 favor ring protonation while electron withdrawers prefer N-protonation. This can be understood if one considers the resonance interactions of the substituent with the ring in the protonated *m*-anisidine (equation 45).

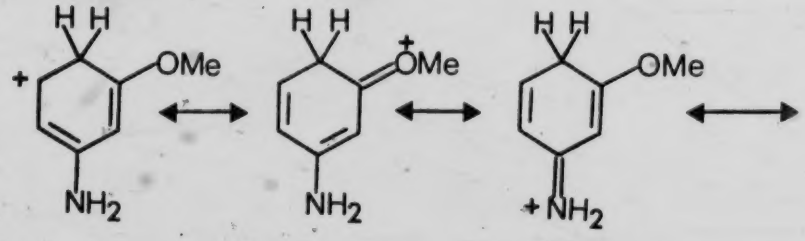

(45)

The formation of positive charge on the ring carbon is stabilized by both the amino- and methoxy groups through resonance interactions. However, in the case of electron-withdrawing substituents, this positive charge would be destabilized by the inductive effects of the substituent and hence N-protonation becomes more favorable than ring protonation.

Figure 23 illustrates the plot of N_{1S} ΔE_B vs $\delta\Delta G°$ of *m*-substituted anilines (relative to aniline) whose values are taken from Table 10 and two straight lines can be drawn for each type of substituent. The electron-withdrawers themselves form a very good correlation line which has a close-to-unity slope (equation 46).

$$N_{1S}\ \Delta E_B = 1.17\ \delta\Delta G° - 0.25\ \text{kcal/mol}\ (r = 0.99) \qquad (46)$$

Table 10. N_{1S} ΔE_B and $\delta\Delta G°$ Values of *m*-Substituted Anilines Relative to Aniline.[a,b]

Compound		N_{1S} E_B (eV)	N_{1S} ΔE_B (eV)[c]	$\delta\Delta G°$ (kcal/mol)[d,e]
45	NH_2	405.30	0.15	-12.8
46	Et	405.33	0.12	- 3.6
47	CH_3	405.34	0.11	- 3.0
48	OH	405.34	0.11	- 3.8
49	OCH_3	405.37	0.08	- 7.2
50	SCH_3	405.39	0.06	- 4.5
15	H	405.45	0	0.0
51	I	405.55	-0.1	1.1
52	Br	405.58	-0.13	2.4
53	CO_2H	405.58	-0.13	-
54	F	405.61	-0.16	3.3
55	Cl	405.66	-0.21	3.3
56	CF_3	405.78	-0.33	6.2
57	CN	405.96	-0.51	9.6
58	NO_2	405.97	-0.52	-

a. N_{1S} E_B values are reported as the average of at least 3 runs and have a precision of >±0.03 eV.

b. Calibrated against an internal standard neon Auger line (E_K = 804.56 eV)[37].

continued.....

Table 10 (continued):

c. $N_{1S}\ \Delta E_B = N_{1S}\ E_B$ (aniline) - $N_{1S}\ E_B$ (substituted aniline); a positive value indicates the base is easier to ionize than aniline.

d. $\delta\Delta G°$ = $\Delta G°$ (substituted aniline) - $\Delta G°$ (aniline); a negative value for $\delta\Delta G°$ indicates the base is stronger than aniline.

e. P. Kebarle, Y.K. Lau and K. Nishizawa, Unpublished results.

Note that the *m*-alkyl substituents lie very close to this correlation line suggesting that the free energy difference between nitrogen and ring protonation cannot be very large. As for the electron donors, least squares analysis reveals some scatter of data points (equation 47).

$$N_{1S}\ \Delta E_B = 0.10\ \delta\Delta G^\circ + 1.75\ \text{kcal/mol}\ (r = 0.52) \qquad (47)$$

The E_B values of these "donors" indicate that they are not very sensitive to the change in substituent judging from the slope of the line in equation 47, probably due to the counterbalancing of inductive and polarization effects. On the other hand, the stability of the ring-protonated species depends on how strong the donor is in terms of its ability to resonance stabilize the positive charge (equation 45).

Although there is no structural information on the orientation of the OCH_3 group (similarly with SCH_3) in *m*-anisidine it may exist with the lone pair either coplanar with or perpendicular to the benzene π-system in the ground state. Regardless of this ground state geometry protonation will allow the lone pair to align with the π ring for stabilization of the positive charge through resonance interaction. Accordingly, the "coplanar" arrangement of the OCH_3 group in anisidine should involve minimal geometry changes upon

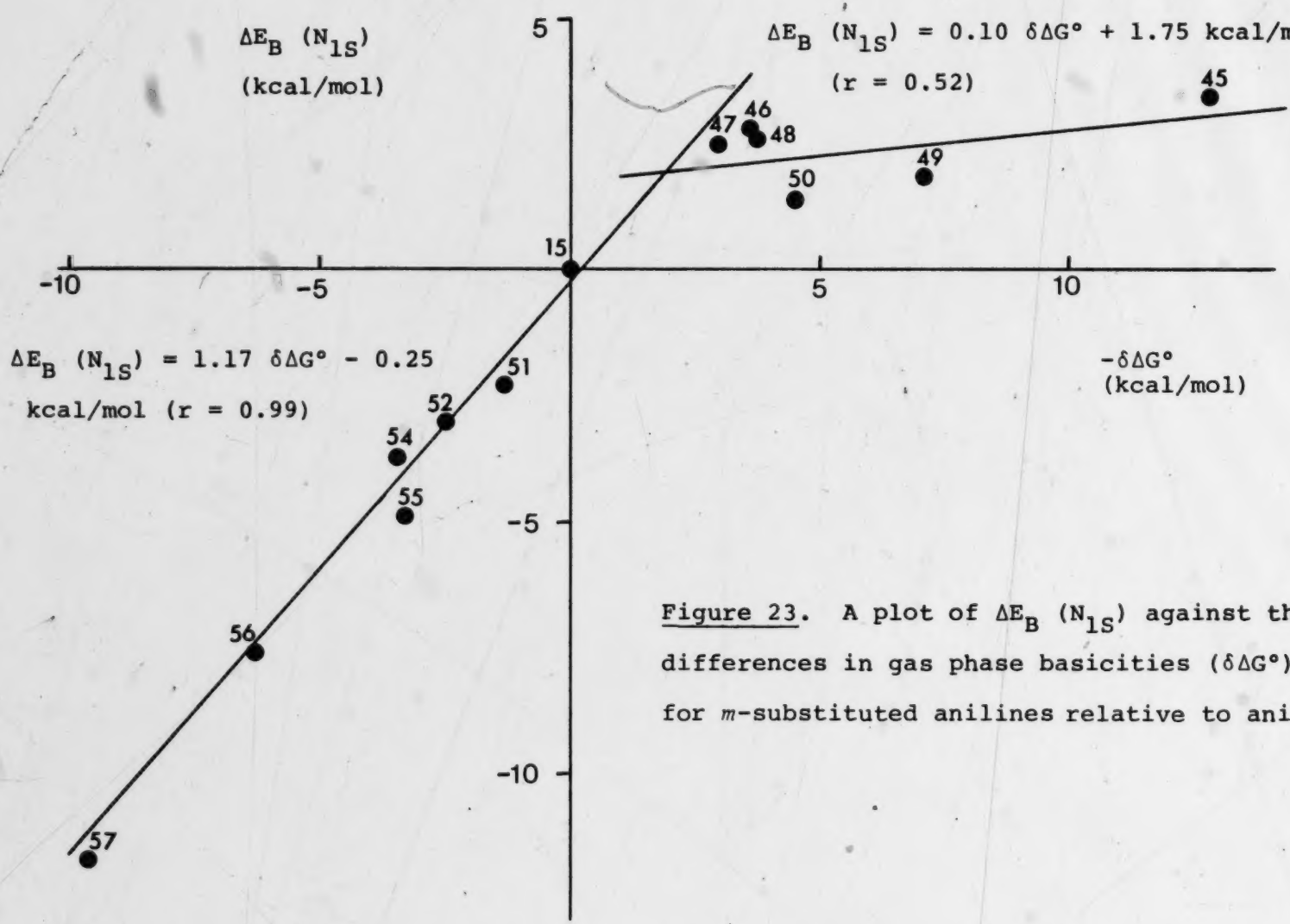

Figure 23. A plot of ΔE_B (N_{1S}) against the differences in gas phase basicities ($\delta\Delta G°$) for *m*-substituted anilines relative to aniline.

protonation while a near 90° turn of the OCH_3 group is expected to be observed for the "perpendicular" arrangement. We have therefore decided to employ MINDO/3 calculations to gain some insight on the conformation of *m*-anisidine. The result of the calculations (with full geometry optimization) indicated that coplanarity of the OCH_3 lone pair with the benzene ring gives a more stable ground state structure (ΔH_f = -30.8 kcal/mol), being 1.6 kcal/mol lower in energy than the "perpendicular" arrangement. This finding is indirectly supported by the work of Houk et al[214] on dimethoxybenzene in which the two electron-donating substituents have their lone pairs aligned with the benzene π system. It is therefore unlikely that geometry changes occurring upon protonation of *m*-anisidine are large enough to account for the deviation, but is satisfactorily explained by ring protonation. It is also interesting at this point to examine the correlation between N_{1S} ΔE_B of *m*-substituted anilines and the corresponding σ-values since it was shown in the last section that pyridines exhibit good correlations between the two values. Figure 24 illustrates the plot of N_{1S} ΔE_B vs σ-parameters[187] and the correlation equation is represented as follows.

$$N_{1S}\ \Delta E_B = -0.81\ \sigma + 0.09\ \text{eV}\ (r = 0.93) \qquad (48)$$

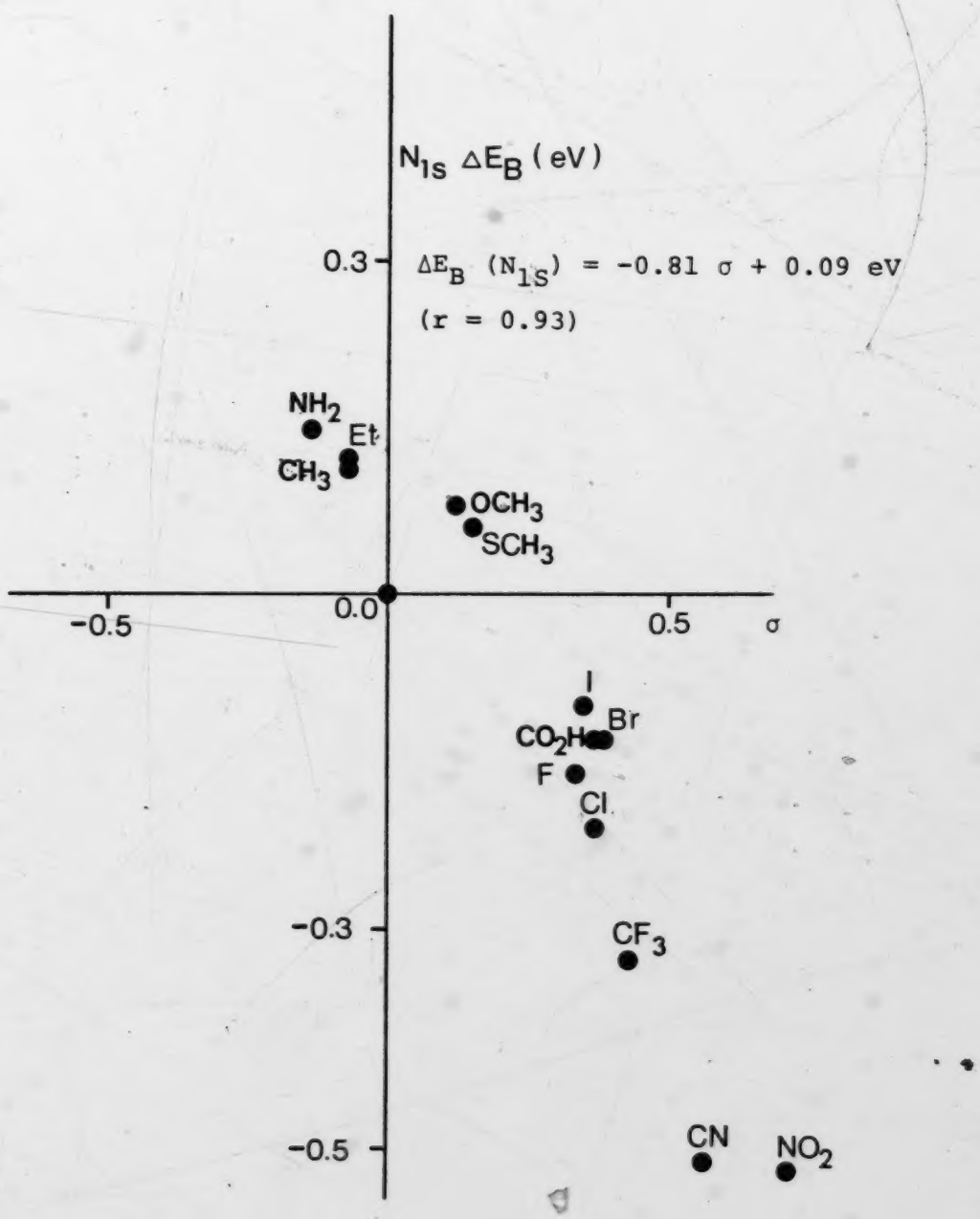

Figure 24. N_{1S} ΔE_B vs σ-values for *m*-substituted anilines relative to aniline.

There is sufficient scatter in the points to indicate some shortcoming in the correlation. It had been shown that the change in ionization constant (ΔpK) of substituted anilines[215] (relative to aniline) correlates well with the σ-values which are derived from benzoic acid ionization. The unexceptional correlation between N_{1S} ΔE_B of *m*-substituted anilines and the σ-values seems to suggest somewhat different substituent effects in the gas phase photoionization of *m*-substituted anilines and in the solution phase ionization of *m*-substituted benzoic acids perhaps due to solvation effects. However, the N_{1S} ΔE_B - σ correlation is better (at least according to the correlation coefficient) for the *p*-substituted anilines (equation 49) suggesting that mechanisms by which the substituents in the *para* position interact with the charged species produced by either aniline N_{1S} photoionization and benzoic acid ionization are similar (Figure 25).

$$N_{1S}\ \Delta E_B = -0.68\sigma - 0.01 \text{ eV } (r = 0.97) \qquad (49)$$

The better correlation found for *p*-substituted anilines was also observed for *p*-substituted fluorobenzenes on F_{1S} - σ plot reported by Siegbahn et al[216]. At this point, we have no explanation as to why the *m*-substituted anilines give a poor correlation with σ-values.

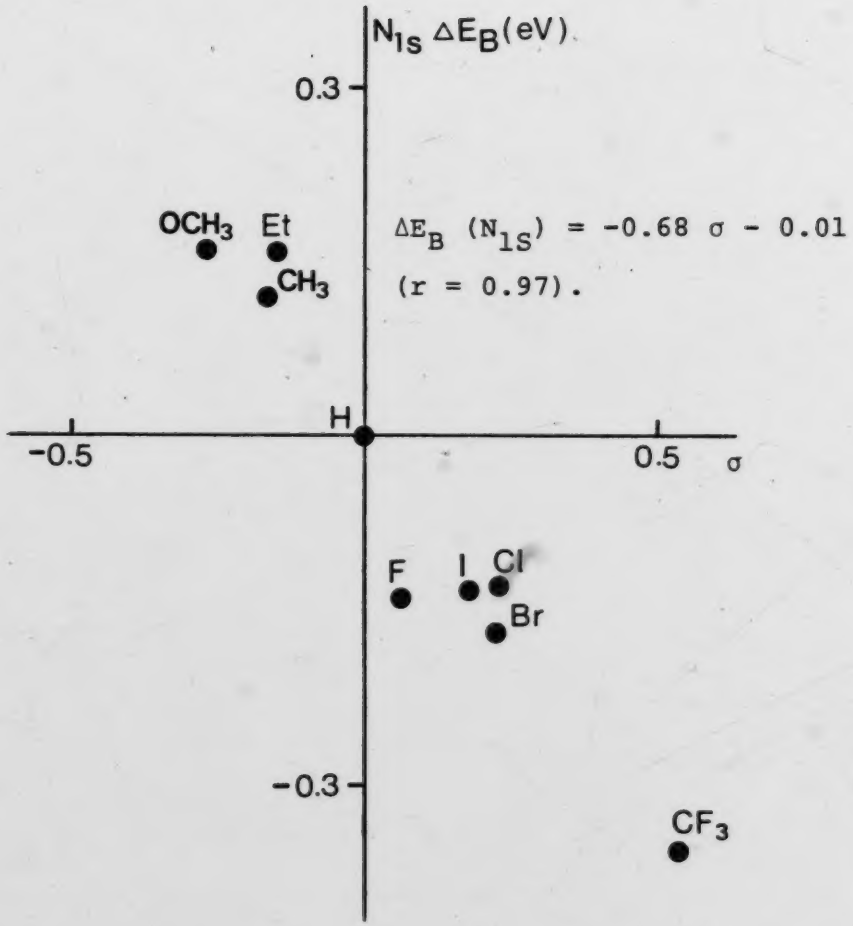

Figure 25. N_{1S} ΔE_B vs σ-values for *p*-substituted anilines relative to aniline.

EXPERIMENTAL

All routine spectral measurements were obtained with the same equipment described in Chapter II. All pyridine and aniline compounds, except the ones identified below, were commercially available and were purified by either sublimation or distillation prior to use. Preparative glpc was done on a HP 5830 A gas chromatograph using a stainless steel column (1/4 in. x 10 ft.) containing 10% polyphenyl ether on Chromosorb WAW-DMCS (80-100 mesh).

The substituted pyridines 3F[217], 2- and 4-NO_2[218], 3-NO_2[219], and 4-OCH_3[220], and N-methyl-2-pyridone[221], pyridine-N-oxide[222], N-phenyl-piperidine[223], N-phenyl-pyrrolidine[215], and benzoquinuclidine[224] were prepared according to existing procedures. The CF_3 substituted pyridines were generously provided by Drs. A.E. Feiring, W.A. Sheppard, and M. Raasch and Mr. E. Wonchoba of the Central Research and Development Department, E.I. Dupont de Nemours and Co., Wilmington, Delaware, 19898. N-hydroxy-2-pyridone, N-ethoxy-2-pyridone and 2-ethoxy-pyridine-N-oxide were kindly given by Dr. J.C. Vederas of this Department. All substituted-naphthalenes were also kindly provided by Prof. P. Kebarle.

4-Chloropyridine

4-Chloropyridine was obtained from the commercially available hydrochloride salt (Aldrich) according to the following procedure. The hydrochloride salt was basified using a saturated $NaHCO_3$ solution, It was then extracted with methylene chloride, which was then dried with anhydrous sodium sulfate and finally removal of solvent gave a red liquid from which after distillation (67-69°C/35 mm) yielded 4-chloropyridine as a colorless liquid (lit.[225] b.p. 147-148°C). All glassware was treated with NH_4OH and oven-dried before use, otherwise the 4-halopyridines tended to decompose during distillation.

4-Bromopyridine

It was prepared the same way as described for 4-chloropyridine. The colorless liquid was microdistilled at a bath temperature of 80°C/20 mm (lit.[226] b.p. 27.5-30°C/0.3-0.5 mm).

4-Fluoropyridine

4-Fluoropyridine was synthesized using a modified procedure of Lyle and Taft[227], and Desai[228]. 4-Amino-pyridine (3.6 gm, 0.038 mol) was dissolved in 16 ml of 48% fluoroboric acid and cooled to 0°C. The amine was diazotized by the addition of 3 gm (0.04 mol) of sodium nitrite in small portions with constant stirring.

The temperature of the solution was kept below 10°C during the addition process. The mixture was then allowed to stand at ice bath temperature for one hour. To decompose the diazonium salt the mixture was warmed slowly to room temperature. After the cessation of N_2 evolution, the solution was quickly cooled to 0°C and was neutralized with solid sodium bicarbonate. The resulting mixture was extracted with 100 ml of methylene chloride and dried over anhydrous sodium sulfate. The solvent was then removed and the residue was distilled (60-62°C/150 mm) to give 0.5 gm (13.6%) of colorless 4-fluoropyridine (lit.[228] b.p. 108°C/757 mm) which was stored over a pellet of sodium hydroxide to prevent decomposition.

3-Dimethylaminopyridine

The conversion of commercial 3-aminopyridine to 3-dimethylaminopyridine was done by the procedure of Clarke, Gillespie and Weisshaus[229]; 4.7 gm (0.05 mol) of the starting material gave after distillation (100°C bath temperature/0.3 mm) 2.9 gm (0.024 mol, 47.5%) of the corresponding dimethylaminopyridine (lit.[230] b.p. 108-110°C/12 mm).

3-Methoxypyridine

This was prepared using the same procedure as in the preparation of 4-methoxypyridine[220] with 3-chloro

pyridine as the starting material. After 3 days of heating at 130°C in a sealed tube using methanol as solvent, a mixture of 3-chloropyridine and 3-methoxypyridine was obtained. The 3-methoxypyridine was then isolated by preparative glpc and micro-distillation (50°C bath temperature/1 mm) to give a colorless liquid (lit.[231] b.p. 43-45°C/1 mm).

CHAPTER IV

DEPENDENCE OF THE π-IONIZATION ENERGY ON THE ORIENTATION OF AN ALLYLIC HYDROXYL OR METHOXYL SUBSTITUENT AS DETERMINED BY UV-PHOTOELECTRON SPECTROSCOPY.

INTRODUCTION

Substituent effects have been of considerable interest to chemists for some time and much effort has been expended in determining the mechanism of interaction between the substituent and the reaction site. These effects are generally considered in terms of inductive[232] and conjugative[233] factors with the former depending on the difference in the electronegativity of the interacting groups as well as their separation, whereas the latter rely on the mutual interaction of orbitals of like symmetry. The two effects either reinforce or oppose each other, thereby introducing uncertainty in the quantitative measurement of one or the other individual effects.

Recently, Pople et al[234-236] performed *ab initio* calculations on the rotational conformers of some simple acyclic molecules containing H, C, N, O and F. They found that for a molecule with two electronegative substituents bridged by a methylene unit the most stable conformation allows an orbital interaction

between the two substituents (equation 50). They suggested an electron transfer process with a π-type

(50)

donation (from X) and a σ-type acceptance (by C-Y) as shown in equation 50. Under this condition, the lone pair in X and the C-Y bond are required to be coplanar for maximum interaction, and consequently the "pair" of electrons in X should be more difficult to ionize when coplanarity is achieved than when the C-Y bond is orthogonal. In principle, one can probe the above prediction by investigating the ionization potential (ip) of this lone pair in X as a function of its orientation to the C-Y bond. As part of our interest in the application of pes to substituent effects we measured the ip's of a number of cyclic compounds in which allylic substituents are either coplanar with or perpendicular to the π-orbital using HeI radiation as the photon source. Our aim in this study was to find out whether there is a rotational dependence of this "bond – no bond" resonance stabilization (equation 50). For our particular case, Y is represented by the

allylic substituent (OR) while the "lone pair" of X is approximated by the π-bond.

Early pes studies on some *bis*-allylic oxygen compounds (45-48)[237,238] with different orientations of the *bis* oxygens relative to the π bond indicated that there is no significant change in the π ip's.

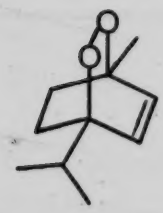

45

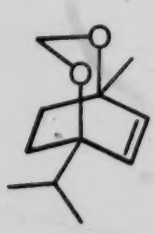

46

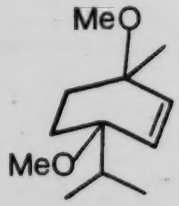

47

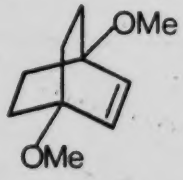

48

This invariance of the π ip's (between 9.65 and 9.70 eV) to the orientation of the *bis*-allylic C-O bonds and their higher values relative to bicyclooctene (π ip = 9.05 eV)[239] seemed to suggest the dominance of inductive effects.

This apparent discrepancy between the experimental and theoretical[234-236] results lead Brown and Marcinko[240] to investigate another series of compounds (49-52) in which only one substituent (ÖR) is involved in the interaction with the π orbital. They have shown a definite variance of the π ip's with the orientation of the substituents in these systems. In view of this orientational effect observed for compounds 49-52 it is

49

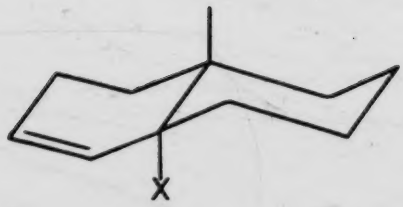

50

X	
a	H
b	OH
c	OMe

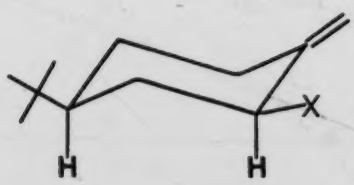

51

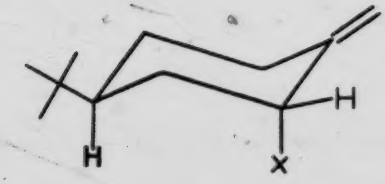

52

interesting to use this pes technique to determine the preferred orientations of similar substituents in systems (53-56) which are not as conformationally rigid

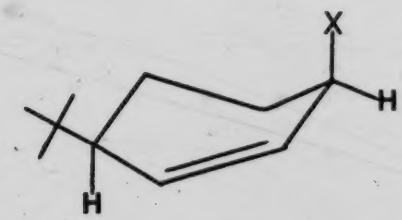

53

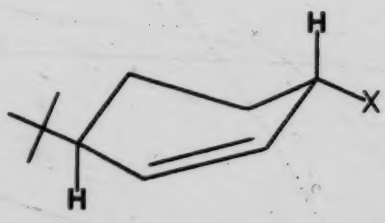

54

X	
a	H
b	OH
c	OMe

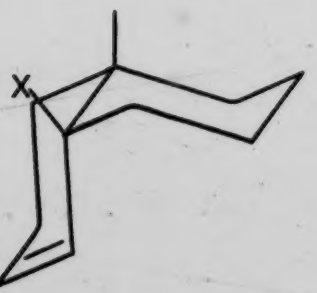

55

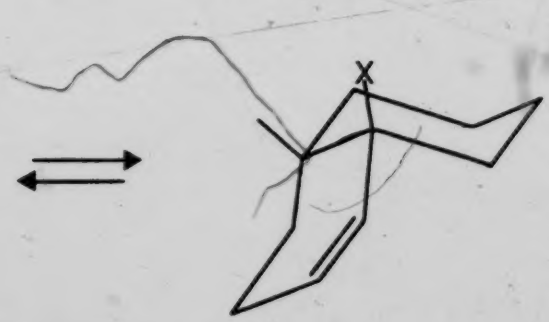

56

as 49-52. Although 53 and 54 contain a *tert*-butyl group, the flexibility provided by the cyclohexene allows the substituent X to be in pseudo-axial (53) and pseudo-equatorial positions (54), respectively. On the other hand, compound 55 can potentially exist in two conformations having the allylic C-X bond co-planar with (55) and orthogonal to (56) the σ-bond. In the following the preferred gas phase conformations of the allylic compounds 53-56 are discussed.

RESULTS

An attempt to determine the dihedral angles (θ and θ') between the allylic methine hydrogen (H_X and $H_{X'}$) and the adjacent vinyl hydrogen H_Y was made on 57 and

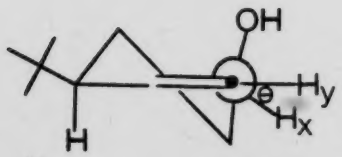

57

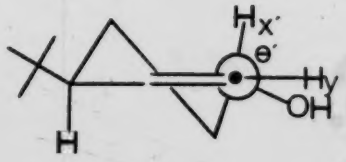

58

58 respectively in order to determine the favorable conformation for these two compounds. This was done by performing proton decoupling experiments based on the observed chemical shifts from the 400 MHz ^1H NMR spectra. Irradiation at the $H_X(H_{X'})$ region and observation on the change in H_Y region allows one to obtain the coupling constant (J) between $H_X(H_{X'})$ and H_Y. These $J_{H_XH_Y}$ and $J_{H_{X'},H_Y}$ were found to be 4.3 and 1.8 Hz respectively. Using the Karplus equation[241] developed for cycloolefins (equation 51), θ and θ' was determined to be about 50° and 65° respectively.

$$J = 10.6 \cos^2\theta \quad (0° \leq \theta \leq 90°) \qquad (51)$$

Note that the derivation of equation 51 did not take into account the effect of allylic electronegative substituents (OH) on the coupling constant between $H_X(H_{X'})$ and

H_Y which may be significant in both 57 and 58. Nevertheless, the difference between θ and θ' still provides a general idea of the difference between the conformations 57 and 58. Assuming that the angle between the OH and $H_X(H_{X'})$ is the usual tetrahedral angle, 109.5°, the dihedral angle between the OH group and the π system in 57 (58) is then equal to 31° (46°). Consequently, one can conclude that compound 57 permits more overlap between the π orbital and the C-O bond than compound 58. One may then observe a difference in the π ip between 57 and 58 from their pe spectra providing there are not specific solvation effects in the solution NMR measurement.

Since 55a serves as the parent compound with which to compare 55b and 55c, it is essential that its structure should be on firm ground. It was prepared from the α,β-unsaturated ketone[242] (59) by a Clemmensen reduction method[243] which could potentially give 55a, 50a, 60 (*cis* and *trans*) and 61, as shown in equation 52.

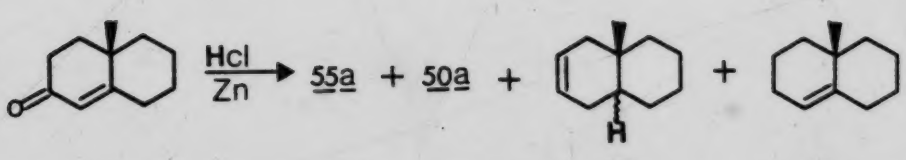

59 60 61 (52)

Compound 50a was produced in 10% yield and was identified by comparison with an authentic sample prepared via an independent route[240].

A 100 MHz ^{1}H NMR spectrum of the major product of the Clemmensen reduction revealed two vinyl protons centered at δ 5.52 indicating that the compound could be either 55a or 60 but not 61. Further support from the ^{13}C NMR data indicating two vinyl carbons separated by 7 ppm which appeared as doublets when proton coupled, and hence compound 61 cannot be the major product. The large ^{13}C chemical shift difference ($\Delta\delta\ ^{13}C$) for the vinyl carbons (7 ppm) seems to be more appropriate for 55a than 60 based on the argument below utilizing the empirical method developed by Roberts et al[244] for the prediction of alkene carbon-13 chemical shifts[245], the vinyl carbons in 60a should be very much the same (predicted $\Delta\delta\ ^{13}C$ = 0.5 ppm) while in 55a they should be quite different (predicted $\Delta\delta\ ^{13}C$ = 4.9 ppm). Comparison of the predicted $\Delta\delta\ ^{13}C$ with that of the experimental one therefore favors 55a. Nevertheless a more definitive proof was carried out by chemical degradation according to equation 53.

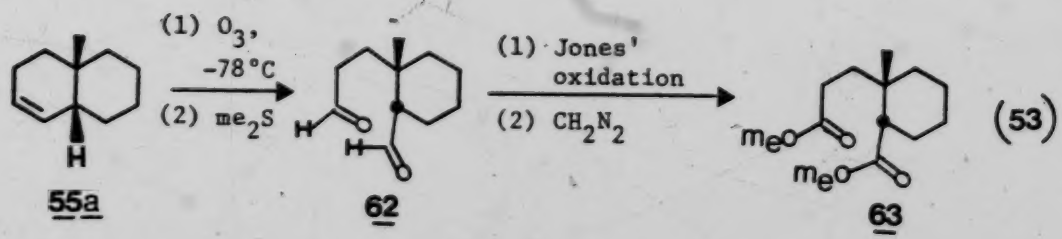

55a 62 63 (53)

Ozonolysis[246] of 55a followed by Jones' oxidation of the presumed dialdehyde intermediate 62 and final treatment with diazomethane gave, after chromatography over silica gel, the diester 63 in good yield. Analysis of the 200 MHz ^{1}H NMR spectrum of 63 showed an integrated areas of the carbonyl α-hydrogens and the methoxyhydrogens in a ratio of 1:2. This confirmed that the structure is 55a since following the same route compound 60 would give a diester having the corresponding integration ratio of 2:3. Utilizing the same chemical degradation procedure on a mixture of 55a and 50a resulted in two isomeric diesters, one corresponding to structure 63 and the other varying slightly in terms of its 200 MHz ^{1}H NMR spectrum. Hence, there is no doubt that the major product from the Clemmensen reduction of 59 is 55a.

The vertical ip's of compounds 53-56 and their saturated analogues (64-66) are shown in Table 11, and the spectra of 53b, 54b, 53c, 54c and 55 are presented in Figures 26-28. The assignments for 53-56 were made by comparing their vertical ip's with those of the saturated analogues. For example, the π-ip of 53a appears at 8.94 eV, while the saturated alcohol 64a exhibits $n_{\ddot{O}H}$ at 9.82 eV. It has been shown previously that with olefins possessing electronegative substituents the ip of each group is increased in the

Table 11. Vertical ionization energies (ip) and assignments for compounds 53, 54, 55, 56, 64, 65 and 66.

Compound		Vertical Ionization Energies (eV) $n_{\ddot{O}R}$	π	$\Delta ip^{a,b}$
53	a = H		8.94	0.0
	b = OH	10.07[d]	9.33	0.39
	c = OCH_3	9.53	9.29[e]	0.35
54	b = OH	10.21[d]	9.18	0.24
	c = OCH_3	9.61	8.97	0.03
55	a = H		8.92	0.0
	b = OH	9.64	9.26	0.34
	c = OCH_3	9.00	9.34	0.42
64	a = OH	9.82		
	b = OCH_3	9.36		
65	a = OH	9.91		
	b = OCH_3	9.32		
66	a = OH	9.45		
	b = OCH_3	9.08		
51[c]	a = H		9.09	0.0
	b = OH	10.15[d]	9.18	0.09
	c = OCH_3	9.55	8.97	-0.12
52[c]	b = OH	9.97[d]	9.37	0.28
	c = OCH_3	9.54	9.30	0.21

a. All values are averages of at least three runs and have a precision of ±0.02 eV unless otherwise noted.

b. Calibrated against argon; $\Delta ip = ip\pi$ (compound) - $ip\pi$ (parent olefin).

c. Reference 240.

c. Tentatively assigned; appears as a well-defined shoulder on the edge of σ-envelope.

d. Precision of ±0.03 eV.

Figure 26. The pe spectra *cis*- and *trans*-4-*tert*-butyl-2-cyclohexen-1-ol (53b and 54b) using argon as an internal reference.

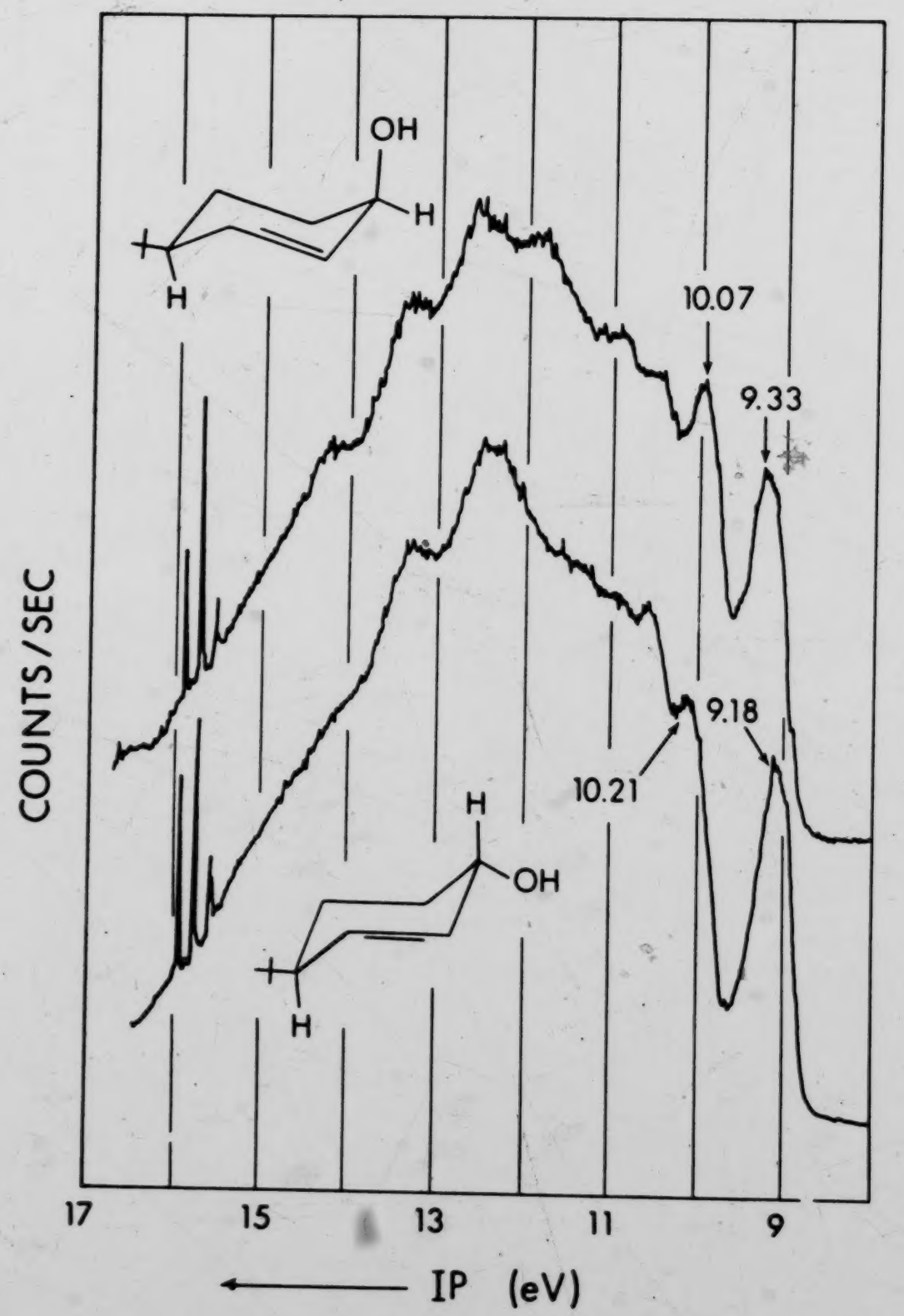
OH
H
H
10.07
9.33
9.18
10.21
H
OH
H
COUNTS/SEC
17
15
13
11
9
IP (eV)

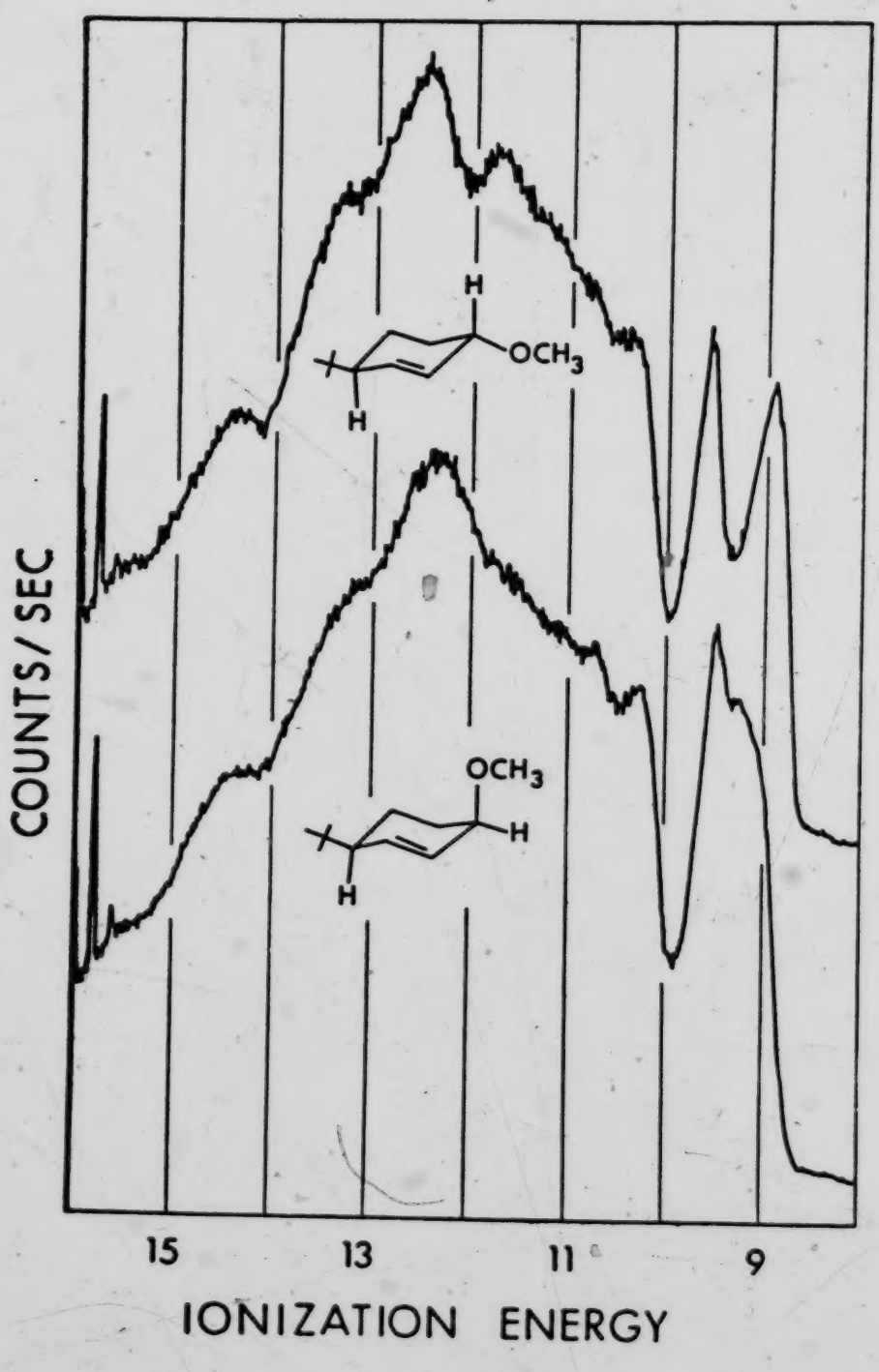

Figure 27. The pe spectra of *cis* and *trans*-3-methoxy-6-*tert*-butylcyclohexene (53c and 54c) using Argon as an internal calibrant.

Figure 28. The pe spectra of 5α-substituted-10α-methyl-Δ^3-octalins (55a,b,c) using Argon as an internal calibrant.

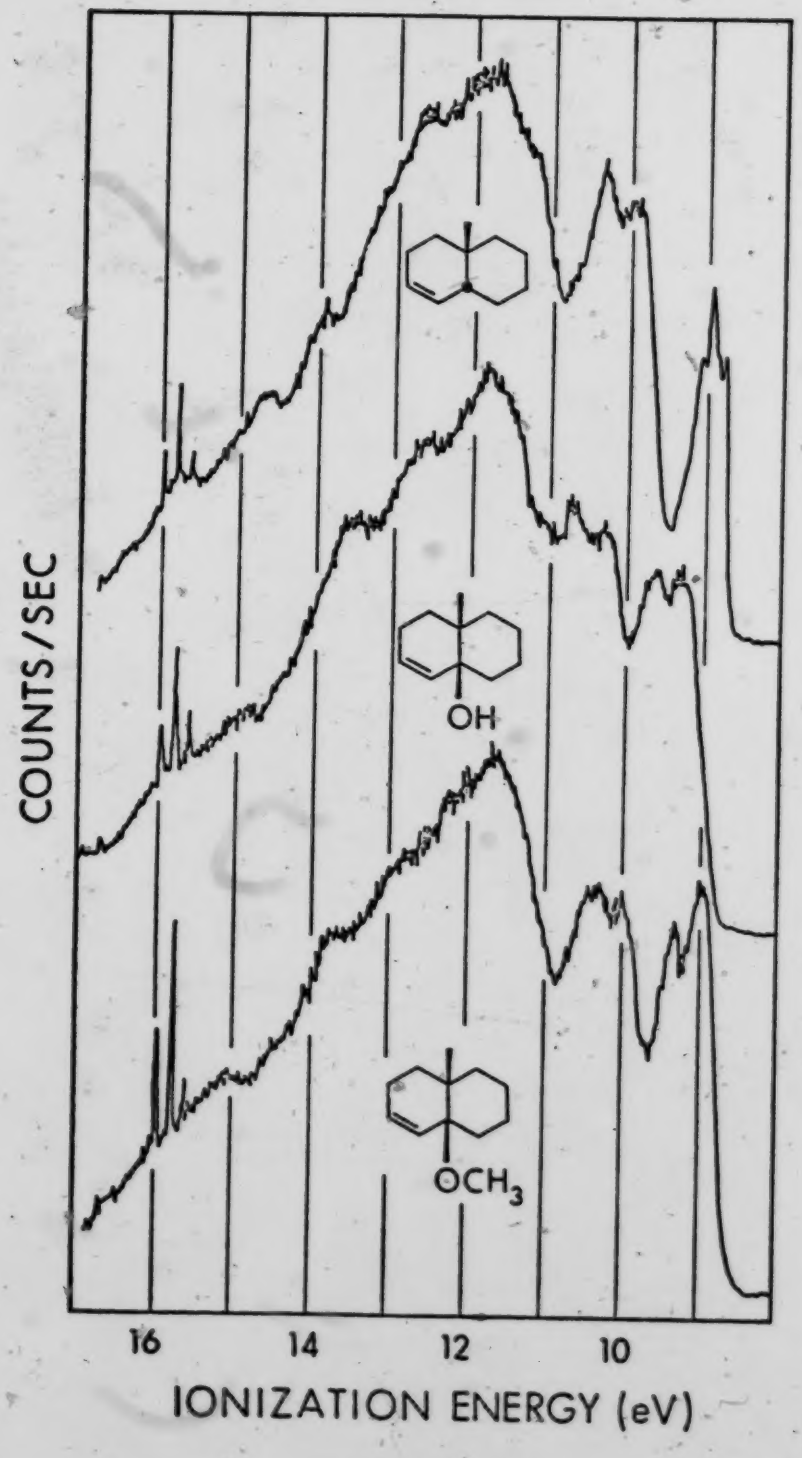

64

65

66

Y	
a	OH
b	OMe

presence of the other[247-252]. Therefore the π-ip in 53b appears at 9.33, 0.39 eV higher than in 53a, while the $\eta_{\ddot{O}H}$ is found to be 10.07, 0.25 eV higher than in 64a. It is a general observation that substitution of a methyl group for hydrogen lowered the ip of $\eta_{\ddot{O}R}$ by between 0.4 and 0.6 eV depending on the system. Thus in the ether 53c, the second ip is assigned to be from the $\eta_{\ddot{O}CH_3}$ orbital (9.53 eV) and the first ip to arise from the π bond (9.29 eV). In a similar fashion, compound 54 was assigned accordingly as shown in Table 11. The assignments of 55 and 56 are more complicated because of the possible equilibrium between them and they will be discussed in detail in the next section.

DISCUSSION

The structure of cyclohexene has been shown to adopt a half-chair conformation from the X-ray crystallographic measurements of some substituted cyclohexenes[253]. It has also been established that for 3-substituted cyclohexenes, electronegative substituents such as OH, OAc[254], Cl[255], and Br[255-256] tend to favor a pseudoaxial position which is in contrast to the usual preference of the equatorial position in the substituted cyclohexane series[257]. This is very similar to the anomeric effect[258-263], in which the axial orientation of an electronegative substituent in the 2-position of a tetrahydropyran is favored over the equatorial one. This effect was first discussed by Lemieux[258-260] in a detailed study of the anomerization of acetylated pento- and hexo-pyranoses and was explained in terms of dipole-dipole interactions between the ring C-O bonds and the anomeric C-X bond. These dipoles form a small angle when the substituent is equatorial (67), while they form a large one when the substituent is axial (68), the two dipoles becoming almost perpendicular.

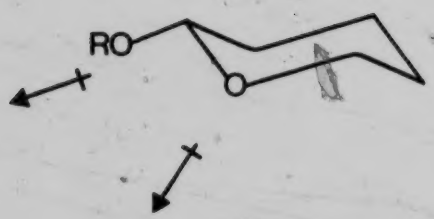

67

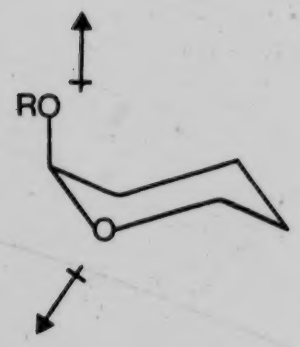

68

Another explanation for this anomeric effect, the rabbit-ear effect[258,262], says that the lone pair-lone pair interaction is significantly larger than either the lone pair-bonding pair or the bonding pair-bonding pair interactions. Structures 69,70 shows that one or less lone pair-lone pair repulsive interaction occurs when the substituent is axial (69) whereas the equatorial substituent experiences two (or less) such interactions (70). The preference for axial orientation is due to this repulsive interaction which destabilizes the equatorial conformation.

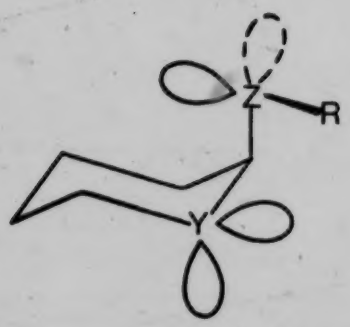

69

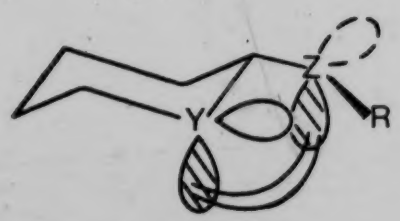

70

A third explanation known as the double bond-no bond resonance was offered[234-236,264-266], in which the charged resonance forms shown in equation 50 contribute to the observed anomeric effect. This can also be interpreted in terms of the overlap between

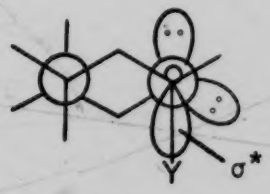

71

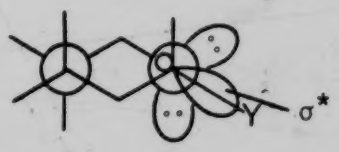

72

the lone-pair electrons on X ($n_{\ddot{X}}$) and the σ^* (anti-bonding) orbital of the C-Y bond (71) which results in the stabilization of X lone pair electrons. Not such a large interaction is possible for the equatorial substituent as shown in 72. This $n_{\ddot{X}}$-σ^* interaction should be maximal when $n_{\ddot{X}}$ and the C-Y bond are in an antiperiplanar position (71), and accordingly, the double bond-no bond resonance predicts a more stable form with Y in the axial position. Lessard et al[256] demonstrated this by a ^{13}C-NMR study of a number of 2-substituted methylenecyclohexanes and 3-substituted cyclohexenes for which the electronegative substituents were found to prefer a pseudo-axial conformation rather than a pseudo-equatorial one.

As shown in Table 11, compounds 53b,c and 54b,c

have very similar pe spectra when compared to their isomers 52b,c and 51b,c, respectively. For the axially oriented electronegative substituents, such as 53b,c and 52b,c, the π bond is markedly stabilized relative to their parent compounds 53a and 51a respectively. On the other hand, the pseudo-equatorial substituents in 54b,c and 51b,c affect the π ip differently; 54b shows a distinct stabilization of 0.24 eV relative to the parent cyclohexene 53a which is diminished (to 0.03 eV) for the ether 54c. However, 51b shows a π ip which is 0.09 eV larger than its *exo*-methylene parent (51a), whereas the ether 51c is destabilized by 0.12 eV relative to 51a. The similarity of the pe spectral data between the anchored models (51b,c and 52b,c) and their flexible counterparts (53b,c and 54b,c) seems to suggest that the dihedral angle between the substituent and the π bond is similar in both systems. This supports our results from the ^{1}H NMR experiments presented in the previous section, since the Drieding models suggest that the C-OR bond in 52 is some 10° from orthogonality while in 51 it is roughly 20-30° from coplanarity with the π bond.

The interpretation of the pe spectra of compound 55 is complicated by the possible presence of two conformations (55 ⇌ 56) in equilibrium. Variable temperature ^{13}C NMR studies[267] of 55a revealed a

roughtly 1:1 ratio of 55a and 56a at -70°C. If the solvent does not interact preferentially with one of the conformers the observed gas phase pe spectrum is probably a result of these two equilibrium structures. However the comparable sharpness and similarity of the π-ionization peak observed for 55a ⇌ 56a to that of 50a[240] suggests that even if both conformers are present in the gas phase, their pe spectra must be very similar. The invariance of this π ip in 55a and 50a indicates the π ionization energy is insensitive to the orientation of the allylic hydrogen or alkyl group.

As for the allylic alcohol 55b and allylic ether 55c, variable temperature ^{13}C NMR data down to -70°C[267] indicate a ratio of 5:1 and 6:1 for 55b:56b and 55c:56c respectively. This suggests that the conformation is more favored when the C-O bond is in alignment with the π-bond and hence allows some stabilizing interaction between them. Table 11 shows that the π-bond in 55b and 55c are more stabilized than 55a by 0.34 eV and 0.42 eV respectively. These large stabilization energies found in 55b,c are similar to that observed previously[240] in the rigid *trans*-isomers 50b,c and thus strongly support a dominant coplanar conformation in the gas phase.

It appears then that in a flexible allylic system,

the electronegative substituent X would tend to orient the C-X bond to allign with the π system so as to allow a stabilizing $\pi - \sigma^*_{C-X}$ interaction resulting in a predominance of one conformation. Although this study deals with cyclohexene series of compounds it is analogous to the anomeric effects proposed for the tetrahydropyran systems discussed earlier. Several literature examples also support the conclusions based on the pe observations made in this investigation. For example, allyl fluoride, chloride and bromide show π ip's at 10.56, 10.34 and 10.18 eV, respectively while propene has a π ionization equaling 9.88 eV[268]. There is experimental evidence[269-271] to suggest that allyl fluoride and chloride exists preferentially in conformations which align C-X bond with the π system although conflicting data for the fluoride have been reported[272]. The pe observations are consistent with either a $\pi - \sigma^*_{C-X}$ interaction or an inductive effect of the allylic substituent on the π system which is then more difficult to ionize. However, only the former argument requires the coplanarity of C-X bond and π system.

Allyl alcohol has been shown by microwave spectroscopy[273] to adopt a conformation where the C-O bond is nearly coplanar with the π system. The observed π ip (10.22 eV)[274] is 0.34 eV higher than that of the parent propene, close to the stabilization found for 58b and 60b in Table 11.

CONCLUSION

The pe spectra of the flexible allylic substituted cyclohexenes 53, 54 demonstrate the preference of these compounds for a conformation in which the π orbital is aligned with the adjacent C-OR σ(σ^*) bond. In the situation where two orientations of the substituent with respect to the π bond are possible, as in compound 55, the conformation described above was found to be the more favorable one (in solution the ratios are 5:1 and 6:1 for 55b:56b and 55c:56c respectively and our gas phase pe spectra are consistent with these ratios). These finding are also supported by the pes results of the allyl systems studied by previous workers[268,273]. Furthermore, the results are consistent with explanations given for the anomeric effect[258-263], however, further investigation is needed to clarify this point.

EXPERIMENTAL

All routine spectroscopic measurements were made on the instruments described in Chapter II and III. All 200 MHz and 400 MHz ^{1}H NMR spectra were obtained using Bruker WH-200 and WH-400 spectrometers, respectively. Melting points and boiling points are reported uncorrected.

3-*tert*-Butylcyclohexene (53a)

Compound 53a was prepared by the procedure of Goering, Reeves and Espy[275]; it was purified by glpc (10% QF-1 on chromosorb P DMCS AW, 3/8" x 16' aluminum column, 110°C): b.p. 80°C/20 mm (lit.[275] 170.5°C/746 mm).

cis and *trans*-4-*tert*-Butyl-2-cyclohexenol (53b and 54b)

Both 53b and 54b were prepared from the same reaction according to the published procedure[276,277] in a 3:7 ratio. Seven grams of this mixture were chromatographed over 350 gm of grade IV alumina (prepared by mixing 35 gm of water with 350 gm of neutral alumina) to give 0.9 gm of pure 53b, m.p. 51-54°C (lit.[278] 44-49) and 6 gm of mixture. Compound 54b was obtained by the published method of Dunkelblum, Levene and Klein[278] from 9 gm of this 3:7 mixture to give 2.5 gm of 54b, m.p. 32-34°C (lit.[278] m.p. 31-32°C).

cis-3-Methoxy-6-*tert*-butylcyclohexene (53c)

Compound 53b (0.25 gm, 1.49×10^{-3} mol) was methylated[279] yielding after microdistillation (70-80°C bath temperature/14 mm), 0.17 gm (63%) of 53c; ^{1}H NMR ($CDCl_3$) δ: 0.89 (s, 9H), 1.20-2.20 (m, 5H), 3.32 (s, 3H), 3.44-3.70 (m, 1H), 5.78 (s, 2H).

Analysis: Calculated for $C_{11}H_{20}O$: C, 78.57; H, 11.90; Found: C, 78.43; H, 11.99.

trans-3-Methoxy-6-*tert*-butylcyclohexene (54c)

Methylation of 54b (0.50 gm, 2.98×10^{-3} mol)[279] gave after final work up and micro-distillation (80°C bath temperature/12 mm) 0.40 gm (74%) of 54c: 100 MHz ^{1}H NMR ($CDCl_3$) δ: 0.88 (s, 9H), 1.12-2.40 (m, 5H), 3.36 (s, 3H), 3.60-4.00 (m, 1H), 5.78 (b s, 2H).

Analysis: Calculated for $C_{11}H_{20}O$: C, 78.57; H, 11.90; Found: C, 78.51; H, 12.11.

10-Methyl-*cis*-3-octalin[280] (55a)

Five grams (0.03 mol) of 10-methyl-4-octalin-3-one[242] was added to amalgamated zinc (prepared from 6.1 gm (0.03 mol) of granular zinc) in a solution of water (6.1 ml) and concentrated hydrochloric acid (6.4 ml) according to the procedure of Davis and Woodgate[243]. After refluxing for 3.5 hours, the mixture was cooled and extracted with ether and the extracts

subsequently dried ($MgSO_4$), filtered, and evaporated to give 4.0 gm (88% yield) of viscous brown oil which proved to be a mixture of 55a and its trans isomer 50a in a 10:1 ratio. Preparative glpc (20% DEGS on Chrom. W DMCS AW, 3/8" x 16' aluminum column, 120°C) yielded first the major isomer 55a which was collected and microdistilled (50°C/5.0 mm) to give a clear liquid; 100 MHz ^1H NMR ($CDCl_3$) δ: 0.94 (s, 3H, 10-CH_3). Exact Mass calculated for $C_{11}H_{18}$: 150.1409; Found: 150.1405.

Degradation of 55a to 63

Twenty-five milligrams (1.67×10^{-4} mol) of 55a was ozonized[246] in 25 ml dry CH_2Cl_2 at -78°C until the solution turned blue. After flushing the solution with O_2 to remove excess ozone, 1 ml of dimethyl sulfide was added and the mixture stirred 2 hours at room temperature. The mixture was then extracted with H_2O, dried over anhydrous Na_2SO_4, and evaporated. The residue was dissolved in 5 ml of acetone and the solution was oxidized by the addition of Jones' reagent, worked up by the addition of H_2O and extracted with CH_2Cl_2 which was subsequently dried over anhydrous Na_2SO_4. Evaporation produced a second residue which was methylated using diazomethane in ether. After removal of ether, the residue was chromatographed over 15 gm silica gel in a 1 mm (diameter) column using 19:1 petroleum

ether:ether to yield 11.4 mg of diester 63; 200 MHz ^{1}H NMR ($CDCl_3$) δ: 0.95 (s, 3H), 2.12-2.40 (m, 3H, (α-H's)), 3.64 (s, OCH_3), 3.66 (s, OCH_3); FT IR (cast film): 1739 cm^{-1}. Exact Mass Calculated for $C_{13}H_{22}O_4$: 242.1518; Found: 242.1511.

cis And *trans*-4-*tert*-butylcyclohexanol (64a and 65a)

Seven grams of commercially available alcohol (4:1 of *trans*:*cis*) was separated as reported[281] to give 1.2 gm of *cis*-isomer 64, m.p. 82-83°C (lit.[281] 81-82°C) and 2.6 gm of *trans*-isomer 65, m.p. 81-82°C (lit.[281] 80-81°C) as well as 3 gm of mixture.

cis-1-Methoxy-4-*tert*-butylcyclohexane (64b)

Methylation[279] of 1.6 gm (1.04×10^{-2} mol) of 64a yielded after microdistillation (100°C bath temperature/15 mm), 0.6 gm (38%) of 64b: 100 MHz ^{1}H NMR ($CDCl_3$) δ: 0.85 (s, 9H), 1.14-2.20 (m, 7H), 3.28 (s, 3H), 3.41 (m, 1H).

Analysis: Calculated for $C_{11}H_{22}O$: C, 77.58; H, 13.02; Found: C, 77.43; H, 12.91.

trans-1-Methoxy-4-*tert*-butylcyclohexane (65b)

Two grams (1.3×10^{-2} mol) of 65a were methylated according to the procedure of Brown, Diner and Sweet[279] giving 1.3 gm (59%) of 65b: 100 MHz ^{1}H NMR ($CDCl_3$) δ: 0.84 (s, 9H), 0.92-1.42 (m, 5H), 1.56-2.28 (m, 4H),

2.84-3.20 (m, 1H), 3.32 (s, 3H).

Analysis: Calculated for $C_{11}H_{22}O$: C, 77.58; H, 13.02; Found: C, 77.28; H, 13.01

Compounds 55 and 66a,b were kindly prepared by R.W. Marcinko.

REFERENCES

1. K. Siegbahn, C. Nordling, R. Fahlman, R. Nordberg, K. Hamain, J. Hedman, G. Johansson, T. Bergmark, S.E. Karlsson, I. Lindgren, and B. Lindberg, "ESCA: Atomic, Molecular, and Solid State Structure Studied by Means of Electron Spectroscopy", Nova Acta Regiae Soc. Sci., Upsaliensis, Ser. IV, Vol. 20 (1967).
2. K. Siegbahn, C. Nordling, G. Johansson, P.F. Heden, K. Hamrin, U. Gelius, T. Bergmark, L.O. Werme, R. Manne, and Y. Baer, "ESCA Applied to Free Molecules", North-Holland, Amsterdam (1969).
3. T.A. Carlson, Physics Today, 25, 30 (1972).
4. C. Nordling, Angew. Chem. Int. Ed., 11, 83 (1972).
5. H.G. Fitzky, D. Wendisch, and R. Holm, Angew. Chem. Int. Ed., 11, 979 (1972).
6. D.A. Shirley, Adv. Chem. Phys., 23, 85 (1973).
7. C.J. Allan and K. Siegbahn in "MTP International Review of Science," Physical Chemistry, Series One, Volume 12, T.S. West, Ed., Butterworths, London (1973), P.1.
8. T.A. Carlson, "Photoelectron and Auger Spectroscopy", Plenum Press, New York (1975).
9. "Electron Spectroscopy: Theory, Techniques and Applications," Volume 1, C.R. Brundle and A.D. Baker, Eds., Academic Press, New York (1977).

10. D.W. Turner, C. Baker, A.D. Baker and C.R. Brundle, "Molecular Photoelectron Spectroscopy", Wiley, London (1970).

11. S.D. Worley, Chem. Rev., 71, 295 (1971).

12. A.D. Baker, Acc. Chem. Res., 3, 17 (1970).

13. A.D. Baker and D. Betteridge," Photoelectron Spectroscopy-Chemical and Analytical Aspects", Pergamon, Oxford (1972).

14. A.D. Baker, C.R. Brundle and M. Thompson, Chem. Soc. Rev., 355 (1972).

15. J.H.D. Eland, "Photoelectron Spectroscopy", Halsted Press, New York (1974).

16. H. Bock and P.D. Mollere, J. Chem. Ed., 51, 506 (1974).

17. W.C. Price in "Advanced Atomic and Molecular Physics," Volume 10, D.R. Bates and B. Bederson, Eds., Academic Press, New York, (1974).

18. J.W. Rabalais, "Principles of Ultraviolet Photoelectron Spectroscopy", John Wiley & Sons, New York, (1977).

19. A. Einstein, Ann. Physik., 17, 132 (1905).

20. T. Koopmans, Physica, 1, 104 (1933).

21. W.G. Richards, Int. J. Mass. Spec. & Ion Phys., 2, 419 (1969).

22. F.L. Pilar, "Elementary Quantum Chemistry", McGraw-Hill, New York (1968).

23. A. Einstein, Ann. Physik., 17, 891 (1905).

24. The Virial theorem states that E_K is proportional to the potential between the electron and the nucleus; details can be found in ref. 7.

25. W. von Niessen, Chem. Phys. Lett., 18, 503 (1973).

26. A. Schweig et al, Chem. Phys. Lett., 32, 163 (1975).

27. A. Schweig et al, Chem. Phys. Lett., 33, 312 (1975).

28. C.E. Mortimer, "Chemistry, A Conceptual Approach," 3rd Edition, D. van Nostrand, New York (1975), P. 25.

29. M.K. Karplus and R.N. Porter, "Atoms and Molecules: An Introduction for Students for Physical Chemistry", Benjamin, New York (1970).

30. J. Franck, Trans. Faraday Soc., 21, 536 (1925).

31. E.U. Condon, Phys. Rev., 32, 858 (1928).

32. F. Daniels & R.A. Alberty, "Physical Chemistry", John Wiley and Sons, New York (1966), P. 301.

33. L. Heroux and H.E. Hinteregger, Rev. Sci. Instr., 31, 280 (1960).

34. The electron multiplier used is a spiraltron manufactured by either Bendix Corporation (Ann Arbor, Michigan 48107, U.S.A.) or Galileo Electro-optics Corporation (Galileo Park, Sturbridge, Mass. 01518, U.S.A.).

35. Details of the ESCA 36 Spectrometer may be found in the MacPherson's Instruction Manual.

36. R.D. Rusk, "Introduction to Atomic and Nuclear

Physics", Appleton-Century Crofts, New York (1964), P. 54.

37. T.D. Thomas and R.W. Shaw, Jr., J. El. Spec. Rel. Phenom., 5, 1081 (1974).
38. L. Åsbrink and J.W. Rabalais, Chem. Phys. Lett., 12, 182 (1971).
39. Manufactured by Hot Watt, Inc. (128 Maple St., Danvers, Mass. 01923, U.S.A.).
40. The ELSPEC Program is an adapted version of the Lawrence Berkeley Laboratories SUNDER Program for deconvoluting spectra.
41. The PLOTTO Program is kindly supplied by Prof. R.G. Cavell.
42. P. Schuster, Chem. Phys. Lett., 3, 433 (1969).
43. J.A. Pople, D.P. Santry, and G.A. Segal, J. Chem. Phys., 43, 129 (1965).
44. J.A. Pople and G.A. Segal, J. Chem. Phys., 43, 136 (1965).
45. J.A. Pople and G.A. Segal, J. Chem. Phys., 44, 3289 (1969).
46. G. Karlström, H. Wennerström, B. Jönsson, S. Forsén, J. Almolöf, and B. Roos, J. Am. Chem. Soc., 97, 4188 (1975).
47. D.W. Williams, Acta. Crystallogr., 21, 340 (1966).
48. J.P. Schaefer and P.J. Wheatly, J. Chem. Soc. A, 528 (1966).

49. A.H. Lowrey, C. George, P.D'Antonio, and J. Karle, J. Am. Chem. Soc., 93, 6399 (1971).

50. A.L. Andreassen, D. Zebelman, and S.H. Bauer, J. Am. Chem. Soc., 93, 1148 (1971).

51. A.D. Isaacson and K. Morokuma, J. Am. Chem. Soc., 97, 4453 (1975).

52. W.J. Hehre, W.A. Lathan, R. Ditchfield, M.D. Newton, and J.A. Pople, Gaussian 70, Program No. 236, Quantum Chemistry Program Exchange, Indiana University.

53. P.A. Kollman and L.C. Allen, Chem. Rev., 72, 283 (1972).

54. K. Morokuma, J. Chem. Phys., 55, 1236 (1971).

55. J.E. Del Bene and W.L. Kochenour, J. Am. Chem. Soc., 98, 2041 (1976).

56. J.E. Del Bene, Chem. Phys. Lett., 44, 512 (1976).

57. S. Kato, H. Kato, and K. Fukui, J. Am. Chem. Soc., 99, 684 (1977).

58. E.M. Fluder and J.R. de la Vega, J. Am. Chem. Soc., 99, 684 (1977).

59. W.H. Here, R.F. Stewart, and J.A. Pople, J. Chem. Phys., 51, 2657 (1969).

60. R. Ditchfield, W.J. Here, and J.A. Pople, J. Am. Chem. Soc., 54, 724 (1971).

61. W.F. Rowe, Jr., R.W. Duerst, and E.B. Wilson, J. Am. Chem. Soc., 98, 4021 (1976).

62. J. Catalan, M. Yanez, and J.I. Fernandez-Alonso,

J. Am. Chem. Soc., 100, 6917 (1978).

63. A.A. Bothner-By and R.K. Harris, J. Org. Chem., 30, 255 (1965).

64. W.O. George and V.G. Mansell, J. Chem. Soc. B, 132 (1968).

65. M.M. Osman, Helv. Chim. Acta, 55, 239 (1972).

66. S.T. Yoffe, P.V. Petrovsky, Ye I. Goryunov, T.V. Yershova, and M.I. Kabachnk, Tetrahedron, 28, 2783 (1972).

67. R.S. Noi, B.A. Ershow, and A.I. Koltsov, J. Org. Chem. USSR (Engl. Trans.) 11, 1788 (1975).

68. C. Nishijima and H. Nakayama, Chem. Lett., 5, (1975).

69. C.J. Selikar and R.E. Hoffmann, J. Am. Chem. Soc., 99, 7072 (1977).

70. H.P. Koch, J. Chem. Soc., 512 (1951).

71. M. Kimura and M. Kubo, Bull. Chem. Soc. Japan, 25, 250 (1952).

72. D.J. Bertelli, T.G. Andrews, Jr., and P.O. Crews, J. Am. Chem. Soc., 91, 5286 (1969).

73. J.W. Emsley, J.C. Lindon, and D.S. Stephenson, Mol. Phys., 27, 641 (1974).

74. L. Weiler, Can. J. Chem., 50, 1975 (1972).

75. J.F. Bagli and M. St. Jacques, Can. J. Chem., 56, 578 (1978).

76. Solvent used in this NMR measurement is a 1:1 ratio of $CFCl_3$ and deuterated acetone.

77. H. Simanouchi and Y. Sasada, Tet. Lett., 2421 (1970).

78. Acta Crystallogr., Sect. B, 29, 81 (1973).

79. M. Kimura and M. Kubo, Bull. Chem. Soc. Japan, 26, 250 (1953).

80. A.C.P. Alves and J.M. Hollas, Mol. Phys., 23, 927 (1972).

81. A.C.P. Alves and J.M. Hollas, Mol. Phys., 25, 1305 (1973).

82. Y. Demura, T. Kawato, H. Kanatomi, and I. Murase, Bull. Chem. Soc. Japan, 48, 2820 (1975).

83. Solvent system used as a 1:1 mixture of $CFCl_3$ (m.p. -110°C) and CD_2Cl_2 (m.p. -95°C).

84. C. Svenson, J.L. Bernstein, S.C. Abrahams, R.C. Haddon, and F.H. Stillinger, J. Am. Chem. Soc., 101, 5759 (1979).

85. F. Carnovale, T.H. Gan, J.B. Peel, and K.D. Franz, Tetrahedron, 35, 129 (1979).

86. SPINDO[87] (Spectroscopic-Potentials-adjusted INDO) method is a modified version of MINDO[88,89] method and is parametrized originally to predict IPs of hydrocarbons. The SPINDO method used by Peel[90] was parametrized to incorporate oxygen atoms in addition to carbon and hydrogen.

87. C. Fridh, L. Åsbrink, and E. Lindholm, Chem. Phys. Lett., 15, 282 (1972).

88. N.C. Baird and M.J.S. Dewar, J. Chem. Phys., 50, 1262 (1969).

89. M.J.S. Dewar and S.D. Worley, J. Chem. Phys., 50,

654 (1969).

90. J.B. Peel and G.D. Willett, Aust. J. Chem., 28, 2357 (1975).

91. K. Hafner, H.E. Kramer, H. Musso, G. Ploss, and G. Shulz, Chem. Ber., 97, 2066 (1964).

92. H.M. Pickett, J. Am. Chem. Soc., 95, 1770 (1973).

93. H. Fuess and H.J. Lindner, Chem. Ber., 108, 3096 (1975).

94. U. Gelius, C.J. Allan, D.A. Allison, H. Siegbahn, and K. Siegbalm, Chem. Phys. Lett., 11, 224 (1971).

95. S. Pignatoro, R. Di Marino, G. Distefano, and A. Mangini, Chem. Phys. Lett., 22, 352 (1973).

96. D.T. Clarke, D.B. Adams, I.W. Scanlan and I.S. Woole, Chem. Phys. Lett., 25, 263 (1974).

97. J. Powling and H.J. Bernstein, J. Am. Chem. Soc., 73, 4353 (1951).

98. A. Schweig, H. Vermeer, and W. Weidner, Chem. Phys. Lett., 26, 229 (1974).

99. D.J. Olszanski, T.J. Anderson, M.A. Newman, and G.A. Melson, Inorg. Nucl. Chem. Lett., 10, 137 (1974).

100. D.P. Spears, H.F. Fischbeck, and T.A. Carlson, J. El. Spec. Rel. Phenom., 6, 411 (1975).

101. P.M. Plaskin, J. Sharma, S. Bulusu, and G.F. Adams, J. El. Spec. Rel. Phenom., 6, 429 (1975).

102. Z.B. Maksic, K. Rupnik, and M. Eckert-Maksic, J. El. Spec. Rel. Phenom., 16, 371 (1979).

103. The high acidity of MA (pKa = 4.64[65]) probably

causes the OH for OD exchange to happen so fast that at the outset of the CH exchange experiment the actual species is HCOCH=C(H)(OD) (6a).

104. J.L. Latham and A.E. Burgess, "Elementary Reaction Kinetics", 3rd edition, Butterworths and Co. (Publishers) Ltd. (1977).

105. L. Melander, "Isotope effects on Reaction Rates", Ronald Press, New York (1964), Chapter 4.

106. R.S. Brown, unpublished results.

107. Assignment is based on the ^{1}H NMR spectrum of β-methoxyacrolein (1b) in which the formyl and hydroxyvinyl protons appear at δ9.43 and 7.45 respectively.

108. F.A. Bovey, "Nuclear Magnetic Resonance Spectroscopy", Academic Press, New York (1969), Chapter 7.

109. R. Hüttel, Chem. Ber., 74(III), 1825 (1941).

110. E.J.J. Grabowski and R.L. Autrey, Tetrahedron, 25, 4315 (1969).

111. N.N. Kalinina, V.T. Klimko, T.V. Protopova, and A.P. Skolinov, J. Gen. Chem. USSR (Engl. Transl.), 32, 2116 (1962).

112. J.W. Cook, A.R. Gibb, R.A. Raphael, and A.R. Somerville, J. Chem. Soc., 503 (1951).

113. H. Nozaki, Z. Yamagati, T. Okada, R. Noyori, and M. Kawanisi, Tetrahedron, 23, 3993 (1967).

114. R.C. Haddon, F. Wudl, M. Kaplan, J.H. Marshall, R.E. Cais, and F.B. Bramwell, J. Am. Chem. Soc., 100, 7629 (1978).

115. K. Hafner, K.H. Vopel, G. Ploss, and C. König, Justus Liebigs Ann. Chem., 661, 52 (1963).

116. J.N. Brönsted, Rec. Trav. Chim., 42, 718 (1923).

117. G.N. Lewis, "Valence and the structure of atoms and molecules", Am. Chem. Soc. Monograph, The Chemical Catalog Co., New York (1923).

118. R.L. Martin and D.A. Shirley, J. Am. Chem. Soc., 96, 5299 (1974).

119 B.E. Mills, R.L. Martin and D.A. Shirley, J. Am. Chem. Soc., 98, 2380 (1976).

120. D.W. Davis and J.W. Rabalais, J. Am. Chem. Soc., 96, 5305 (1974).

121. J. March, "Advanced Organic Chemistry: Reactions, Mechanisms, and Structure", McGraw-Hill, New York (1968), P. 19.

122. T.H. Lowry and K.S. Richardson, "Mechanism and Theory in Organic Chemistry", Harper and Row, New York (1976).

123. J.S. Jen and T.D. Thomas, J. Am. Chem. Soc., 97, 1265 (1975).

124. T.X. Carroll, S.R. Smith and T.D. Thomas, J. Am. Chem. Soc., 97, 659 (1975).

125. S.R. Smith and T.D. Thomas, J. Am. Chem. Soc., 100, 5459 (1978).

126. F.M. Benoit and A.G. Harrison, J. Am. Chem. Soc., 99, 3980 (1977).

127. R.G. Cavell and D.A. Allison, J. Am. Chem. Soc., 99, 4203 (1977).

128. A.J. Ashe, III, M.K. Bahl, K.D. Bomben, W-T. Chan, J.K. Gimzewski, P.G. Sitton, and T.D. Thomas, J. Am. Chem. Soc., 101, 1764 (1979).

129. R.W. Taft in "Proton Transfer Reactions", E. Calden, V. Gold, Eds., Chapman and Hall, London (1975), P. 31.

130. ΔG° of amino-, and dimethylamino pyridines were taken from the work of Aue: D.H. Aue, H.M. Webb, M.J. Towers, C.L. Liotta, C.J. Alexander, and H.P. Hopkins, J. Am. Chem. Soc., 98, 854 (1976).

131. Y.K. Lau, P.P.S. Saluja, P. Kabarle, and R.W. Alder, J. Am. Chem. Soc., 100, 7328 (1978).

132. We thank Prof. Taft for informing us about corrected ΔG° values.

133. J. Catalán, O. Mó, P. Pérez, and M. Yáñez, J. Am. Chem. Soc., 101, 6520 (1979).

134. D.W. Davis, D.A. Shirley, and T.D. Thomas, J. Am. Chem. Soc., 94, 6565 (1972).

135. D.W. Davis, D.A. Shirley, and T.D. Thomas, J. Chem. Phys., 56, 671 (1972).

136. D.T. Clark, D. Kilcast, and W.K.R. Musgrave, J. Chem. Soc. D, 516 (1971).

137. D.T. Clark, D. Kilcast, D.B. Adams, and W.K.R. Musgrave, J. El. Spec. Rel. Phenom., 1, 227 (1972/73).

138. T. Ohta, T. Fujikawa, and H. Kuroda, Bull. Jpn. Chem. Soc., 48, 2017 (1975).

139. B.C. Trudell and S.J.W. Price, Can. J. Chem., 55, 1279 (1977).

140. B.C. Trudell and S.J.W. Price, Can. J. Chem., 56, 538 (1978).

141. D.W. Davis and D.A. Shirley, Chem. Phys. Lett., 15, 185 (1972).

142. D.A. Shirley, Chem. Phys. Lett., 16, 220 (1972).

143. D.W. Davis, M.S. Banna, and D.A. Shirley, J. Chem. Phys., 60, 237 (1974).

144. D.W. Davis and D.A. Shirley, J. El. Spec. Rel. Phenom., 3, 137 (1974).

145. A.R. Katritzky and J.M. Lagowski in "Adv. Heterocycl. Chem., Volume 1", A.R. Katritzky, Ed., Academic Press, New York, (1963) P. 312.

146. A. Albert and J.N. Phillips, J. Chem. Soc., 1294 (1956).

147. S.F. Mason, J. Chem. Soc., 674 (1958).

148. É.S. Levin and G.N. Rodianova, Doklady Akademii Nauk SSSR, 164, 584 (1965).

149. P. Beak and F.S. Fry, J. Am. Chem. Soc., 95, 1700 (1973).

150. P. Beak, F.S. Fry, J. Lee, and F. Steele, J. Am. Chem. Soc., 98, 171 (1976).

151. P. Beak, J.B. Covington, and S.G. Smith, J. Am. Chem. Soc., 98, 8284 (1976).

152. P. Beak, Accts. Chem. Res., 10, 186 (1977).

153. M.J. Cook, S. El-Abbady, and A.R. Katritzky, J. Chem. Soc. Perkin II, 1652 (1977).

154. C. Guimon, G. Garrabe, and G. Pfister-Guillouzo, Tet. Lett., 2585 (1979).

155. R.J. Gillespie and T. Birchall, Can. J. Chem., 41, 148 (1963).

156. V.P. Kabanor and S.N. Khar'kov, J. Applied Chem. U.S.S.R. (Engl. Transl.), 48, 2784 (1975).

157. J.E. Sarneski, H.L. Surprenant, and D.N. Reilley, Spectrosc. Lett., 9, 885 (1976).

158. L. Diop, C. Belin, and J. Potier, J. Chim. Phys.-Chim. Biol., 73, 207 (1976).

159. P. Stilbs, S. Forsen, and J.S. Hartman, J. Chem. Soc. Perkin Trans. 2, 556 (1977).

160. H. Moehrle et al, Monatsh. Chem., 109, 1295 (1978).

161. J.F. Hinton, A. Beeler, D. Harpool, R.W. Briggs, and A. Pullman, Chem. Phys. Lett., 47, 411 (1977).

162. P. Kollman and S. Rothenberg, J. Am. Chem. Soc., 99, 1333 (1977).

163. R.W. Alder, P.S. Bowman, W.R.S. Steele, and D.R. Winterman, Chem. Commun., 72[illegible] (1968).

164. F. Hibbert, J. Chem. Soc., Chem. Commun., 463 (1973).

165. R.W. Alder and J.E. Anderson, J. Chem. Soc., Perkin II, 2086 (1973).

166. H. Einspahr, J.B. Robert, R.E. Marsh, and J.D. Roberts, Acta. Cryst., B29, 1611 (1973).

167. M.R. Truter and B.L. Vickery, J. Chem. Soc. Dalton, 395 (1972).

168. MINDO/3, Quantum Chemistry Program Exhange No. 279, R.C. Bingham, M.J.S. Dewar, and D.H. Lo, J. Am. Chem. Soc., 97, 1285 (1975).

169. S.K. Pollack, J.L. Devlin III, K.C. Summerhays, R.W. Taft, and W.J. Hehre, J. Am. Chem. Soc., 99, 4583 (1977).

170. K.D. Summerhays, S.K. Pollack, R.W. Taft, and W.J. Hehre, J. Am. Chem. Soc., 99, 4585 (1977).

171. E.M. Arnett in "Proton Transfer Reactions", E. Calden, V. Gold, Eds., Chapman and Hall, London (1975), P. 79.

172. H.L. Retcofsky and R.A. Friedel, J. Phys. Chem., 71, 3592 (1967).

173. H.L. Retcofsky and R.A. Friedel, J. Phys. Chem., 72, 290 (1968).

174. H.L. Retcofsky and R.A. Friedel, J. Phys. Chem., 72, 2619 (1968).

175. J.A. Pople and M. Gordon, J. Am. Chem. Soc., 89, 4253 (1967).

176. H. Basch, Chem. Phys. Lett., 5, 337 (1970).

177. U. Gelius, G. Johansson, H. Siegbahn, C.J. Allan, D. Allison, J. Allison, and K. Siegbahn, J. El. Spec. Rel. Phenom., 1, 285 (1972/73).

178. R.E. Block, J. Magn. Resonance, 5, 155 (1971).

179. W.E. Swartz and D.M. Hercules, Anal. Chem., 43, 1066 (1971).

180. G.D. Mateescu and J.L. Riemenschneeder in "Electron Spectroscopy", D.A. Shirley, Ed., North-Holland Publishing Co., Amsterdam (1972), P. 661.

181. B.J. Lindberg, J. El. Spec. Rel. Phenom., 5, 149 (1974).

182. M. Witanowski, T. Saluvere, L. Stefaniak, H. Janiuszewski, and G.A. Webb, Mol. Phys., 23, 1071 (1972).

183. M.E. Schwartz, Chem. Phys. Lett., 6, 631 (1970).

184. B. Bak, L. Hansen-Nygaard, and J. Rostrup-Andersen, J. Mol. Spectrosc., 2, 361 (1958).

185. D. Liberman, Bull. Am. Phys. Soc., 9, 731 (1964).

186. L. Hedin and G. Johansson, J. Phys. B, 2, 1336 (1969).

187. C.D. Ritchie and W.F. Sager in "Progress in Physical Organic Chemistry, Vol. 2", S.G. Cohen, A. Streitwieser, Jr., R.W. Taft, Eds., Interscience, New York (1964), P. 323.

188. S. Ehrenson, R.T.C. Brownlee, and R.W. Taft in Progress in Physical Organic Chemistry, Vol. 10", A. Streitwieser, Jr., R.W. Taft, Eds., Interscience, New York (1973), P. 1.

189. H.H. Jaffé, Chem. Rev., 53, 191 (1953).

190. R.W. Taft, E. Price, I.R. Fox, I.C. Lewis, K.K. Andersen, and G.T. Davis, J. Am. Chem. Soc., 85, 709 (1963).

191. R.W. Taft, E. Price, I.R. Fox, I.C. Lewis, K.K. Andersen, and G.T. Davis, J. Am. Chem. Soc., 85,

3146 (1963).

192. R.C. Bingham, M.J.S. Dewar, and D.H. Ho, J. Am. Chem. Soc., 97, 1296, 1303, 1307, 1311 (1975).

193. N. Bodor and R. Pearlman, J. Am. Chem. Soc., 100, 4946 (1978).

194. B.S. Freiser, R.L. Woodin, and J.L. Beauchamp, J. Am. Chem. Soc., 97, 6893 (1975).

195. D.P. Martinsen and S.E. Buttrill, Jr., Organic Mass Spec. 11, 762 (1976).

196. Y.K. Lau and P. Kebarle, J. Am. Chem. Soc., 98, 1320 (1976).

197. L.K. Nash, "Elements of Chemical Thermodynamics", Addison-Wesley, Massachusetts (1970), P. 134.

198. D.H. Aue, L.D. Betowski, W.R. Davidson, M.T. Bowers, P. Beak, and J. Lee, J. Am. Chem. Soc., 101, 1361 (1979).

199. Corrected according to $\Delta G°_{300} = \frac{\Delta G°_{600} + \Delta H°}{2}$. We thank Dr. Y.K. Lau for providing us with the $\Delta H°$ values for compounds in ref. 165.

200. D.G. Lister, J.K. Tyler, J. Chem. Soc., Chem. Comm., 152 (1966).

201. J.C.D. Brand, D.R. Williams, and T.J. Cook, J. Mol Spectrosc., 20, 359 (1966).

202. R.A. Kydd and P.J. Krueger, Chem. Phys. Lett., 49, 539 (1977).

203. M. Qwack and M. Stockberger, J. Mol. Spectrosc., 43, 87 (1972).

204. N.W. Larsen, E.L. Hansen, and F.M. Nicolaisen, Chem. Phys. Lett., 43, 584 (1976).

205. C.C. Stramitz and H.H. Schmidtke, Theoret. Chim. Acta., 42, 13 (1976).

206. J.W. Smith, J. Chem. Soc., 81 (1961).

207. A. Hastie. D.G. Lister, R.L. McNeil, and J.K. Tyler, J. Chem. Soc., Chem. Comm., 108 (1970).

208. C.W.N. Cumper and A. Singleton, J. Chem. Soc. (B), 1096, 1100 (1967).

209. M.J. Aroney, K.E. Calderbank, R.J.W. LeFévre, and R.K. Pierens, J. Chem. Soc. (B), 561 (1968).

210. V. Vilkov and T.P. Timasheva, Proc. Acad. Sci. U.S.S.R. Chem. Soc. (Engl. Transl.), 161, 261 (1965).

211. W.J.E. Parr and R.W. Wasylishen, J. Mol. Struct., 38, 272 (1977).

212. T.J. Zielinski, D.L. Breen, and R. Rein, J. Am. Chem. Soc., 100, 6266 (1978).

213. G. Klopman, A. Andreozzi, A.J. Hopfinger, O. Kilkuchi, and M.J.S. Dewar, J. Am. Chem. Soc., 100, 6267 (1978).

214. G.M. Anderson III, P.A. Kollman, L.N. Domelsmith, and K.N. Houk, J. Am. Chem. Soc., 101, 2344 (1979).

215. A.I. Biggs and R.A. Robinson, J. Chem. Soc., 388 (1961).

216. B. Lindberg, S. Svensson, P.Å. Malmquist, E. Basilier, U. Gelius, and K. Siegbahn, Chem. Phys. Lett., 90, 175 (1976).

217. A. Roe and G.F. Hawkins, J. Am. Chem. Soc., 69, 2443 (1947).

218. R.H. Wiley and J.H. Hartman, J. Am. Chem. Soc., 73, 494 (1951).

219. A. Fischer, W.J. Galloway, and J. Vaughan, J. Chem. Soc., 3591 (1964).

220. A. Albert and J.N. Phillips, J. Chem. Soc., 1294 (1956).

221. P. Beak, J. Bonham, and J.T. Lee, J. Am. Chem. Soc., 90, 1569 (1968).

222. E. Ochiai, J. Org. Chem., 18, 534 (1953).

223. C.H. Hornig and F.W. Bergstorm, J. Am. Chem. Soc., 67, 2110 (1945).

224. J. Meisenheimer, O. Finn, and W. Schneider, Ann., 420, 219 (1920).

225. "Beilstein Handbuch Der Organischen Chemie, Volume 20", F.K. Beilstein, Ed., Julius Spinger, Berlin, Germany (1935), P. 231.

226. J.P. Wibaut, J. Overhoff, and H. Geldof, Rec. Trav. Chim., 54, 807 (1935).

227. J.L. Lyle and R.W. Taft, J. Heterocyclic Chem., 9, 745 (1972).

228. P.B. Desai, J. Chem. Soc. Perkin I, 1865 (1973).

229. H.T. Clarke, H.B. Gillespie, and S.Z. Weisshaus, J. Am. Chem. Soc., 55, 4571 (1933).

230. A. Binz and O. von Schickkh, Chem. Ber., 68, 315 (1935).

231. L. Marion and W.F. Cockburn, J. Am. Chem. Soc., 71, 3402 (1949).

232. L.M. Stock, J. Chem. Educ., 49, 400 (1972).

233. R. Hoffmann, Acc. Chem. Res., 4, 1 (1971).

234. L. Radom, W.J. Hehre, and J.A. Pople, J. Am. Chem. Soc., 93, 289 (1971).

235. L. Radom, W.J. Hehre, and J.A. Pople, J. Am. Chem. Soc., 94, 2371 (1972).

236. J.A. Pople, Abstracts, 172nd National Meeting of the American Chemical Society, San Francisco, Aug. 1976, No. PHYS-79.

237. R.S. Brown, Can. J. Chem., 53, 3439 (1975).

238. R.S. Brown, Can. J. Chem., 54, 805 (1976).

239. P. Bischof, J.A. Hashmall, E. Heilbronner, and V. Hornig, Helv. Chim. Acta., 52, 1745 (1969).

240. R.S. Brown and R.W. Marcinko, J. Am. Chem. Soc., 100, 5721 (1978).

241. G.V. Smith and H. Kriloff, J. Am. Chem. Soc., 85, 2016 (1963).

242. B. Branchaud, T. Maestrone, and P.S. Zoretic, Tet. Lett., 527 (1975).

243. B.R. Davis and P.D. Woodgate, J. Chem. Soc., 5943 (1965).

244. D.E. Dorman, M. Jautelat, and J.D. Roberts, J. Org. Chem., 36, 2757 (1971).

245. G.C. Levy and G.L. Nelson, "Carbon-13 Nuclear Magnetic Resonance for Organic Chemists", Wiley-Interscience, New York (1972), P. 60.

246. J.J. Pappas and W.P. Keaveney, Tet. Lett., 4273 (1966).

247. B.J.M. Neijzen, R.F. Schmitz, G.W. Klumpp, and D.A. de Lange, Tetrahedron, 31, 873 (1975).

248. D. Chadwick, D.C. Frost, and L. Weiler, J. Am. Chem. Soc., 93, 4320, 4962 (1971).

249. R.S. Brown, Can. J. Chem., 54, 1521 (1976).

250. Angew. Chem., Int. Ed., Engl., 12, 307 (1973).

251. G. Worrell, J.W. Verhoeven, and W.N. Speckamp, Tetrahedron, 3525 (1974).

252. E.J. McAlduff, P. Caramella, and K.N. Houk, J. Am. Chem. Soc., 100, 105 (1978).

253. R.A. Pasternak, Acta. Cryst., 4, 316 (1951)

254. Y. Senda and S. Imaizumi, Tetrahedron, 30, 3813 (1974).

255. K. Sakashita, J. Chem. Soc. Japan, 81, 49 (1960).

256. J. Lessard, P.V.M. Tan, R. Martino, and J.K. Saunders, Can. J. Chem., 55, 1015 (1977).

257. E.L. Eliel, N.L. Allinger, S.J. Angyal, and G.A. Morrison, "Conformational Analysis", John Wiley and Sons, New York (1965).

258. R.U. Lemieux in "Molecular Rearrangements, Volume 2", P. de Mayo, Ed., Interscience, New York (1964), P. 709.

259. R.U. Lemieux, Pure Appl. Chem., 25, 527 (1971).

260. H. Booth and R.U. Lemieux, Can. J. Chem., 49, 777 (1971).

261. E.L. Eliel, Acc. Chem. Res., 3, 1 (1970).

262. E.L. Eliel, Angew. Chem., Int. Ed. Engl., 11, 739 (1972).

263. S.J. Angyal, Angew. Chem., Int. Ed. Engl., 8, 157 (1969).

264. C. Romers, C. Altona, H.R. Buys, and E. Havinga, Top. Stereochem., 4, 39 (1969).

265. S. David. O. Eisenstein, W.J. Hehre, L. Salem, and R. Hoffman, J. Am. Chem. Soc., 95, 3806 (1973).

266. C. Braddeley, Tet. Lett., 1645 (1973).

267. L.M. Browne, R.E. Klinck, and J.B. Stothers, Org. Magn. Reson., 12, 561 (1979).

268. H. Schmidt and A. Schweig, Angew. Chem., Int. Ed. Engl., 12, 307 (1973).

269. R.E. Rondeau and L.A. Harrah, J. Mol. Spectrosc., 21, 332 (1966).

270. C. Sourisseau and B. Pasquier, J. Mol. Struct., 12, 1 (1972).

271. E. Hirota, J. Mol. Spectrosc., 35, 9 (1970).

272. E. Hirota, J. Chem. Phys., 42, 2071 (1965).

273. A.N. Murty and R.F. Curl, J. Chem. Phys., 46, 4176 (1967).

274. G.W. Mines and H.W. Thompson, Spectrochim. Acta, 29, 1377 (1973).

275. H.L. Goering, R.L. Reeves, and H.H. Espy, J. Am. Chem. Soc., 78, 4926 (1956).

276. P.L. Barili, G. Bellucci, G. Berti, M. Golfarini, F. Marioni, and V. Scartoni, Gazzetta Chimi. Italiana, 104, 107 (1974).

277. E.W. Garbisch, Jr., J. Org. Chem., 30, 2109 (1965).

278. E. Dunkelblum, R. Levene, and J. Klein, Tet., 28, 1009 (1972).

279. R.K. Brown, U.E. Diner, and F. Sweet, Can. J. Chem., 44, 1591 (1966).

280. 10-Methyl-*cis*-3-octalin was prepared by R.W. Marcinko.

281. S. Winstein and N.J. Holness, J. Am. Chem. Soc., 77, 5562 (1955).